

**CELL AND MOLECULAR MEDIATORS INVOLVED IN DAMAGE AND REPAIR IN
EMPHYSEMA USING MOUSE MODELS**

by

Nisha Sambamurthy

B.Tech Industrial Biotechnology, Anna University in Chennai, 2007

Submitted to the Graduate Faculty of
The School of Medicine in partial fulfillment
of the requirements for the degree of
Doctor of Philosophy

University of Pittsburgh

2014

UNIVERSITY OF PITTSBURGH

SCHOOL OF MEDICINE

This dissertation was presented

by

Nisha Sambamurthy

It was defended on

February 27, 2014

And approved by

Chairperson: Tim D. Oury, MD, PhD, Professor, Department of Pathology

Prabir Ray, PhD, Professor of Medicine and Immunology, Department of Immunology

Sally Wenzel, MD, Professor of Medicine, Departments of Medicine and Pathology

Naftali Kaminski, MD, Professor of Internal Medicine, Chief of Pulmonary, Critical

Care and Sleep Medicine, Yale School of Medicine

Dissertation Advisor: Steven D. Shapiro, MD, Professor of Medicine, Department of

Medicine

Copyright © by Nisha Sambamurthy

2014

**CELL AND MOLECULAR MEDIATORS INVOLVED IN DAMAGE AND REPAIR
IN EMPHYSEMA USING MOUSE MODELS**

Nisha Sambamurthy

University of Pittsburgh, 2014

Chronic obstructive pulmonary disease (COPD) is the third leading cause of morbidity and mortality in the United States and an epidemic worldwide. COPD pathologically manifests as emphysema, which is characterized by the abnormal and permanent airspace enlargement. Current research strives to understand the exact sequence of events triggering and leading to the progression of this disease, with the continued hope of finding a cure. The overarching aim of the current study was to investigate the role for the receptor for advanced glycation end products (RAGE) and a distal bronchial progenitor cell population (DBPCs) in mediating alveolar damage and repair using murine models of emphysema.

RAGE has gained importance in the context of COPD in the past decade. Highly expressed in normal adult lung tissue; its expression is altered in the context of lung injury. The present study tests the hypothesis that RAGE mediates cigarette smoke induced alveolar injury based on its previously described pro-inflammatory function. RAGE knockout mice (RAGE^{-/-}) were used to investigate the contribution of this receptor towards the development of cigarette smoke induced emphysema. Our data indicates RAGE's key contribution towards cigarette smoke induced emphysema, mediated through neutrophil recruitment and increased loss of tissue elastance.

Emphysema is thought to result from the disruption of a delicate balance that exists within the alveolar compartment; accentuated by failure at endogenous attempts to repair in the

presence of extensive inflammation and loss of underlying basement membrane. Using a transgenic mouse line (CC10-Cre x Rosa26-LacZ) developed in our laboratory, we trace and confirm the migration of a distal bronchial progenitor cell population from the bronchoalveolar duct junction (BADJ)/ terminal bronchioles into the adjacent injured alveolar compartment. We further confirm our findings in a knock-in mouse line (CC10-iCre X Rosa26-LacZ) and thereby authenticate the contribution of these progenitor cells towards repopulating the injured alveolus.

This study shows that RAGE mediates early neutrophil recruitment leading to the pathogenic progression of alveolar damage and elucidate the contribution of a CC10 expressing bronchial progenitor arising from the distal airways leading to alveolar repopulation in the context of emphysema.

TABLE OF CONTENTS

PREFACE.....	XIV
ACKNOWLEDGEMENTS	XV
NOMENCLATURE.....	XX
1.0 CHRONIC OBSTRUCTIVE PULMONARY DISEASE (COPD).....	1
1.1 BURDEN OF COPD.....	1
1.2 RISK FACTORS CONTRIBUTING TO COPD.....	2
1.2.1 Cigarette smoking and genetic factors	2
1.2.2 Age and gender.....	3
1.2.3 Occupational exposure, outdoor and indoor air pollutants	3
1.3 COPD- PATHOPHYSIOLOGY	4
1.3.1 Pathogenic mechanisms in Emphysema	5
1.3.1.1 Protease- anti-protease imbalance.....	6
1.3.1.2 Inflammation	7
1.3.1.3 Oxidative stress	8
1.3.1.4 Loss of alveolar structure and apoptosis.....	10
1.4 COPD-ASTHMA OVERLAP.....	11
1.5 COPD-DIAGNOSIS AND ASSESSMENT	11
1.6 COPD-TREATMENT.....	13

1.7	ANIMAL MODELS OF EMPHYSEMA	15
1.7.1	Protease and chemical injury models.....	16
1.7.2	Cigarette smoke model	17
1.7.3	Naturally occurring airspace enlargement in genetic mutant mice	18
1.7.4	Gene targeted mice and transgenic mice with airspace enlargement	19
1.7.5	Cigarette smoke mediated Emphysema in gene-targeted mice	20
2.0	THE RECEPTOR FOR ADVANCED GLYCATION END PRODUCTS (RAGE) MEDIATED NEUTROPHIL RECRUITMENT DRIVES THE PATHOGENIC PROGRESSION OF EMPHYSEMA	22
2.1	RAGE- BACKGROUND	23
2.1.1	RAGE – structure, isoforms, ligands and signaling.....	23
2.1.2	RAGE in the lung.....	25
2.1.3	RAGE and COPD	25
2.2	RAGE-MATERIALS AND METHODS	26
2.2.1	RAGE knockout mice	26
2.2.2	Cigarette smoke models.....	27
2.2.2.1	Chronic cigarette smoke model	27
2.2.2.2	Acute cigarette smoke model	27
2.2.3	Respiratory mechanics measurements.....	27
2.2.4	Tissue processing for histology and morphometry	28
2.2.5	Gills staining for morphometric assessment.....	28
2.2.6	Morphometry	29
2.2.7	Lung tissue homogenate preparation and immunoblotting.....	29

2.2.8	Bronchoalveolar lavage fluid collection and processing.....	30
2.2.9	Cytospin preparation and analysis.....	30
2.2.10	Serum collection	31
2.2.11	Statistical analysis	31
2.3	RAGE-RESULTS	32
2.3.1	Absence of RAGE affects the alveolar dimensions at baseline and protects from alveolar enlargement on chronic cigarette smoke exposure.	32
2.3.2	Effect of RAGE on lung physiology	35
2.3.3	Cigarette smoke induced apoptosis is RAGE-dependent on chronic smoke exposure	37
2.3.4	Impaired neutrophil recruitment observed in RAGE -/- mice on acute cigarette smoke exposure.....	38
2.4	RAGE-DISCUSSION.....	41
2.5	RAGE- FUTURE DIRECTIONS.....	45
3.0	A DISTAL BRONCHIAL PROGENITOR CELL (DBPC) POPULATION CONTRIBUTES TO ALVEOLAR REPAIR IN EMPHYSEMA USING MOUSE MODELS	49
3.1	DBPC- BACKGROUND.....	50
3.1.1	Epithelial cell populations in the lung.....	50
3.1.2	Alveolar repair in normal and emphysematous lungs	51
3.1.3	Pulmonary epithelial progenitor cell populations.....	53
3.1.4	Potential involvement of other cell lineages towards lung epithelial repair	54

3.1.5	Bioengineering lung tissue <i>ex vivo</i>	56
3.2	DBPC- MATERIALS AND METHODS.....	57
3.2.1	Lineage tracing of distal bronchial progenitor cells	57
3.2.1.1	Transgenic mouse model- CC10-Cre; ROSA-LacZ	57
3.2.1.2	Cre specificity in the CC10-Cre; ROSA-LacZ transgenic mouse ..	59
3.2.1.3	Constitutive knock-in mouse model- CC10-iCre; ROSA-LacZ	59
3.2.2	Murine models of Emphysema	60
3.2.2.1	Porcine pancreatic elastase (PPE) model.....	60
3.2.2.2	Cigarette smoke model	60
3.2.3	Lung tissue processing- X-Gal staining.....	61
3.2.4	β -gal ⁺ lineage tagged cell quantification	61
3.2.5	Morphometry	62
3.2.6	Isolation of bronchoalveolar stem cells (BASCs) by fluorescence activated cell sorting (FACS)	62
3.2.7	Immunofluorescence staining	64
3.3	DBPC- RESULTS.....	64
3.3.1	Bronchoalveolar stem cells detected at the bronchoalveolar duct junction in normal lung tissue.....	64
3.3.2	Expansion of BASC population with emphysema associated alveolar injury	66
3.3.3	Migration of distal bronchial progenitor cells from the terminal bronchiole in the context of alveolar injury.....	69

3.3.4	Distal bronchial progenitor cells enter the alveolar space in response to emphysema associated alveolar injury	70
3.3.5	Lineage tagged distal bronchial progenitor cells give rise to alveolar type-II and alveolar type-I epithelial cells	73
3.3.6	Lineage tagged cells emanate from the BADJ and repopulate the alveoli in a constitutive CC10-iCre; Rosa-LacZ knock-in mouse line in the context of PPE associated injury	78
3.4	DBPC- DISCUSSION.....	80
3.5	DBPC- FUTURE DIRECTIONS	85
APPENDIX A: SELECTIVITY AND SPECIFICITY OF RAT-CC10 PROMOTER EXPRESSION IN CC10-CRE; ROSA-LACZ TRANSGENIC MICE		88
APPENDIX B: RAGE EXPRESSION ON CHRONIC CIGARETTE SMOKE EXPOSURE		91
BIBLIOGRAPHY		97

LIST OF TABLES

Table 1: Quantification of airspace enlargement using lung morphometry	33
--	----

LIST OF FIGURES

Figure 1: Lack of RAGE leads to enlarged airspaces at baseline and protects from progressive airspace enlargement on chronic cigarette smoke exposure	34
Figure 2: Smoke-exposed RAGE ^{-/-} mice show no reduction in lung tissue elastance on bronchoconstriction when compared to their air-exposed controls.....	36
Figure 3: RAGE expression contributes to apoptosis on chronic cigarette smoke exposure.	38
Figure 4: RAGE mediates early recruitment of neutrophils in response to acute cigarette smoke exposure	40
Figure 5: Lineage tracing distal bronchial epithelial cells	58
Figure 6: Detection of bronchoalveolar stem cells (BASCs) at the bronchoalveolar duct junction	65
Figure 7: Expansion of BASC in the terminal BADJ on emphysema-associated injury.....	68
Figure 8: Migration of distal bronchial progenitor cells from the terminal bronchi in response to alveolar injury	70
Figure 9: Migration of Distal bronchial progenitor cells from the BADJ into the injured alveolar compartment of the lung	72
Figure 10: β -Gal ⁺ lineage tagged cells arising from the terminal bronchi give rise to AT-I and AT-II epithelial cells post-PPE injury.....	74

Figure 11: SP-C expressing β -Gal⁺ lineage tagged cells visualized around the BADJ on PPE exposure 76

Figure 12: β -Gal⁺ lineage tagged cells arising from the terminal bronchi give rise to AT-I and AT-II epithelial cells post-cigarette smoke induced injury..... 77

Figure 13: Migration of β -Gal⁺ lineage tagged cells from the BADJ into the damaged alveoli in the knock-in mouse model 79

Figure 14: β -Gal⁺ lineage tagged cells emanating from the BADJ into the alveolar space express SP-C 80

Figure 15: Cre expression limited to the airways and not found in the lung parenchyma. 89

Figure 16: Rat CC10 promoter expression is airway specific even on injury. 90

Figure 17: Immunofluorescence for RAGE shows no alteration of expression on cigarette smoke exposure 94

Figure 18: Quantification of RAGE isoforms indicates no alteration in membrane RAGE expression on chronic smoke exposure..... 95

PREFACE

Chapters of this dissertation may contain results, figures and discussion from a manuscript I will be submitting as first author.

Nisha Sambamurthy, Adriana S Leme, Tim D Oury, Steven D Shapiro. The receptor for advanced glycation end products (RAGE) contributes to the pathogenic progression of emphysema in mice. (Pending Publication). 2014

ACKNOWLEDGEMENTS

“It is good to have an end to journey toward; but it is the journey that matters, in the end.”

— Ernest Hemingway

So as I inch closer toward the end of this journey through my PhD, I realize that these past several years have truly been life altering. As much as I have had the opportunity to grow as a scientist and get better at the craft, I have also grown as a person and learnt to appreciate the day-to-day wonders of life. I am grateful to a lot of amazing people who made this journey possible and but more importantly worthwhile.

I have been fortunate to have the distinct pleasure of working with Dr. Steven Shapiro, who perhaps saw a spark in me when I first approached him to pursue a rotation in his lab during the summer of 2008. I am glad he decided to take me under his wing when I asked to join the lab as his graduate trainee and for having been instrumental to my growth as a scientist. In addition to giving me the intellectual freedom to direct my own projects, he has encouraged me to present my ideas at conferences and supported my training in areas that didn't always fit into the expertise of the lab. I admire his ever-positive attitude and how he keeps going strong even with a jam-packed day. Thank you Steve for your guidance, support and mentorship! I hope I can make you proud someday.

My thesis advisory committee has been extremely critical to my scientific growth, their direction and willingness to extend collaborative projects has been key to steering me through

my PhD especially at times when I felt lost. Dr.Oury, thank you for being an excellent chair, for being approachable, flexible and open to discussing science or just matters of life. Dr.Ray, I am grateful for your critical scientific input in all our discussions, your practical approach to problem solving and for being the backbone of my committee. Dr. Kaminski, I appreciate your willingness to collaborate on ideas and for staying with me even after moving to Yale. Dr. Wenzel, thank you for being that calm force that keeps our discussions centered and for encouraging me at times when all I had to show was negative data. Each of you has been vital to my development to this point, your wisdom, experience, criticism and focus has helped hone skills that I hope will carry me through life.

I am extremely grateful to Dr. Majd Mouded, who was like a big brother to me when I first stepped into the lab and will continue to remain so. During my initial rotation at the lab and later when I joined the lab, Majd, Eduardo and I had a great team dynamic. Dr. Eduardo Egea was a great teacher, who initially trained me on a lot of the techniques he had mastered and a great team partner. Most of all, Majd and Eduardo made going to lab fun, exciting and one I would look forward to. Majd always made himself available to discuss ideas, troubleshoot experiments and provided hands-on training at critical scientific reasoning especially at the time I was preparing for my qualifying exam. I am indebted to Majd for his mentorship; he exemplified a morally grounded, frank, straightforward and self-assured individual who I hope to emulate. A lot of the initial groundwork with the transgenic mice and techniques used in investigating the distal bronchial epithelial cell population discussed in Chapter 3.0 of my thesis is credited to both Eduardo and Majd, without whose significant contributions I would not have had the tools to explore further.

I have had the good fortune of associating and working with a lot of good people during my time in Dr. Shapiro's laboratory, some who have seen me from the start of my journey, some who shared parts of this journey and some who are sharing these last few years of my journey. Dr. Adriana Leme, I am grateful for your technical input especially with the RAGE project, your willingness to share your expertise these past several years and for being a well-wisher. I have enjoyed our many discussions on work life balance, thank you for lending me a patient ear and empathizing especially during the rough times. Dr. Alyssa Gregory, thank you for helping with troubleshooting experiments, for sharing your experience through graduate training and for helping with techniques to test ideas. Thank you Dr. Murat Kaynar for being a well-wisher and my constant bay partner over these years. I would also like to thank Christine Burton for taking good care, breeding and genotyping mice used in this study. Further, I greatly appreciate the friendly learning environment created by both past and present members of the Shapiro laboratory: Dr. Clint Robbins, Dr. Naoto Minematsu, Dr. Anna Perry, Dr. Nadine Dandachi, Dan Frederick, Dr. Takao Tsuji, Dr. Saeko Takahashi, Robin Chambers, Dr. McGarry Houghton, Dr. Annerose Berndt, Clint Cario, Brittany Agostini, Heather Metz, Dr. Lin Zhu, Laura Williams, Egemen Tutuncuoglu, Neil Kelly, John Paul, Dr. Veli Bakalov and Josiah Radder. Thank you Andrew Metz for taking care of smoking all the mice for my experiments especially with the acute smoke exposure experiments and Stephen Scott for helping with this in the past year.

Outside the Shapiro lab, I have had the good fortune to collaborate, learn techniques and exchange ideas with Dr.Pavle Milutinovic and Beth Oczypok from Dr.Oury's laboratory, Dr.Nandini Krishnamoorthy and Mahesh Raundhal from Dr.Ray's laboratory and Dr.Kusum Pandit, Dr.Jadranka Milosevic and Dr.John Tedrow from Dr.Kaminski's laboratory during his time at the University of Pittsburgh. In particular, I would like to thank Dr. Shanmugam

Nagarajan for his support and generously sharing his insights. Thank you, Kimberly Fuhrer at the *in situ* laboratory, who has been incredibly accommodating of my last minute requests to process samples and rushing my slides all along the way. I would like to thank all the personal assistants, especially Mrs. Paula Nave and Mrs. Mary Williams for finding a way to make room for me on some very busy calendars. All the graduate school administrators have been extremely helpful and made it easy to stay on top of my paper work through this process, I specially thank Mrs. Cindy Duffy, Mrs. Shari Tipton, Mrs. Carol Williams, Ms. Jennifer Walker and Ms. Clare Gauss.

These years in graduate school would certainly be incomplete without the strong support system I have had in the form of my friends and fellow graduates: Sriram, Ashwini and Hetu, Pradeep, Bharat, Vani, Varsha and Rk, Jhun, Saketh, Tarun, Reety, John, K'Ann and Madhav, Uday, Anindya, Vineet, Katy, Arvind and Sharanya, Prerna, Kristia, Azime and Matt, Martha and Bob, Tatiana, Vidya, Anne, Jyoti and Navin, Prashanth and Shruti. Thank you all for sharing in numerous experiences at varying points in time that I will always cherish and for making me feel at home in Pittsburgh. I am extremely grateful to Beloo aunty, Navin uncle and Nenoo aunty, for being my extended US family and taking special care of me.

Words fall short as I describe how grateful I feel for my family back in India, their strength, support, unconditional love and blessings is why I find myself where I am today. I am forever indebted to my mom and dad who have instilled in me a sense of responsibility, compassion and a strong value system. I am truly fortunate to have been born to them and for the countless struggles and sacrifices they made to give my sister and me a chance to dream bigger. I am forever grateful to my sister Neeraja and my grandparents for their unflinching faith in me. Finally, I am thankful for having had the chance through graduate school to meet my husband Balaji. He truly has been my better half through these past several years, my best critic and my

patient friend. He has celebrated in my successes and encouraged me never to give up especially when times got hard. In marrying him I have been adopted by his loving family for which I feel glad.

“We cannot do great things on this earth, only small things with great love”

-Mother Teresa

NOMENCLATURE

A1AT	α 1 anti-trypsin	ECM	extracellular matrix
A549	human lung adenocarcinoma cell line	EGF	epithelial growth factor
AQP-5	aquaporin 5	Egr-1	early growth response gene-1
AT-I	alveolar type-I epithelial cell	ESC	embryonic stem cell
AT-II	alveolar type-II epithelial cell	FACS	fluorescence activated cell sorting
ATRA	all trans retinoic acid	FEV1	forced expiratory volume 1
BADJ	bronchoalveolar duct junction	FGF/FGFR	fibroblast growth factor/ fibroblast growth factor receptor
BALF	bronchoalveolar lavage fluid	FM	fluorescence microscopy
BAPN	lathyrogen β -aminopropionile	FVC	forced vital capacity
BASC	bronchoalveolar stem cell	G	tissue damping
BCA	bicinchoninic acid assay	G-CSF	granulocyte colony stimulating factor
β -Gal	beta-galactosidase	GAG	glucosaminoglycan
BMDMSC	bone marrow derived mesenchymal stem cells	GAPDH	glyceraldehyde 3-phosphate dehydrogenase
BSA	bovine serum albumin	GWA	genome wide association
C	dynamic compliance	H	tissue elastance
c-Myc	cellular homolog of myelocytomatosis viral oncogene v-Myc	HDAC	histone deacetylases
cAMP	cyclic adenosine monophosphate	HEK293	human kidney cell line
CC10	clara cell secretory protein 10 or CCSP or Scgb1a1	HGF	hepatocyte growth factor
CD	cluster of differentiation	HMGB1	high mobility group box 1
CHAPS	3-[(3-Cholamidopropyl)dimethylammonio]-1-propanesulfonate	HRP	horseradish peroxidase
CL	chord length or mean linear intercept	HSC	hematopoietic stem cell
CM	confocal microscopy	ICAM-1	intercellular adhesion molecule-1
COPD	chronic obstructive pulmonary disease	IFN	interferon
Cre	cre recombinase	IL	interleukin
CSE	cigarette smoke extract	iPSC	induced pluripotent stem cell
CT	computed tomography	IT	intratracheal
DAPI	4', 6-diamidino-2-phenylindole	Klf4	kruppel-like factor 4
DBPC	distal bronchial progenitor cells	LacZ	lac operon Z encodes β -galactosidase enzyme
DLCO	diffusing capacity of the lung for carbon monoxide	LCN2	lipocalin-2
E	dynamic elastance	LPS	lipopolysaccharide

LVRS	lung volume reduction surgery	RAR	retinoic acid receptor
m-RAGE	membrane RAGE	RAW246.7	murine macrophage-like cell line
MAPK	mitogen activated protein kinase	RBC	red blood cell
MCP-1	monocyte chemotactic protein-1	Rn	airway resistance
MMP	matrix metalloproteinase	ROSA26	ROSA β geo26
NADPH	nicotinamide adenine dinucleotide phosphate	s-RAGE	soluble RAGE
NBF	neutral buffered formalin	Sca1	stem cell antigen-1
NE	neutrophil elastase	SDS	sodium dodecyl sulfate
NF- κ B	nuclear factor kappa-light chain-enhancer of activated B cells	SNP	single nucleotide polymorphism
Oct3/4	octamer-binding transcription factor 3/4	SOD	superoxide dismutase
PAGE	polyacrylamide gel electrophoresis	Sox2	(sex-determining region Y)-box2
PBS	phosphate buffered saline	SP-A/B/C/D	surfactant protein A/B/C/D
PDE4	phosphodiesterase-4	SV40	simian virus 40
PDGF	platelet derived growth factor	TGF	transforming growth factor
PECAM	platelet endothelial cell adhesion molecule	TIMP	tissue inhibitor of matrix metalloproteinase
PN	post natal	TLR	toll like receptor
PPE	porcine pancreatic elastase	TNF	tumor necrosis factor
PVDF	polyvinylidene fluoride	Tsk	tight skin mice
R	dynamic resistance	TTF-1	thyroid transcription factor-1
R3/1	rat alveolar type-I cell line	VEGFR-2	vascular endothelial cell growth factor receptor 2
RAGE	receptor for advanced glycation end products	Wnt	wingless-related integration site
RAGE ^{-/-}	RAGE deficient mouse on a C57BL/6J background	X-gal	5-bromo 4-chloro 3-indolyl β -D-galactopyranoside
RAGE ^{+/+}	wildtype mouse on a C57BL/6J background	X-RAGE	an isoform of RAGE, membrane bound and possibly N-glycosylated

1.0 CHRONIC OBSTRUCTIVE PULMONARY DISEASE (COPD)

Chronic obstructive pulmonary disease (COPD) is estimated to affect greater than 24 million individuals across the United States of America [1]. It has been formally defined by the Global Initiative of Chronic Obstructive Lung Disease (GOLD) as “ a common preventable and treatable disease, characterized by persistent airflow limitation that is usually progressive and associated with an enhanced chronic inflammatory response in the airways and the lung in response to noxious particles and gases” [2]. Irreversible airflow limitation is a common byproduct of this disease, which comes in varying degrees of contribution from small airways disease (obstructed bronchi) and extensive destruction of the alveolar parenchyma (emphysema).

1.1 BURDEN OF COPD

COPD is largely a preventable disease, however it still remains a major cause of morbidity and mortality throughout the world. The Global burden of disease predicts that COPD will become the third leading cause of death globally by 2020 and newer estimates predict that it will be the fourth leading cause by 2030 [3]. Other co-morbid chronic conditions such as musculoskeletal diseases, metabolic diseases, cardiovascular diseases, hematological diseases, gastro-intestinal diseases to name a few increase the morbidity observed in COPD patients and make treatment more difficult [4]. Being the third leading cause of death in the United States, COPD presents a

significant economic and social burden to the country at large. Although the estimates are far from being exact due to various limitations in data availability, population sizes etc. they do serve as an indicator of rising costs to the national healthcare sector. The major contributor to these costs comes from hospitalization and related outpatient services [5].

1.2 RISK FACTORS CONTRIBUTING TO COPD

1.2.1 Cigarette smoking and genetic factors

Perhaps the most predominant factor leading to the development of COPD comes in the form of cigarette smoke exposure [6]. However, ~10 % present with COPD in absence of cigarette smoke exposure. The interaction of cigarette smoke and other environmental exposures and the genetic make up of an individual largely determine their susceptibility to developing the disease. One of the best and well-characterized examples of this comes from COPD patients deficient for a serine protease inhibitor α_1 anti-trypsin (A1AT), which is usually ~1 to 3 % of all cases. Low levels of A1AT in combination with exposure to cigarette smoke or toxic fumes can elevate the development of emphysema [7], although some A1AT patients can develop emphysema without smoking.

Matrix metalloproteinase12 (MMP-12), also known as macrophage elastase produced by macrophages have been described to play a vital pro-inflammatory role in the distal lung in response to cigarette smoke induced emphysema [8, 9]. An investigation of single nucleotide polymorphisms (SNP) in this gene as a function of forced expiratory volume in 1 second (FEV₁) in approximately 8300 subjects, led to the discovery of a significant association between the

minor allele of SNP rs2276109 in the MMP-12 gene and a decreased risk of smoke induced COPD [10].

1.2.2 Age and gender

Age has been attributed to be a factor to consider in the development of COPD [7]. However, it remains unclear if age by itself contributes to the development of this disease or if it is a manifestation of cumulative exposures through the course of one's life that manifest as the disease in one's later years in addition to diminished endogenous repair processes. Gender, is another factor that has been studied and its contribution as a factor debated. In the past, COPD had been associated to have a higher prevalence in men compared to women owing to greater exposure to cigarette smoke or occupational fumes [11, 12]. However, more recent studies indicate that women are more susceptible to the damaging effects of cigarette smoke in comparison to their male counterparts [13].

1.2.3 Occupational exposure, outdoor and indoor air pollutants

Occupational exposure to noxious dusts, fumes or vapors probably does not initiate but contributes to COPD. An analysis involving over 10,000 subjects showed almost 19.2% of the COPD cases were exposed to work-related exposures [14]. The occupations that were reported to have the highest odds includes freight, stock, material handlers, record processing and distribution clerks, vehicle mechanics and the armed forces [14]. The risks of occupational exposures leading to COPD in less regulated, lower income countries are greater than in better-regulated, high-income countries. Further, indoors exposure to burning of biomass fuel (wood,

cow dung, coal, crop residues etc.) to cook and heat without sufficient ventilation pose a major risk of acquiring COPD especially in developing countries [15, 16]. Outdoor air pollutants mainly vehicular and industrial air pollution poses a lower risk to the development of COPD in comparison to indoor pollutants. About 2% of the COPD cases may arise from outdoor pollution in middle to lower income countries and less than 1% in developed countries [7]. Other risk factors include exposures and respiratory infections during early childhood and adolescence when the lungs are developing which can pre-dispose these individuals to developing COPD later in life due to limited functional reserve. Additionally, socio-economic status can influence exposures to cigarettes, indoor/outdoor pollutants, nutrition and incidence of infections.

1.3 COPD- PATHOPHYSIOLOGY

COPD manifests through a variety of abnormalities throughout the respiratory tract including chronic bronchitis in the upper airways, small airway obstruction and emphysema in the alveolar compartment of the lung. Small airway obstruction and emphysema are characterized by significant airflow limitation. In the airways there is narrowing of the airway lumen due to mucus hyper-secretion, abnormal inflammatory response and fibrosis. In the alveolar space breakdown of extracellular matrix particularly the elastic cable network by excessive proteolytic activity leads to reduced elastic recoil manifesting as reduced airflow. Airflow limitation is typically progressive and distinguished by an abnormal and chronic inflammatory response to inhaled noxious gases or particulate matter (including industrial and environmental pollutants), in the case of COPD it is mostly due to long-term exposure to cigarette smoke. The common

symptoms of this disease include shortness of breath (lack of sufficient gas exchange) and persistent cough with phlegm (increased mucus production).

Bronchitis is the inflammation of the cells lining the upper airways and bronchi. Acute bronchitis characterized by coughing may accompany a cold and typically clears within a span of 2 weeks. Chronic bronchitis, on the other hand is accompanied by prolonged coughing with sputum production for almost a month, 3 months of a year, over two consecutive years. Chronic bronchitis is commonly characterized by excessive mucus production leading to narrowing of airway lumen and inflammatory cell infiltration of the bronchial epithelium. Mucus producing goblet cells lining the airways proliferate (hyperplasia) and increase their production of mucus (hypertrophy) contributing to this phenotype.

Emphysema is characterized by the permanent destruction and enlargement of alveoli. It may or may not manifest clinically in isolation of chronic bronchitis. This component of COPD is thought to manifest from noxious gas exposure inducing cellular oxidative stress, loss of alveolar epithelium (by apoptosis or necrosis) and proteolysis of the extracellular matrix (ECM) functioning as a scaffold for the alveolar epithelial cells to adhere. Airflow limitation that in emphysema may occur through loss of alveolar ECM leading to the collapse of the alveolar structure and subsequent to this loss of the alveolar unit leading to collapse of the distal bronchi further constricting their lumen contributing to insufficient airflow.

1.3.1 Pathogenic mechanisms in Emphysema

The pathologic enlargement and inflammation of the alveolar compartment of the lung characterize emphysema. Our understanding of mechanisms that serve as triggers instrumenting

such damage and destruction of the lung parenchyma is a work in progress. Exposure to cigarette smoke is critical. Other environmental factors may contribute as well including respiratory infections. Genetic factors are also important and several have been identified since the identification of alpha-1-antitrypsin over 50 years ago. Some genes that have been suggested to be associated with the disease from multiple genome wide associated studies, include interleukin-6 receptor (IL-6R), hedgehog interacting protein (HHIP), family with sequence similarity 13 member A1 (FAM13A), iron-responsive element binding protein (IREB2) and a nicotinic acetylcholine receptor (CHRNA 3/5) locus to name a few [17]. Currently, established mechanisms propose an imbalance of protease-anti-protease levels, oxidant induced injury, increased inflammation, inhibition of histone de-acetylases and alveolar wall cell apoptosis. Genetically mutated/targeted mice applied to cigarette smoke exposure have served and continue to serve as good models to study relative contributions of different genes and exogenous agents towards lung alveologenesis and emphysematous destruction of the alveolar compartment.

1.3.1.1 Protease- anti-protease imbalance

The protease-anti-protease hypothesis has been the main proposed mechanism of emphysema for over half a century now. A delicate balance between proteases that breakdown connective tissue and anti-proteases that protect from this destruction; closely dictate lung maintenance [18]. The first example of this came from work by Laurell and Eriksson who found that patients deficient for α_1 anti-trypsin (A1AT) were at an increased risk of early development of emphysema [19]. A1AT, a protein made by the liver, inhibits neutrophil-derived neutrophil elastase in the lung, the absence of which allows for uncontrolled elastin degradation leading to emphysema. Gene mutations in A1AT can lead to the production of abnormal protein that is unable to leave the liver and enter circulation [20]. Further, clinical studies have shown an increased prevalence of

COPD in patients with chronic liver disease [21]. Several other proteases have later been implicated in connective tissue damage using animal models of emphysema (discussed later). Elastin seems to be the critical target of proteases, the loss of which can lead to loss of elastic recoil important to alveolar function. In addition to degrading elastin/connective tissue components, proteases produce elastin fragments that displayed chemotactic potential serving in a positive feedback loop to recruit more inflammatory cells (mainly macrophages and neutrophils) to propagate alveolar destruction [8, 22, 23].

1.3.1.2 Inflammation

Study of bronchial biopsies from smokers with mild-moderate COPD indicated elevated inflammation in their lungs [24]. Both the innate and adaptive immune systems have been shown to be active in emphysema. The recruitment of inflammatory cells to the lung environment leads to release of proteases and cytokines that mediate alveolar destruction and aberrant lung remodeling. The most dramatic of which are the macrophages that comprise the vast majority of inflammatory cells in the lung parenchyma and show a 5-10 fold increase in recruitment to the lung on chronic cigarette smoke exposure [25]. Morphometric analysis of macrophages in the tissue and alveolar spaces of patients with emphysema indicated a 25-fold increase in macrophage numbers when compared to normal smokers [26]. Macrophages once activated by cigarette smoke can secrete elastolytic matrix metalloproteinases (MMPs) like MMP-9 and MMP-12 (macrophage elastase). Neutrophil elastase may also be found in macrophages once they are taken up from apoptotic neutrophils [27, 28]. Further activated macrophages secrete other nuclear factor κ B (NF- κ B) transcription regulated cytokines like tumor necrosis factor α (TNF- α), interleukin-8 (IL-8), monocyte chemotactic protein-1 (MCP-1), leukotriene B₄ and various CXC chemokines that serve to attract neutrophils and lymphocytes into the lung [29, 30].

Cigarette smoke has been shown to increase the circulating levels of neutrophils and reduce the deforming capacity of these cells thereby sequestering them in the circulating capillaries [31]. Neutrophils have the potential to secrete neutrophil elastase, proteinase 3, cathepsin G and MMPs 8 as well as 9 capable of destroying connective tissue leading to emphysema [32, 33].

Several studies have observed an increase in T lymphocytes in the lung parenchyma and airways of smokers, with a higher increase in CD8+ T cells in comparison to CD4+ T cells [26, 34-36]. This observation was mirrored in mice using cigarette smoke induced emphysema that showed a predominance of T cells which had a direct correlation with the extent of emphysema [37]. Specifically, CD8+ cells have been shown to be capable of mediating cytolysis and apoptosis of alveolar epithelial cells through the release of perforins, TNF- α and granzyme-B [38].

Imbalances in levels of histone acetylases and deacetylases (HDACs) have been ascribed to chromatin remodeling resulting in pro-inflammatory gene expression therefore enhancing inflammation in the lung. Macrophages isolated from the lungs of cigarette smokers as well as animals exposed to cigarette smoke express reduced levels of HDAC [39, 40]. Reduced levels of HDAC result in the unwinding of the chromatin, allowing access to transcription factors to transcribed inflammatory genes. Conclusive evidence is yet to be gathered to confirm this proposed mechanism.

1.3.1.3 Oxidative stress

Cigarette smoke comprises of a complex mix of chemicals, free radicals and reactive oxidants. The equilibrium between extracellular and intracellular anti-oxidants that fight the toxic insult from noxious gases or vapors is essential to normal lung function. It is when this

equilibrium is disturbed oxidative stress occurs. Human leukocytes isolated from smokers have been described to release increased numbers of oxidants as compared to non-smokers [41]. This finding showcased increased oxidative stress in the lungs of smokers caused by the progressive accumulation of macrophages and neutrophils in the alveolar space. Free radicals generated by oxidative stress can attack polyunsaturated fatty acids on the cell membrane causing lipid peroxidation. This leads to the generation of hydrogen peroxides and long-lived aldehydes that perpetuate the damage. Further support for this finding comes from analysis of plasma and BALF from healthy smokers and COPD patients with acute exacerbations who had elevated levels of lipid peroxidation products and compared to healthy non-smokers [42-44].

Cigarette smoke-induced oxidant damage has been shown to partially damage elastin and collagen promoting damage by elastases and collagenases respectively [45]. Further, cigarette smoke has been shown to interfere with elastin synthesis and repair of damaged elastin leading to emphysematous changes [46]. Oxidants (like reactive oxygen species) have been known to potentiate proteolytic activity in COPD by the activation of these protease precursors [47]. Further direct oxidation of methionine residues in the active site of A1AT have been shown to inhibit this enzyme's activity and though to contribute to the imbalance [48, 49]. Anti-oxidant enzymes characterized in the lungs of normal healthy individuals include superoxide dismutase (SOD), catalases and glutathione system [50]. Although studies have shown elevated glutathione levels in the BALF of chronic smokers [51], subsequent investigations have indicated that cigarette smoke depleted glutathione in a dose-dependent manner implying insufficient levels to counter-act oxidative damage under acute smoke exposures [42]. Thus, the abnormal alveolar enlargement may result from oxidative stress (constituting cigarette smoke) on epithelial cells,

resulting in perpetuation by inflammatory cells in the airspaces in parallel with impaired cellular repair (anti-oxidant enzymes).

1.3.1.4 Loss of alveolar structure and apoptosis

Surfactants are thought to contribute towards alveolar structure and integrity. Studies conducted blocking neutral lipid metabolism in lysosomal acid lipase knockout mice developed emphysema, had elevated levels of neutrophils and macrophages, increased expression of pro-inflammatory cytokines and MMPs [52]. Further the mice lacking surfactant protein A, C and D showed emphysema and inflammation-related alterations in their lungs [53]. Additionally, clinical studies have indicated that elevated serum levels of SP-D may act as a biomarker for patients with stable COPD as compared to their healthy controls [54, 55]. The alveolar space and the cells lining it share a certain degree of plasticity allowing for them to adjust on a continuous basis, disruption of this balance can lead to emphysematous changes.

Alveolar cell apoptosis and loss of alveolar structural equilibrium (matrix loss) had been thought to be instrumental to the development of emphysema [56]. Contrary to these findings, epithelial cell apoptosis induced by intra-tracheal microcystine (apoptosis inducer) in mice showed changes in lung morphology that were similar to mild acute lung injury camouflaged as emphysema; different from alveolar changes in mice that received porcine pancreatic elastase (PPE) [57]. Apoptosis of epithelial cells may not be the initiating event leading to emphysema, but rather a downstream event of other triggers that are yet to be uncovered.

1.4 COPD-ASTHMA OVERLAP

COPD shares features that are common with asthma, namely both are inflammatory diseases that affect the small airways, characterized by bronchial hyper-responsiveness and bronchoconstriction due to increased mucus production leading to air-flow limitation. At the same time they also are distinctly different; in that COPD affects both the airways as well as the alveoli, while asthma exclusively affects the airways. Besides both being chronic inflammatory diseases, the nature of inflammation observed is quite different [58]. In COPD, the inflammatory response is mostly characterized by macrophages, neutrophils, and cytotoxic CD-8⁺ T-lymphocytes [35, 59]. In contrast, the inflammatory response in asthma is mainly eosinophil and CD4 T-lymphocyte driven. There is clinical data to indicate that the nature of inflammation dictates the response to treatment by pharmaceutical drugs. Corticosteroids have been shown to be more efficacious in treating eosinophilic asthma as compared to the more neutrophilic COPD [60, 61]. Clinically asthma and COPD do co-exist in some cases, which make its diagnosis challenging especially in older patients and its treatment complicated [62].

1.5 COPD-DIAGNOSIS AND ASSESSMENT

A patient who presents with symptoms that include shortness of breath and chronic cough with sputum and has prior exposure to any of the risk factors discussed in the earlier section is to be diagnosed for COPD [2]. In addition, the complete medical history of the patient needs to be assessed in conjunction with their diagnosis to tailor treatment to the patient's needs.

Spirometry provides a reproducible and objective measure of airflow limitation. It is used to measure the maximum amount of air exhaled after a maximal inspiration (forced vital capacity, FVC) and the volume of air exhaled with the first second of this expiration (forced expiratory volume-1, FEV₁). The ratio of these two parameters (FEV₁/FVC) collected from the spirometric assessment is then calculated and evaluated in comparison to a reference table additionally accounting for age, gender, height, weight etc [63]. Further, a FEV₁/FVC ratio < 0.7 on bronchodilation is used to confirm airway constriction and make a definitive diagnosis of COPD [2].

Since COPD is often a progressive disease occurring over a prolonged span in time; it does have systemic effects such as weight loss, musculoskeletal dysfunction and nutritional abnormalities [64]. Several studies highlight an increased risk in patients with COPD of developing other chronic diseases; this is particularly striking in the case of COPD and lung cancer. The precise reason for this association is not completely understood, but may be related to the lack of effective clearance of carcinogens or presence of common susceptibility genes or similar sensitivity to environmental risk factors [65-68].

Additional analysis may involve imaging through X-Ray or a computed tomography (CT) scan of the chest. A1AT genetic screening may also be performed if the patient presents with emphysema in the lower lobes or has a familial history. Body plethysmography is used to measure lung volumes and the diffusing capacity (DL_{CO}) to determine the functional capacity of the lungs as a result of emphysema. In determining the need for additional oxygenation, the patient's oxygen saturation is tested by pulse oximetry. Assessing exercise capacity through a walk test may also indicate the level of physical disability or improvement in physiological function as an effect of clinical rehabilitation [2].

1.6 COPD-TREATMENT

Smoking cessation is clearly the best way to prevent COPD and blunt the natural progression of COPD. This may involve the adoption of nicotine replacement strategies such as nicotine patches, gum or spray, which have all shown to significantly aid in abstinence from smoking [69-71]. Recent myocardial infarction or stroke, unstable coronary artery disease or untreated peptic ulcer diseases may be reasons to withhold treatment by nicotine replacement [72]. Weight loss and nutritional deficiencies are common manifestations in patients with advanced COPD; hence their diet needs to be a balanced one with sufficient caloric intake accompanied by exercise to prevent muscle atrophy and insufficient nutrition [2].

Pharmacologic treatment options for COPD used in isolation or combination include bronchodilators like Beta₂ (β_2) agonists, anti-cholinergics as well as inhaled corticosteroids and phosphodiesterase-4 (PDE-4) inhibitors. Bronchodilators enable the opening up of constricted airways by modulating airway smooth muscle tone, in doing so they help improve lung function (increase FEV₁) and the emptying of the lungs. The most important of these are β_2 -agonists, which act on β_2 adrenergic receptors present on airway smooth muscle cells causing the release of cyclic adenine mono-phosphate (c-AMP) which counter-acts broncho-constriction. Ipratropium, oxitropium and tiotropium bromide (long-acting) are commonly used anti-cholinergics that aid in blocking the binding and further activation by acetocholeline on muscarinic receptors, which impact the underlying airway tone. Inhaled short-acting anti-cholinergics provide longer bronchodialatory effect in comparison to short-acting β_2 -agonists, evident up to 8 hours from the time of administration [73]. Anti-Cholinergics may act to reduce mucus hypersecretion, however β_2 -agonists and mucolytics may have no contribution [74]. Inhaled corticosteroids are used to treat inflammation, however their efficacy in COPD as opposed to

asthma in terms of countering pulmonary and systemic inflammation is debated. Further the long-term effects and safety of using inhaled corticosteroids is still to be determined. Roflumilast, a PDE-4 inhibitor (anti-inflammatory) recently approved for COPD; has been shown to reduce moderate to severe exacerbations in 15-20% of patients with severe to very severe COPD who received this in combination with an inhaled corticosteroid [75].

Supplementary pharmacologic treatments may include A1AT augmentation therapy for patients deficient in A1AT (rare and expensive), antibiotic treatment[76], vasodialators [77], mucolytic agents [78], anti-oxidant agents, vaccines [79] and immunoregulators [80].

COPD patients with chronic respiratory failure and low resting levels of oxygen (hypoxemia) showed significantly improved survival rates with long term oxygen therapy [81]. Non-invasive ventilation is increasingly used to treat stable very severe COPD. Long term oxygen therapy implemented in combination with external ventilation has been used in patients who present with daytime hypercarbia (increased levels of circulating carbon-dioxide) leading to better survival with no improvement to quality of life [82].

Severe COPD patients with upper lobe emphysema and low exercise capacity make suitable candidates for lung volume resection surgery (LVRS); which involves removal of portions of the lung (pneumectomy) to reduce increased inflation from loss of alveolar units of the lung [83]. The procedure is thought to improve the mechanical efficiency of respiratory muscles by enabling them to better generate pressure. Further exacerbations are reduced through improved elastic recoil following surgery that in turn improves the expiratory flow of air [84]. A major limitation of LVRS remains that it has high mortality than medical management of severe COPD [85]. Lung transplantation on the other hand has led to regaining better functional capacity and quality of life. One of the major challenges has been availability of matched donor

organs and associated costs. COPD patients who undergo lung transplants are often faced with issues such as immune rejection, infections (fungal, viral or bacterial) and lymphoproliferative diseases [86].

Most treatment strategies currently used in the clinical realm cater to treating the symptoms associated with COPD; these provide temporary relief and delay mortality at best. While attempts continue to be made to understand the underlying cause of this complex disease, we are still far from finding a cure for it.

1.7 ANIMAL MODELS OF EMPHYSEMA

A number of different animals have been used to study emphysema over the years including monkeys, sheep, dogs, guinea pigs and rodents. However, in more recent times mice have proven to be the best model to study this disease given our elaborate understanding of their genome, relative ease of genetic manipulation, short breeding times with large litters and availability of probes/antibodies allowing for greater investigation [87]. The extent to which mice or other animal models do and do not replicate human physiological and pathologic processes must be kept in mind while trying to extrapolate findings in animal models to corresponding processes in humans. The use of exogenous agents such as proteases, oxidants, particulates, inhibitors and cigarette smoke have been used to model characteristic features of human emphysema. In addition, naturally occurring and genetically engineered mutants that result in airspace enlargement enable for better understanding of the roles of genes especially during lung development and even later in life.

1.7.1 Protease and chemical injury models

Protease injury models date back to the studies performed by Gross, who instilled papain in rats and described emphysematous alterations in their lungs 50 years ago [88]. Intra-tracheal instillation of porcine pancreatic elastase (PPE) led to an initial loss in elastin and collagen in the lung. PPE exposure resulted in permanent loss of the alveolar extracellular matrix (ECM) thereby distorting the lung architecture. Although elastin and glucosaminoglycan (GAG) levels were restored later in the model; collagen levels remained enhanced. On close investigation of the elastin fiber assembly it was noted to have an abnormal morphology, similar to that seen in patients with emphysema [89]. Intra-tracheal PPE lead to an initial breakdown of elastin, which was followed by an endogenous inflammatory response leading to progressive damage observed. Studies performed using lathyrogen β -aminopropionile (BAPN), which inhibited cross-linking of elastin and collagen fibers resulted in worse emphysema implying the presence of attempts at endogenous repair [90]. Proteases such as PPE, neutrophil elastase, papain, proteinase-3 has been shown to contribute to panlobular emphysema and are useful to study the downstream effects of protease injury [91]. Human emphysema on the other hand develops as a result of prolonged exposures to cigarette smoke and hence the short-term protease-model may not mirror a homologous progression of the disease. The PPE model initially was thought to be limited to the study of mediators working downstream of protease injury in the lung, however given that most of the emphysema at 3-4 weeks is due to endogenous inflammation and destruction, it might replicate human disease better than previously thought. It also provides a simple model to perform preliminary analysis of downstream events particularly in the context of alveolar repair [92].

Repeated endotoxin (lipopolysaccharide, LPS) administration was shown to result in airspace enlargement [93]. Nitrogen dioxide and ozone, common oxidants in air predominantly caused lung injury [87]. Cadmium chloride (major constituent of cigarette smoke), coal dust and silica caused varying degrees of alveolar injury or fibrosis. Vascular endothelial cell growth factor receptor – 2 (VEGFR-2) inhibitor, used to model non-inflammatory emphysema; was characterized by airspace enlargement, alveolar epithelial cell apoptosis and loss of pulmonary arterial branching [94, 95]. Several other chemical agents have been utilized in the study of emphysema yet none have been able to reflect the damage induced by chronic cigarette smoke exposure in its entirety.

1.7.2 Cigarette smoke model

The cigarette smoke model involves the delivery of smoke from burning cigarettes into a chamber with controlled airflow dynamics. The first successful description of this model was in 1990; guinea pigs were exposed to 10 cigarettes a day, 5 days a week, over 1,3,6 and 12 months and shown to develop emphysematous changes in their lungs and displayed similar lung dynamics on pulmonary function testing as found in humans [96]. Prolonged exposure to cigarette smoke led to neutrophilia, progressive accumulation of macrophages and CD4+ T-lymphocytes. Halting cigarette smoke exposure failed to reverse the airspace enlargement observed [97].

Murine models of cigarette smoke exposure involved the use of previously described smoking chambers [98]. Mice can breathe only through their noses, their tracheas are mildly populated by ciliated epithelial cells thereby not enabling for much filtering of air inhaled. However, mice are able to tolerate 2 cigarettes at a time at least twice a day without their

carboxyhaemoglobin levels reaching toxic levels for over several months and develop a phenotype with similarities to that seen in human COPD. The airways in mice are sparsely populated by mucus producing cells, which are mostly if not always found in the trachea. Their airways are composed of ciliated epithelial cells and Clara cells, nevertheless they lack goblet cells. Mouse airways display much less branching than human airways and they further lack respiratory bronchioles. C57BL/6 and A/J strains of mice have extensive ciliated cells lining their airways with an increased density in the proximal regions. Long-term (~2 months) cigarette smoke exposure does not affect the numbers of clara cells, on the contrary it causes a loss in ciliated epithelial cells lining the airways and accumulation of inflammatory cells [92]. Neutrophils are the first to arrive in the lung from the very first cigarette followed subsequently by macrophages and T-lymphocytes. The early neutrophil recruitment is accompanied by significant breakdown of lung elastin and collagen. Antibodies against polymorphonuclear leukocytes and intraperitoneal administration exogenous A1AT have been shown to block this early neutrophil recruitment and elastin breakdown [99]. Mouse alveoli show increased inflammatory cell recruitment and alveolar enlargement in response to chronic cigarette smoke exposure similar to the response seen in humans. The enlargement in alveolar spaces was accompanied by an increase in alveolar duct size by 3-6 months and injury was mainly macrophage-mediated [100]. The extent of alveolar space enlargement seems to be mouse strain-dependent, which in turn allows for future investigation of genes linked to COPD susceptibility.

1.7.3 Naturally occurring airspace enlargement in genetic mutant mice

Several inbred strains of mice have been known to spontaneously develop mutations leading to certain identifiable phenotypes. The airspace enlargement observed in these mice arises from

developmental abnormalities rather than targeted lung destruction. A classic example of this was observed in the case of tight skin (Tsk+/-) mice. The Tsk+/- mice have abnormal alveolar development and progressive airspace enlargement; resulting from a mutation in fibrillin-1 involved in elastin assembly [101]. Other mutant strains previously described to develop enlarged alveoli include pallid mice [102], blotchy mice [103, 104] and beige mice [105].

1.7.4 Gene targeted mice and transgenic mice with airspace enlargement

Advances in mouse genetic engineering have enabled gene-targeted approaches that allow the over-expression a specific gene or deletion of a gene of interest either under an endogenous cell-specific promotor (knock-in or knock-out) or by random insertion in the mouse genome (transgenic). This has facilitated the study of effects of loss or gain of a single gene under regulated experimental conditions thereby elucidating mechanistic aspects of the disease.

Mouse embryonic lung development begins at around embryonic day 9.5, however alveologenesis involving the septation of the alveoli in the distal lung occurs between post-natal days 4 to 14 [106]. Loss of genes involved in laying down elastin fibers or it's cross-linking can contribute significantly to the loss of structural integrity of the lung and impaired alveolar development. Platelet derived growth factor-A (PDGF-A), fibrulin-5, elastin and retinoic acid receptor- γ (RAR γ) knockout mice deficient in elastin production or assembly had impaired alveolar septation [107-110]. A functional deletion of fibroblast growth factor receptor-3 and 4 (FGFR-3 and FGFR-4) important for lung development shows increased collagen deposition with no change in structural elastin and abnormal alveologenesis [111].

Some gene-targeted mice develop spontaneous airspace enlargement with age. Mice carrying a targeted deletion of surfactant protein-D (SP-D) and tissue inhibitor of matrix

metalloproteinase-3 (TIMP-3) start of with normal lungs but develop progressive airspace enlargement as they age. This effect has been linked to matrix metalloproteinases (MMP) and inflammatory responses mediated by loss of these genes [112, 113].

Phenotypes observed in transgenic mouse models of emphysema may not completely reflect the exact features of disease due to the random integration of the transgene into the mouse genome, which could result in certain off-target effects [87]. The over-expression of platelet derived growth factor-B (PDGF-B), Interleukin-11 (IL-11), IL-6 and transforming growth factor- α in the lung were linked with developmental abnormalities [114-116]. Inducible over-expression of IL-13, interferon- γ (IFN- γ) and mice over-expressing human MMP-1 has been observed to develop abnormally enlarged airspaces similar to human disease [117-119].

1.7.5 Cigarette smoke mediated Emphysema in gene-targeted mice

Mouse strains deficient for specific proteases were exposed to long-term cigarette smoke to study the effect of loss of the specific gene towards alveolar maintenance or destruction. Elevated levels of expression of MMP-12 (or macrophage elastase) had been reported on human macrophages isolated from smokers in addition to immunohistochemistry staining on lung tissue from patients with emphysema. MMP-12 deficient mice (MMP-12^{-/-}) were exposed to chronic cigarette smoke over 6 months and found to lack emphysema when compared to their wild-type counterparts [8]. This study inferred that MMP-12 was not only required for alveolar macrophage recruitment but also for alveolar destruction [120]. Neutrophil elastase inhibited by A1AT, when genetically deleted in mice rendered partial protection from long-term cigarette smoke induced emphysema [121]. These studies indicate the importance of elastases and inflammatory cell involved in the lung microenvironment leading to the development and

progression of the disease. Further, mice that were deficient for both tumor necrosis factor- α receptor type-I and II and IL-1 β type-I receptor were protected from intratracheal porcine pancreatic elastase (PPE) exposure [122]. While MMP-9 is augmented in human subjects with emphysema, MMP-9 deficient mice were shown to develop similar inflammation and airspace enlargement on smoke exposure as their wild-type counterparts indicating the action of other compensatory mechanisms [123].

2.0 THE RECEPTOR FOR ADVANCED GLYCATION END PRODUCTS (RAGE) MEDIATED NEUTROPHIL RECRUITMENT DRIVES THE PATHOGENIC PROGRESSION OF EMPHYSEMA

The Receptor for advanced glycation end products (RAGE) acts as a pattern recognition receptor and is highly expressed in the adult lung under normal conditions. Several studies in the recent years have pointed towards its involvement in chronic lung disease. In the current investigation, we aim to define the contribution of RAGE in the pathogenesis of emphysema using a RAGE global knockout (RAGE^{-/-}) strain of mouse. RAGE^{-/-} mice exposed to chronic cigarette smoke demonstrated partial protection from cigarette smoke induced alveolar enlargement when compared to their wild-type (RAGE^{+/+}) counterparts. The RAGE^{-/-} mice exposed to room air showed airspace enlargement at baseline when compared to their room-air exposed wild-type controls, indicating a role for RAGE in alveolar development. Lung physiology measurements displayed a significant decrease in tissue elastance of wild type mice that were exposed to cigarette smoke compared to their room-air exposed controls on bronchoconstriction. Such a change in tissue elastance was not observed in the RAGE^{-/-} smokers when compared to their air-exposed controls. Macrophages and neutrophils have been attributed as the main inflammatory cell types that are recruited to the inflamed lung where they release proteases leading to progressive damage. A significant impairment in recruitment of neutrophils was observed on acute cigarette smoke exposure in RAGE^{-/-} mice as compared to their wild type counterparts.

The results from our study define a role for RAGE in promoting alveolar enlargement on cigarette smoke exposure, through neutrophil recruitment and perhaps increased loss of elastance.

2.1 RAGE- BACKGROUND

2.1.1 RAGE – structure, isoforms, ligands and signaling

The receptor for advanced glycation end products (RAGE) was initially isolated and characterized from bovine endothelium [124]. RAGE, based on computation analysis of its amino-acid structure was found to share homology with the immunoglobulin superfamily [125]. The extracellular domain of RAGE contains one “V” type domain involved in ligand binding and two “C” type domains. Full-length RAGE in addition to the extracellular domain has a transmembrane domain and a cytosolic tail (43 amino acid) involved in intracellular signaling [125].

The other isoform of RAGE, soluble RAGE (sRAGE); lacks the transmembrane and intracellular domains found in full-length RAGE. sRAGE acts as a decoy receptor and binds to ligands that would normally bind full-length membrane bound RAGE, thereby blunting RAGE-ligand mediated downstream signaling. Hence sRAGE has been thought to play a protective role by binding RAGE ligands and preventing their negative interaction with membrane bound RAGE. RAGE binding ligands like HMGB1 and S100A8/A9 complex also bind and signal through the toll-like receptor 4 (TLR4) [126-128]. The soluble form of the receptor (s-RAGE) exerts antagonistic effects by binding these ligands and preventing their signaling through

membrane bound RAGE (m-RAGE) or other receptors like TLR4. Although the mechanisms by which it is produced are not clear, some studies suggest that is produced by proteolytic cleavage of membrane RAGE and some others suggest its directly produced by alternative splicing of RAGE mRNA [129-132].

Several ligands are known to interact with RAGE, such as DNA binding high mobility group box 1 (HMGB1) [133], S100 protein family members [134], advanced glycation end products (AGEs) [135], glycosaminoglycans [136], beta amyloid proteins [137] and extracellular matrix components like collagen I, collagen IV and laminin [138, 139]. Additionally, RAGE has been shown to heterodimerize with β_2 integrin Mac-1 on leukocytes [140]. Ligands that bind RAGE may not specifically bind to and signal only through RAGE, an example being HMGB1 that can also bind to toll-like receptor-2 and 4 (TLR2 and TLR4) [141, 142].

Binding of ligands to extracellular domain of RAGE triggers an intracellular signaling cascade mediated by the cytoplasmic domain. Diaphanous-related formin 1 (mDia1) belonging to the actin and microtubule polymerization family of proteins was shown to bind to the intracellular domain of RAGE and signal through Rac1 and Cdc42 mediating cellular migration pathways [143]. Activation of RAGE by binding of AGE-albumin demonstrated the activation of p21- Ras driven mitogen activated protein kinase (MAPK) signaling cascade, which in turn activates nuclear factor κ B (NF- κ B) that translocates to the nucleus and begins transcription [144]. NF- κ B acts as a master transcriptional regulator and is capable of initiating the transcription of pro-inflammatory factors such as interleukin-6 (IL-6), tumor necrosis factor- α (TNF- α) and interferon- β (IFN- β) [145-148]. NF- κ B has additionally been shown to function in a positive feedback loop and leads to an upregulation in RAGE expression in the presence of

elevated levels of RAGE ligands. While there is overall consensus that RAGE signaling leads to NF κ B nuclear translocation, the sequence of intra-cellular signaling events is poorly understood.

2.1.2 RAGE in the lung

The membrane bound form of RAGE (m-RAGE) is highly expressed in normal adult lung tissue and has been shown to localize to the basolateral membrane of differentiated alveolar type-I epithelial cells [149]. RAGE is also expressed on bronchial smooth muscle cells, vascular endothelial cells, alveolar macrophages & transitioning alveolar type-II epithelial cells in the alveolar parenchyma (F. Katsuoka, 1997; J Bret et al, 1993).

In vitro studies performed utilizing a human embryonic kidney cell line (HEK293) transfected with full length RAGE illustrated the role of RAGE in cell adhesion and spreading on collagen IV matrix [139]. These findings highlighted the contribution of RAGE to epithelial, and perhaps alveolar type-I cell (AT-I) cell adhesion, spreading and facilitating gaseous exchange in the lung. Further, expression of RAGE predominantly on AT-I epithelial cells (M. Shirasawa, 2004) indicates its potential contribution to alveologenesis and the maintenance of normal lung homeostasis.

2.1.3 RAGE and COPD

Deregulated expression of RAGE in lung tissue has been observed in various animal injury models and clinical studies of pulmonary disorders such as fibrosis (L.E. Hanford, 2003; J.M. Englert, 2008; L. Ramsgaard, 2008), non-small cell lung adenocarcinoma [150-155] and acute lung injury [131, 156, 157]. Black and coworkers, showed elevated intensity of staining for

RAGE in the alveolar walls of lung tissue from smokers with COPD [158]. Decreased levels of soluble RAGE, which acts in an antagonistic fashion to RAGE, were detected in the bronchoalveolar lavage fluid (BALF) from the lungs of chronic smokers with COPD [159, 160]. RAGE expression was increased following *in vitro* exposure to cigarette smoke extract in rat (R3/1) cells and human (A549) cells [161]. Further investigation by the same group demonstrated that RAGE expressed by alveolar macrophages stimulated by intra-tracheal delivery of cigarette smoke extract elicited an inflammatory response [162]. Together these studies indicate a potential role for RAGE in the pathogenesis of COPD. However, the direct involvement and contribution of RAGE to the development of emphysema has not been explored thus far.

2.2 RAGE-MATERIALS AND METHODS

2.2.1 RAGE knockout mice

RAGE^{-/-} mice were originally generated from a founder RAGE knockout colony provided by Dr. A. Bierhaus (University of Hiedelberg, Germany) [163]. RAGE^{-/-} mice were backcrossed until 10 generations into the C57BL/6J background. Eight to twelve week old female mice were used in all the experiments designed. Age, sex and background matched wild type (C57BL/6J) mice were obtained from Jackson Laboratories. The animals underwent strict quarantine when transferred between animal facilities within the university. All animal experiments were reviewed and approved by the University of Pittsburgh Institutional Animal Care and Use Committee

2.2.2 Cigarette smoke models

2.2.2.1 Chronic cigarette smoke model

RAGE^{-/-} and wild type mice were exposed to 2 unfiltered cigarettes, 2 times a day, 5 days a week over 6 months using a smoking chamber [96] that had been adapted for use with mice [8]. The controls in each group were exposed to room-air and housed along with their smoke exposed counterparts. This model was characterized by acute neutrophilic inflammation followed by accumulation of macrophages and lymphocytes within days.

2.2.2.2 Acute cigarette smoke model

RAGE^{-/-} and wild type mice were exposed to 2 unfiltered cigarettes. The controls in each group did not receive any cigarette smoke, instead were exposed to room air. This model was used to study neutrophil recruitment, which peaks generally around 4 hours post-exposure.

2.2.3 Respiratory mechanics measurements

We measured airway resistance (R_n), tissue damping (G), tissue elastance (H), dynamic resistance (R), dynamic elastance (E) and dynamic compliance (C) in response to methacholine challenge (Sigma, St. Louis, MO) using a computer-operated ventilator (Flexivent, Scireq, Montreal, QC). The mice were anesthetized intraperitoneal with pentobarbital sodium (60mg/kg), a tracheotomy was performed and the animal attached to a mechanical ventilator. Each animal was given deep lung inflation to open out the airways and baseline pressure-volume-flow measurements were captured. The animal was further exposed to phosphate buffered saline (1x

PBS) followed by increasing concentrations of methacholine (1, 3, 10 & 30mg/ml) through a nebulizer for 10 seconds and their responses were recorded.

The responses recorded using a forced oscillation technique were then fitted to a constant phase model to compute the various parameters. We then plotted these parameters as a function of the log transformed concentrations of methacholine to analyze the dose-response. The slopes of the curves generated indicate differences in overall responses between strains and their treatments.

2.2.4 Tissue processing for histology and morphometry

The mice were sacrificed by carbon dioxide inhalation, their chest wall exposed and their trachea was cannulated. The lungs were inflated with 10% normal buffered formalin (NBF) under 25cm water pressure for ten to fifteen minutes and processed as previously described [164]. The inflated lungs were further fixed in 10% NBF before being processed for paraffin embedding. Serial mid-sagittal sections were obtained and the desired staining performed.

2.2.5 Gills staining for morphometric assessment

The paraffin embedded parasagittal lung sections were de-paraffinized at 60°C for 30 minutes, followed by rehydration in xylenes and a gradient of ethanols. The rehydrated sections were then rinsed in distilled water for 5 minutes and stained in modified Gills stain (1:1 Harris hematoxylin: Harris Gills no.3 stain) overnight at room temperature. The sections were then washed in distilled water, fixed in dilute ammonium hydroxide for 5 minutes and dehydrated through ethanols and xylene. Cover slips were added to the slides and let to air-dry.

2.2.6 Morphometry

Ten random fields of gills stained sections per animal were captured under 200X magnification using NIS-elements program as described earlier (5,6) (Nikon, Tokyo, Japan). The sections were analyzed using Scion Image (Scion Corp., Fredrick, MD) avoiding all ambiguous areas, airways, smooth muscle and vasculature. The computed average chord length (CL) served as a measure of the average alveolar diameter from each experimental subject and enabled quantification of alveolar enlargement (a measure of emphysema).

2.2.7 Lung tissue homogenate preparation and immunoblotting

Whole lung tissue isolated from the mice were first homogenized in isotonic buffer with CHAPS detergent (50 mM Tris-HCl, pH 7.4, 150 mM NaCl, 10 mM CHAPS) with protease inhibitors (100 μ M 3,4-dichloroisocoumarin (DCI), 10 μ M trans-epoxysuccinyl-L-leucylamido- (4-guanidino) butane (E-64), 2 mM o-phenanthroline monohydrate- all from Sigma) and then sonicated briefly. The protein concentration of the total lung homogenates was quantitated using the BCA standard protein assay kit (Thermo Fisher). 50 μ g of protein per sample was separated by SDS-PAGE and transferred to PVDF membranes as described previously [165]. The membranes were blocked overnight in 5% nonfat dry milk/PBST for an hour at room temperature. The membranes were then incubated with 1:1000 Rabbit anti-mouse caspase-3 (Cell Signaling) primary overnight at 4°C and 1:2,000 anti-rabbit HRP secondary antibodies for 1 hr at room temperature. The membranes were washed with PBST (3x for 10 min) between primary and secondary antibody incubation. The reactive bands were visualized using the

chemiluminescence method (SuperSignal West Pico, Pierce). The same membranes were probed with GAPDH (1:500; Cell Signaling) as loading controls.

2.2.8 Bronchoalveolar lavage fluid collection and processing

At the various points of time post- acute cigarette smoke exposure; batches of mice were sacrificed by carbon dioxide narcosis. The chest cavity was exposed and the trachea of the mice was cannulated using a 22-gauge intravenous catheter. The lungs of the animal were lavaged with 0.75 ml of 1x PBS three times. The volume returned from each lavage was collected and recorded. The lavage fluid was centrifuged at 300 G for 5 minutes at 4°C and the supernatant separated for supplementary analysis. The cell pellet was then re-suspended in hypotonic solution to lyse red blood cells (RBC) and then centrifuged at 300 G for 5 minutes at 4°C. The supernatant containing lysed RBCs was discarded and the pellet resuspended in 1x PBS. A small fraction of this cell suspension was used to determine total cell counts using a hemacytometer and the remainder (approximately 200µl) was used to prepare cytopins.

2.2.9 Cytopsin preparation and analysis

The cytopins were prepared at 500rpm for 5 mins and let to air dry. The cytopins were then stained using a modified romanowsky stain, for 30 seconds in each of the 3 solutions and then rinsed in running distilled water. The slides were let to air-dry before being imaged using a bright field microscope. Five to ten random fields were counted per animal (approximately 300 cells) depending on the total number of cells recovered. The different cell populations were

recorded and their calculated percentages were used to extrapolate their individual counts in 1 ml of lavage fluid, using the total cell counts estimated earlier.

2.2.10 Serum collection

After sacrificing the mice, the fur and body wall was severed to expose their abdomen. The diaphragm was punctured to enable collapse of the lungs and a small incision was made to access the chest cavity. The inferior vena cava was severed, leading to the collection of blood in the chest cavity. The blood was drawn using a one ml syringe and collected in a serum separator tube (BD biosciences). These tubes were then centrifuged at 10,000 RPM for 10 minutes at 4 degrees centigrade. The serum thus obtained was separated into a fresh tube and stored at -80°C for later analysis.

2.2.11 Statistical analysis

The quantitative data collected was analyzed using the Graphpad Prism 5 (Graphpad Prism Inc., La Jolla, CA). The values were represented as means \pm standard error mean. An unpaired 2-tail student T-test was performed to determine statistical significance between strains and treatments. A p-value < 0.05 was considered statistically significant.

2.3 RAGE-RESULTS

2.3.1 Absence of RAGE affects the alveolar dimensions at baseline and protects from alveolar enlargement on chronic cigarette smoke exposure.

The contribution of RAGE to cigarette smoke induced emphysema was investigated by exposing RAGE^{-/-} mice to either chronic cigarette smoke or room-air for 6 months. Age and sex matched wild-type (C57BL/6J background) control mice were similarly exposed to cigarette smoke and room-air. Gills stained lung sections were examined for histologic and morphometric changes in the alveolar compartment as detailed in the Materials and Methods section. Wild-type (C57BL/6J) mice exposed to cigarette smoke (Figure 1, Panel B) displayed enlarged alveoli when compared to their room air exposed controls (Figure 1, Panel A). This histological observation was supported by morphometric analysis of chord lengths (CL), a measure of the alveolar diameter, as described in the materials and methods. As visualized in Figure 1E and Table 1, the wild-type mice exposed to cigarette smoke showed a 13.5% increase (p-value < 0.005) in chord length ($29.7 \pm 11.3 \mu\text{m}$) when compared to their air-exposed controls ($26.2 \pm 4.2 \mu\text{m}$). These results were replicated in a second study group with n=5-6 mice per strain per treatment group. A 14% increase in CL was observed in the second batch of chronic smoke exposed wild-type mice (Table 1). The alveolar enlargement observed in the wild type mice on cigarette smoke exposure was in corroboration with the expected phenotype.

RAGE^{-/-} mice demonstrated enlarged airspaces in the absence of smoke exposure (Figure 1, panel C) compared to wild type (Figure 1, panel A). The mean chord length of RAGE^{-/-} mice exposed to room air ($30.1 \pm 3.6 \mu\text{m}$) was significantly higher (p-value=0.00002) than room air exposed wild-type mice ($26.2 \pm 4.2 \mu\text{m}$) (Table 1). This trend was preserved in the

second batch of mice that were lavaged once before their lungs were inflated with 10%NBF for morphometric analysis. The enlarged airspaces observed in mice lacking RAGE expression likely represents altered alveolar development.

Cigarette-smoke exposure in the RAGE^{-/-} mice did not lead to a significant increase in chord length as compared to their air-exposed controls (31.2±18.6µm vs. 30.1±3.6µm, p-value=0.45) (Figure 1 and Table 1). Together these results imply that the absence of RAGE contributes to the development of emphysema. RAGE^{-/-} mice were significantly protected from cigarette smoke induced airspace enlargement. Hence, airspaces in RAGE^{-/-} mice are enlarged at baseline but protected from progressive enlargement in response to cigarette smoke.

Table 1: Quantification of airspace enlargement using lung morphometry

Group	N/group	Batch #1				Batch #2				
		CL (SEM)	% increase with Sm	P-value (vs. Nsm)	P-value (vs. WT-NSm)	N/group	CL (SEM)	% increase with Sm	P-value (vs. Nsm)	P-value (vs. WT-NSm)
WT (NSm)	5	26.19(0.16)	-	-	-	5	28.38 (0.52)	-	-	-
WT (Sm)	5	29.72(0.38)	13.47	0.0049	-	5	32.36 (0.99)	14.02	0.012	-
RAGE ^{-/-} (NSm)	5	30.13(0.12)	-	-	<0.0001	5	32.22 (0.45)	-	-	0.0005
RAGE ^{-/-} (Sm)	4	31.02(0.60)	2.95	0.4455	0.00376	6	34.82 (0.52)	8.06	0.0043	<0.0001

Mean chord length (CL) data from 2 independent experiments of chronic cigarette smoke exposures. Wild-type (WT) mice were C57BL/6J background, congenic with the RAGE^{-/-} mouse strain. The CL, the standard error of the mean (within the parentheses) as well as the percentage increase in CL with smoke exposure is displayed. The p-value indicated was derived from a 2-tailed student t-test.

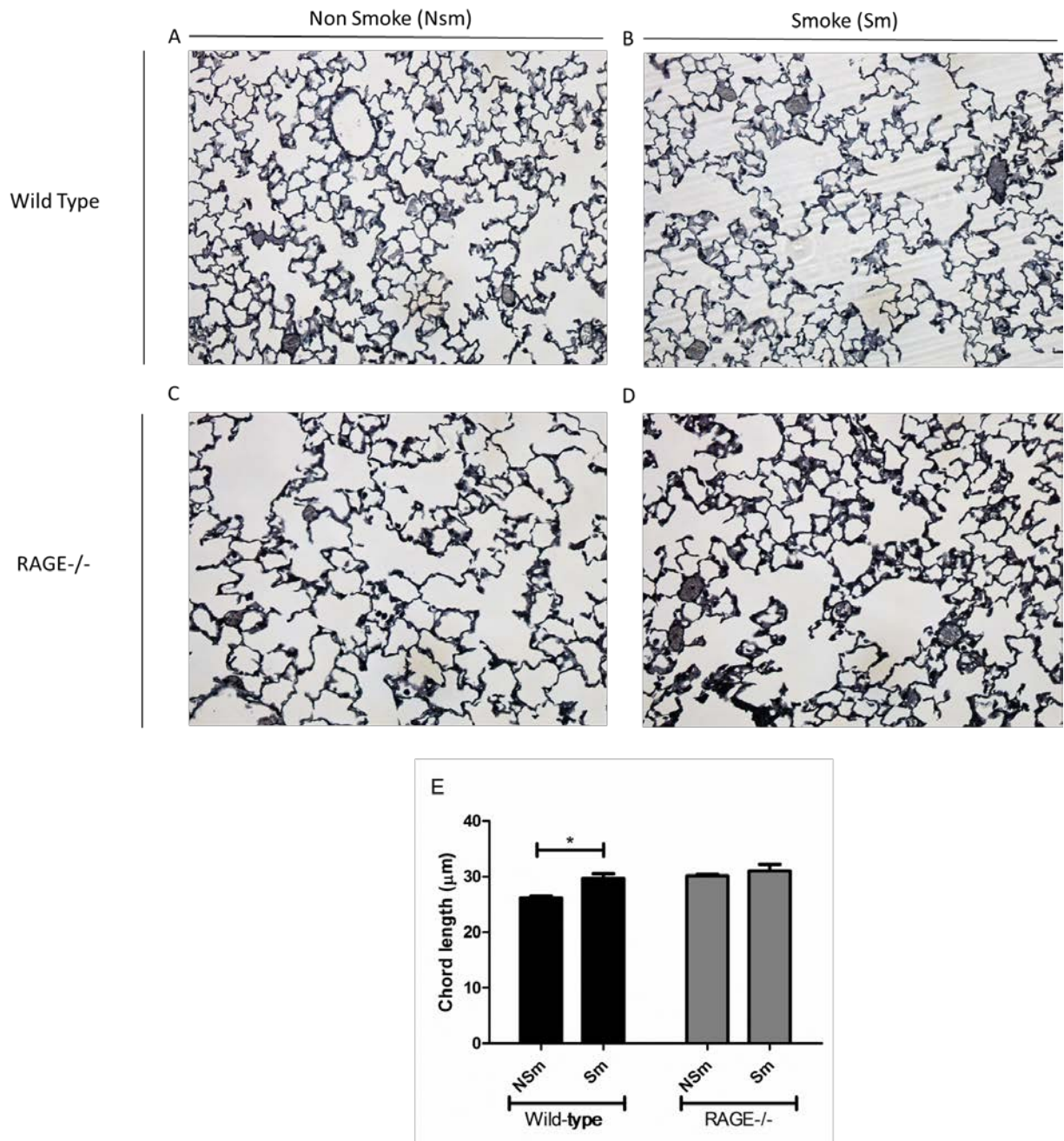


Figure 1: Lack of RAGE leads to enlarged airspaces at baseline and protects from progressive airspace enlargement on chronic cigarette smoke exposure

Panels A-D show representative images of H&E stained sections of the lungs from the different treatment groups. Wild-type mice exposed to smoke (B) showed enlarged airspaces compared to their air-exposed controls (A). RAGE-/- mice showed no visually detectable difference in alveolar size on smoke exposure (D) when compared to their air-exposed controls (C). Panel E shows a graphical representation of Batch # 1- the mean chord length (µm), a

measure of alveolar diameter, calculated in each strain and treatment group. The * indicates a p-value < 0.05 on an unpaired 2-tailed student t-test, specifying statistical significance. The error bars indicate the standard error mean (SEM) for each group.

2.3.2 Effect of RAGE on lung physiology

To investigate the effect of RAGE on general lung tissue dynamics, pulmonary function testing was performed on the RAGE^{-/-} mice and wild-type mice with and without exposure to chronic cigarette smoke. Tissue elastance (H) acts as a measure of energy conservation in the lung tissue, a decrease in H as seen in emphysema would imply a decrease in capacity of the lung to return to its original form on removal of external distending forces. Wild-type smoke exposed mice showed a significant decrease (p-value=0.048) in lung tissue elastance (H) in a dose-dependent manner to methacholine challenge when compared to their room-air exposed controls (Figure 2, panel A). Although emphysema was too mild to detect differences in tissue elastance (H) at baseline, addition of methacholine brought out significantly reduced elasticity with smoke exposure, which correlated with the significantly enlarged alveoli observed in these mice on morphometric analysis (Figure 1E & Table 1).

RAGE deficient mice at baseline did not display any difference in tissue elastance (H) irrespective of their exposure to cigarette smoke or room-air when compared to their wild-type counterparts. However, on challenge with 30mg/ml of methacholine the RAGE^{-/-} air-exposed mice (Figure 2A) displayed a trend towards decreased tissue elastance (75.29 cmH₂O/ml) as compared to the air-exposed wild-type mice (101.65 cmH₂O/ml). Chronic smoke exposure in RAGE deficient mice did not lead to any reduction in lung tissue elastance compared to their room-air exposed RAGE^{-/-} control mice. RAGE^{-/-} mice irrespective of their exposure to

cigarette smoke or room-air had similar changes in H when compared with wild-type chronic smoke exposed mice on bronchodilation. While differences in H were observed with smoke exposure, we did not appreciate any changes in dynamic compliance, C (Figure 2B).

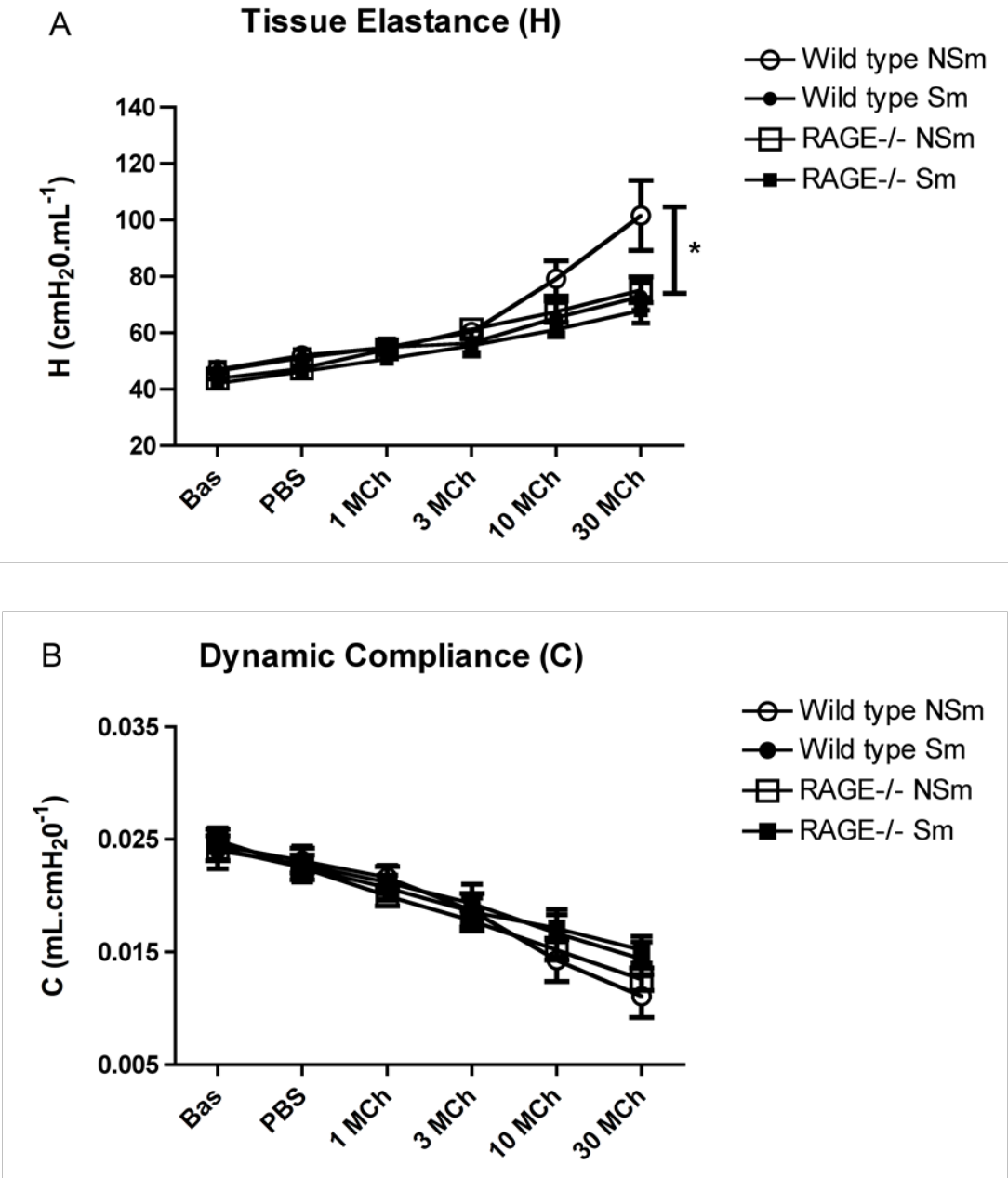


Figure 2: Smoke-exposed RAGE^{-/-} mice show no reduction in lung tissue elastance on bronchoconstriction when compared to their air-exposed controls

Respiratory mechanics of RAGE^{-/-} mice and wild type mice (n=5-10 mice per strain per treatment group) previously exposed to cigarette smoke or room air was assessed using a mechanical ventilator (Flexivent) as described in the methods section. **Panel A** indicates a significant reduction in lung tissue elastance in wild type smokers (●) as compared to the air-exposed controls (○) on bronchocontraction. However, RAGE^{-/-} mice show no reduction in lung tissue elastance (H) on cigarette smoke exposure (■) (or methacholine challenge) compared to their controls (□). **Panel B**-Dynamic lung compliance (C) was not significantly altered on methacholine challenge in either mouse model irrespective of cigarette smoke exposure. * P-value < 0.05 indicates statistical significance.

2.3.3 Cigarette smoke induced apoptosis is RAGE-dependent on chronic smoke exposure

Alveolar endothelial and epithelial apoptosis is well characterized in cigarette smoke-induced COPD that correlates with the loss of alveolar tissue [95]. To investigate the role of RAGE in mediating cellular damage in response to cigarette smoke exposure, total lung homogenates from RAGE^{-/-} and wild-type mice were probed for caspase-3 as a marker of apoptosis. Concurrent with previous studies, cleavage of caspase-3 was elevated in the wild-type smoke-exposed mice when compared to their air-exposed controls. Western blotting for caspase-3 indicated reduction in cleaved caspase-3 (17,19kDa) levels in the RAGE^{-/-} smokers compared with wild-type smokers (Figure 3). The pro-caspase (35kDa) levels were similar between the wild type and RAGE^{-/-} mice irrespective of their exposure to cigarette smoke or room air (Figure 3). Wild-type mice exposed to cigarette smoke had elevated cleaved caspase-3 levels when compared to their air-exposed controls. In the absence of RAGE, no alteration in cleaved caspase-3 levels was observed in total lung homogenates from cigarette smoke exposed and air exposed mice. Subsequent repetition of this blot confirmed these observations in an n=6 per strain per treatment group.

Consistent with morphometry and physiology these findings suggest protection from cellular damage in response to cigarette smoke mediated injury in RAGE^{-/-} mice, leading to a decreased loss of the underlying matrix and manifesting in significant protection from cigarette smoke induced emphysema.

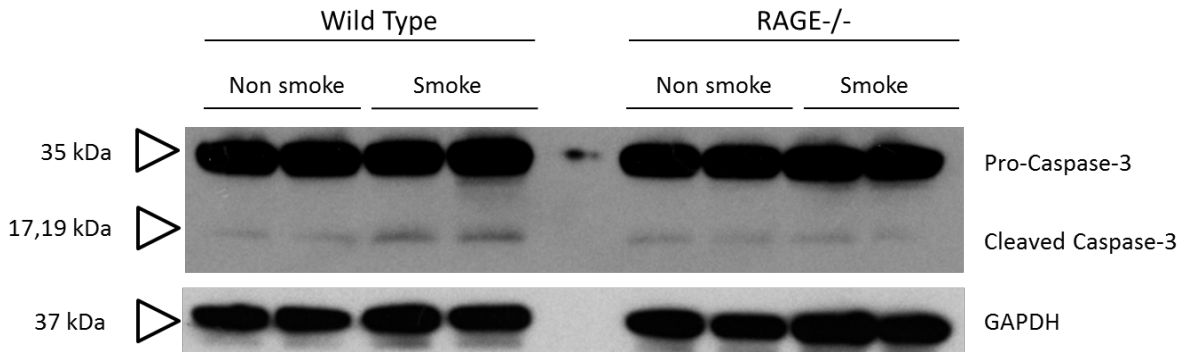


Figure 3: RAGE expression contributes to apoptosis on chronic cigarette smoke exposure.

Lung homogenates (50µg per well) harvested from RAGE^{-/-} and wild-type mice (n=2/strain/treatment) exposed to chronic cigarette smoke were separated by an SDS-PAGE and immunoblotted for caspase-3. Pro-caspase 3 (35kDa) levels were unaltered irrespective of the exposure of cigarette smoke or room air in both RAGE^{-/-} and wild type mice. GAPDH (37kda) was used as an internal control. Cigarette smoke exposure led to caspase-3 cleavage in wild type mice, but not RAGE^{-/-} mice.

2.3.4 Impaired neutrophil recruitment observed in RAGE^{-/-} mice on acute cigarette smoke exposure.

Emphysema results from inflammatory cell-mediated elastolysis. Moreover RAGE has been shown to mediate the adhesion and recruitment of inflammatory cells (Chakavis T, 2003 & 2004). Upon exposure to cigarette smoke, neutrophils are recruited within hours and return to normal within 24 hours. Macrophages and lymphocytes are not as acutely responsive but appear to accumulate over time. Following six months of cigarette smoke exposure we observed

macrophage accumulation. However, we did not detect any differences in chronic macrophage exposure or MMP-12 production (unpublished data) in the RAGE^{-/-} mice on long-term smoke exposure.

Acute smoke exposure led to no change in total BALF cell counts (Figure 4A), although there was a significant neutrophil accumulation in wild-type mice but not in RAGE^{-/-} mice (Figure 4B). Specifically, at four hours post-acute smoke exposure wild-type mice showed an eight-fold increase (p-value= 0.018) in neutrophils recruited when compared to their room-air exposed controls (Figure 4B). The macrophage or monocyte and lymphocyte counts were unaltered at 4 hours post-acute smoke exposure in the wild-type mice as compared to their room-air exposed controls (Figure 4C and D). In contrast, the RAGE^{-/-} mice showed no significant increase (p-value=0.475) in neutrophils at 4 hours post-smoke exposure (Figure 4B) compared to their room-air exposed controls. There was no significant difference in the macrophage, monocyte and lymphocyte counts from the BALF of RAGE^{-/-} mice at 4 hours post-acute smoke exposure when compared to their air-exposed controls (Figure 4, panels C and D). These observations indicate the critical involvement of RAGE in the early recruitment of neutrophils on acute smoke exposure and in emphysema.

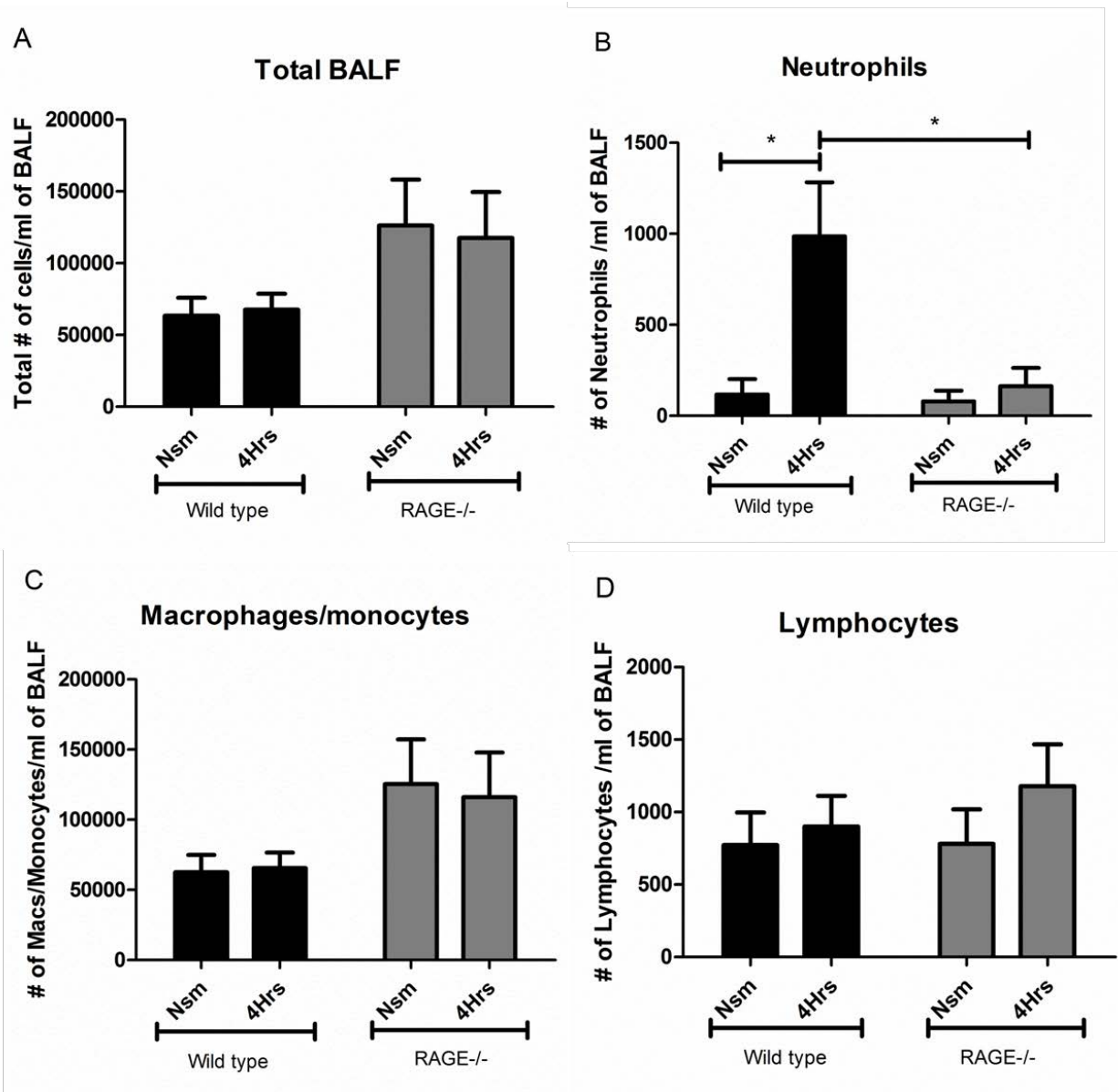


Figure 4: RAGE mediates early recruitment of neutrophils in response to acute cigarette smoke exposure

The bronchoalveolar lavage fluid (BALF) collected from the lungs of RAGE^{-/-} (grey bars) and wildtype (black bars) mice (n=8-15 per strain per group) was used to stain and quantify cells that had migrated into the fluid lining the alveoli. **Panel A** indicates the total cell counts obtained from the BALF of the different treatment groups on acute cigarette smoke exposure. RAGE^{-/-} mice display significantly reduced recruitment of neutrophils at 4 hours post-smoke exposure as compared to their wild-type counterparts (**Panel B**). There was no significant alteration observed in the number of macrophages or monocytes (**Panel C**) and lymphocytes (**Panel D**) recruited in either the RAGE^{-/-}

or wild-type mice at 4 hours post-acute smoke exposure. (* p-value ≤ 0.05 indicating statistical significance). The error bars indicate the standard error mean (SEM) within each group/treatment/time point

2.4 RAGE-DISCUSSION

Upon long-term exposure to cigarette smoke, despite having enlarged airspaces at baseline, RAGE^{-/-} mice did not develop significant airspace enlargement compared to RAGE^{+/+} mice. Protection from smoke-induced emphysema in RAGE^{-/-} mice was based upon morphometry with less increase in airspace dimensions, physiology with less loss of elastance, and less cellular damage and apoptosis. Mechanistically, this was related to impaired neutrophil recruitment in the absence of RAGE.

Enlarged alveolar dimensions at baseline in RAGE^{-/-} mice suggest a role for RAGE during alveolar development. RAGE is expressed highly on alveolar type-I (AT-I) cells under normal conditions [166, 167] and is a marker of terminal differentiation on these cells [139]; hence the absence of RAGE may contribute to defective differentiation of the alveolar epithelial cells in the lung parenchyma. Of note, mouse models that over-express human RAGE have been described to have poor alveolar septation during post-natal development [168]. These findings combined with our observation of enlarged airspaces in the RAGE^{-/-} mice (Figure 2C) point toward a requirement for RAGE in normal alveolar development.

RAGE has been implicated as having a role in COPD. Clinical studies demonstrated increased staining for advanced glycation end products (AGE) and RAGE in lung sections from COPD

patients with an FEV1 <80% predicted, this was equivalent to GOLD stage 2-4 [158]. Additionally, this increased intensity of RAGE staining was significantly elevated in the alveolar walls when compared to the airways. Further, lower plasma levels of soluble RAGE (sRAGE) correlated with increased severity of emphysema in COPD patients when compared to controls who lacked airflow obstruction [160]. These findings were corroborated by observations in a larger COPD patient cohort [169]. In vitro studies performed using a rat alveolar type-I cell line (R3/1), human alveolar type-II cell line (A549) and a murine macrophage-like cell line (RAW246.7) showed upregulated expression of RAGE and RAGE ligands upon exposure to cigarette smoke extract (CSE) [161]. In this study we directly confirmed a role for RAGE in the pathogenesis of emphysema by using RAGE deficient mice exposed to chronic cigarette smoke and show that they are significantly protected from smoke induced airspace enlargement.

Inflammation associated destruction of lung tissue, particularly elastin, has been the basis for the pathogenesis of emphysema [90, 170, 171]. The elastase: antielastase hypothesis has stood the test of time for over 50 years [19, 88, 172, 173]. With respect to inflammation, acute cigarette smoke exposure leads to transient recruitment of the short-lived neutrophils to the lung. Recruitment and loss within 24 hours is repeated throughout our 6-month smoking study. Hence, despite representing a small percentage of the total cells recovered by BAL, there is a large contribution of neutrophil burden elicited by smoking. Upon prolonged smoke exposure, longer-lived lymphocytes and macrophages accumulate in the lung.

Both neutrophils and macrophages interact to promote emphysema, largely through their elastases: neutrophil elastase (NE), macrophage elastase (MMP-12) and perhaps MMP-9 expressed by both neutrophils and macrophages [121]. In our study, RAGE deficiency impairs

neutrophil accumulation but not macrophage numbers and MMP-12 content (not shown). In this study, RAGE appears to be essential for neutrophil recruitment demonstrated by the fact that RAGE^{-/-} mice have only ~17% the neutrophils in response to cigarette smoke exposure than wild-type mice do, which corresponded to ~78% protection against emphysema. Hence, these studies further support the importance of neutrophils in emphysema and suggest that RAGE is involved in cigarette smoke induced recruitment of neutrophils into the lung.

RAGE when engaged by its ligands has been shown to activate intracellular NF- κ B mediated chemokine/cytokine transcription, thereby perpetuating inflammatory cell recruitment in other acute and chronic inflammatory disease models [174-177]. In addition AGE-RAGE signaling may up-regulate the expression of several adhesion molecules through NF- κ B activation namely E-selectin, intercellular adhesion molecule-1 (ICAM-1) and vascular adhesion molecule-1 (VCAM-1) specifically on endothelial cells [178, 179]. In fact, RAGE has been identified as a counter-receptor for the leukocyte β 2 Integrin Mac-1 facilitating its adhesion and recruitment across the vasculature [180].

We now extend the importance of RAGE to cigarette smoke related neutrophil but not macrophage recruitment. We tested many pro and anti-inflammatory cytokines and chemokines in our model but we were unable to detect differences in their circulating levels (not shown). Either the changes were too subtle to detect, or alternative mechanisms exist in this model that require further investigation.

The contribution of extracellular matrix destruction versus cellular apoptosis has been debated. Clearly loss of alveolar tissue and consequently enlarged airspaces requires both the loss of

structural cells and extracellular matrix (ECM). Whether the events are separate or one leads to the other (and which one initiates) is less clear. However it is plausible that the loss of ECM leads to anoikis (death following matrix detachment). Alternatively, cell death could lead to inflammation. In this study, we observed increased apoptosis in the RAGE^{+/+} mice exposed to 6 months cigarette smoke that correlated with emphysema. We interpret this to confirm our emphysema phenotype; although this observation sheds no additional light on the mechanism. This is consistent with previous studies have also found a role for RAGE in promoting apoptosis in other lung models [162].

Lung physiology of the RAGE^{+/+} mice show a significant decrease in lung tissue elastance on methacholine challenge mirroring the phenotype observed with chronic cigarette smoke exposure. In the absence of RAGE we find that there was no loss of lung tissue elastance with methacholine challenge (Figure 2A), this finding correlated with the partial protective phenotype observed on chord length quantification in the RAGE^{-/-} mice (Table 1). Together, these observations suggest that loss of RAGE, despite leading to abnormal alveolar development, confers protection from further airspace enlargement in response to cigarette smoking.

The current study adds RAGE to a growing list of mediators of emphysema and confirms the importance of neutrophil recruitment. Further understanding of mechanisms of neutrophil recruitment could lead to novel therapy that is badly needed for this devastating and common disease, although cigarette-smoking cessation remains most important. As the era of precision medicine arrives, RAGE polymorphisms could also be a factor that identifies smokers who are either resistant or susceptible to COPD [159]. Single nucleotide polymorphisms (SNPs) in the

minor allele (T allele) within exon 3 of RAGE gene, which converts a glycine at the 82nd position into serine (G82S) present within the ligand-binding pocket increases affinity for AGE ligands and enhances its ligand binding function [181, 182]. A recent clinical study in a Chinese population suggested that smokers with the G82S polymorphism in their RAGE gene had an elevated risk of developing COPD[183]. This finding along with future studies holds the promise of better evaluation of individual susceptibilities to this disease and its possible prevention.

2.5 RAGE- FUTURE DIRECTIONS

The results of this study demonstrate that RAGE is required for progression of emphysema in mice. The enlargement of airspaces observed in the RAGE deficient mice on exposure to room-air, additionally suggest its involvement in the development of the alveolar compartment. Expression of RAGE in other organ systems that undergo branching morphogenesis such as the kidney and neurite outgrowth post-peripheral nerve injury confirm its critical function in organ development and repair [184, 185]. Furthermore, moderate over-expression of human RAGE in mice during post-natal alveolar development demonstrated its involvement in secondary alveolar septation resulting in enlarged airspaces [168]. This observation was corroborated by a different group that over-expressed mouse RAGE in a doxycycline inducible mouse model that showed similar alveolar enlargement with poorly fused basement membrane and decreased collagen deposition [186]. RAGE expression is significantly elevated in the lung during post-natal alveologenesis in AT-I cells at post-natal day-4 (PN4) through PN10. Moreover, its expression was positively regulated by early growth response gene-1 (Egr-1) and negatively regulated by thyroid transcription factor-1 (TTF-1) [161]. Although our findings along with other published

studies highlight a role for RAGE in alveolar development, we still do not understand the exact role of this receptor during lung development and adult lung homeostasis. Future studies would involve trying to dissect molecules lying downstream or upstream of RAGE that facilitate the process of alveolarization. In the RAGE^{-/-} mice, one could begin by investigating Egr-1 and TTF-1 expression to check for any differences in levels of expression during post-natal alveolar septation.

Lung fibroblasts mainly synthesize elastin during lung development [187, 188]. In vitro experiments involving the over-expression of mouse RAGE or sRAGE in mouse lung fibroblasts indicated an elevation in elastin mRNA synthesis [189]. Since AT-I epithelial cells are the primary source of RAGE expression, a potential direction to investigate is if the loss of RAGE expression especially on the structural cells in RAGE deficient mice influences the amount of elastin synthesized by the alveolar fibroblasts especially during alveolar development. By measuring desmosine and isodesmosine levels (a measure of elastin) in lung tissue [190] from RAGE deficient mice and comparing it to their wild-type (RAGE^{+/+}) controls, we may attempt to explain the enlarged airspaces observed in the room-air exposed RAGE^{-/-} mice (Figure 1C) in our chronic smoke experiments.

Toll-like receptor-4 (TLR4) has been linked with RAGE to signal through similar pathways leading to inflammation in patients with type-II diabetes [191]. Subsequently, TLR4 deficient mice have been shown to elevate NADPH oxidase (NOX3) expression in their lungs leading to an increase in oxidant activity [192]. Investigation of NOX3 expression in the absence of RAGE expression, using RAGE^{-/-} mice that are exposed to cigarette smoke and comparing them to their room air exposed controls may provide some insight into their oxidative stress bearing capacity. Additionally, RAGE and TLR4 share several common ligands such as HMGB1

[128, 133], S100A8/A9 [193, 194] and lipopolysaccharide (LPS)[195, 196] which may mediate their effects through TLR4 in the absence of RAGE expression. Hence it may be worthwhile investigating if cigarette smoke induced deregulation of RAGE ligand expression may mediate some or none of their effects through alternate pathways, namely TLR4 mediated signaling. One way of studying this could be through exogenous administration of RAGE ligands such as recombinant HMGB1 into RAGE^{-/-} mice and monitoring their inflammatory response through analysis of their bronchoalveolar lavage fluid (BALF). Elevated HMGB1 has been suggested to mediate neutrophilic inflammation albeit in asthma [197]. The results of this study will further indicate if elevated levels of HMGB1 or any other RAGE ligand is capable of initiating an inflammatory response independent of RAGE. An alternate investigation may incorporate using a double knockout mouse deficient for TLR4 and RAGE, to study the effect of cigarette smoke induced HMGB1 accumulation [198] on the cells mediating innate immunity.

A number of studies correlate the levels of sRAGE to the extent of disease, however the exact mechanisms by which sRAGE levels are altered are not clear. Reduced levels of systemic sRAGE were reported in a group of stable COPD patients when compared to their healthy controls and further reduction in sRAGE levels was reported in those patients during acute COPD exacerbations [169]. These observations were confirmed later by a different research group in a larger cohort of COPD subjects who observed greater loss in pulmonary function with reduced circulating levels of soluble RAGE [160]. Despite soluble RAGE being largely attributed to have an antagonistic function to membrane bound RAGE [199], there are studies that indicate that sRAGE may have agonist functions as well [200, 201]. The effect exerted by sRAGE may depend on the levels of RAGE ligands present in the context of normal lung homeostasis or injury. Therefore, one approach could be to investigate the contribution of

sRAGE in the context of cigarette smoke induced injury in RAGE^{-/-} mice. Since RAGE^{-/-} mice show partial protection from chronic cigarette smoke exposure, one would expect that if sRAGE played an antagonistic function that the RAGE^{-/-} mice would show greater protection on cigarette smoke exposure. On the other hand, if sRAGE plays a more agonistic role we would expect that the RAGE^{-/-} mice do much worse on cigarette smoke exposure. By understanding the role of sRAGE in the context of emphysema, we can aim to translate our findings to potential therapeutic solutions. A novel large molecule RAGE inhibitor (TTP4000) is currently in the clinical developmental phase for treating Alzheimer's disease (Transtech Pharma Inc.) and could potentially find therapeutic utility in chronic lung diseases in the near future. The realization of which would evidently need for us to have a better understanding of the mechanisms by which different RAGE ligands specifically bind and signal through RAGE in the context of disease.

3.0 A DISTAL BRONCHIAL PROGENITOR CELL (DBPC) POPULATION CONTRIBUTES TO ALVEOLAR REPAIR IN EMPHYSEMA USING MOUSE MODELS

Understanding cellular events that initiate endogenous reparative mechanisms and the reasons for their failure in progressive inflammatory diseases such as emphysema will provide much needed insight as to how we may one day better treat this disease. Alveolar repair is a complex process with multiple components that require coordination to bring functionality to the alveolus. These include maintaining an intact basement membrane, repopulation of damaged alveolar epithelium and building tight junctions between the epithelial and endothelial layers to facilitate gaseous exchange. The current study will focus on understanding the role of a distal bronchial epithelial (progenitor) cell towards alveolar repair, which forms a component of this multi-step reparative process.

To study the contribution to alveolar repopulation of this previously identified distal bronchial progenitor cell, we developed a transgenic mouse line that enabled us to lineage trace these cells and their movement from the distal bronchi into the surrounding alveolar epithelium in the context of injury. Transgenic mice were exposed to cigarette smoke or intratracheal PPE and their lungs were analyzed at the end of the experiment to monitor the contribution of these distal bronchial progenitor cells (DBPCs). Our observations indicate a significant contribution of the DBPCs in the alveolar compartment of the lung post-injury with increased migration and

potential repopulation of alveolar epithelial cells. Further these observations were validated using a knock-in mouse model, which confirmed our findings in the initially developed transgenic mouse model.

Overall our findings point towards a significant contribution of the DBPC population in the alveolar compartment amplified by injury and their capacity to repair the alveolar epithelial cell population.

3.1 DBPC- BACKGROUND

3.1.1 Epithelial cell populations in the lung

Mouse lungs are comprised of a variety of epithelial cell populations. The trachea and proximal airways are typically lined with basal cells, ciliated cells, goblet cells and small numbers of neuroendocrine cells. The distal and terminal bronchi are composed mostly of non-ciliated columnar Clara cells [202]. The alveolar compartment of the lung is mainly comprised of two types of cells alveolar type-I (AT-I) and alveolar type-II (AT-II) cells [203]. AT-I epithelial cells make up approximately 95% of the alveolar compartment of the lung. AT-I cells and endothelial cells joined by a fused basement membrane form the air-blood barrier across which gaseous exchange occurs. AT-I cells are known to mainly regulate alveolar fluid balance and surfactant protein secretion by alveolar type-II (AT-II) cells in the lung [204-207]. On the other hand, AT-II epithelial cells populate the remaining ~5% of the alveolar epithelium. These cells are cuboidal and are interspersed between AT-I cells, commonly characterized by lamellar bodies and microvilli on their apical surface [203]. AT-II cells are involved in the production, secretion and

resorption of pulmonary surfactants in response to stretch vital in providing the required surface tension that prevents the alveoli from collapsing [208].

3.1.2 Alveolar repair in normal and emphysematous lungs

The general assumption has been that once the alveolus is damaged or fails to develop properly there is rarely any successful spontaneous attempt at alveolar repair or regeneration of the lost alveoli. We continue to explore and try to understand the role of putative endogenous progenitors that aid in maintaining this fragile alveolar compartment that is exposed to external and internal stresses as well all fend us against toxic insults on a daily basis.

Evidence for alveolar repair mechanisms in rodent models sheds light on possible contributors of such endogenous repair. Adult mice that were ovariectomized displayed lesser surface area and larger alveoli when compared to their controls. After 3 weeks of estrogen treatment these ovariectomized mice showed alveolar regeneration [209]. Other studies involving calorie restriction of the diets of adult rats showed changes in the lung as early as 2 hours similar to those seen during the activation of apoptosis. However, by the end of 72 hours the rats showed significant alveolar loss. After 15 days on the calorie-restricted diet, when the rats were returned to a calorie-enriched diet they displayed alveolar regeneration within a span of 72 hours [210]. These studies were instrumental in providing insight into regenerative cues that were capable of inducing alveolar remodeling.

Elastin fibers are one of the most complicated to repair as they are molecularly complex, have slow turnover and require a number of helper proteins to facilitate its assembly [170]. In the context of emphysema, inflammatory cell secrete proteases that attack these long-lived fibers and cause their degradation. The elastin fragments generated by this elastolytic activity further serve

to recruit more inflammatory cells furthering the damage [23]. Tropoelastin monomers secreted by myofibroblasts form the basal unit; these monomers aggregate in presence of fibrils and are cross-linked by lysyl oxidase. These larger conglomerates of elastin then leave the cell surface and fuse with microfibrils in the extracellular space (composed of fibrillins). Once associated with the microfibrils, these elastin aggregates coalesce forming even larger aggregates. The final maturation process of the elastin fibers involves cross-linking of newly formed elastin aggregates with the microfibrils while removing older fibers. This multi-step proposed model of elastin assembly demands both extensive energy and cellular resources, which are precious to the cell. In addition when levels of functional elastin are below a critical threshold, attempts at repair after injury become unproductive and can lead to further progression of emphysema [211].

Retinoids, a vitamin A derivative, have been shown to be essential to the development of many organs including the lung. Retinoids are stored as retinyl esters in lipid-laden fibroblasts in the lung, which is its second largest storage site [212]. All-trans retinoic acid (ATRA), a biologically active form of retinoids, has been shown to regulate elastin in the lung [213]. Further, when ATRA was supplemented post-natally during alveolar septation in rats there was an increase in numbers of alveoli but did not show any increase in alveolar surface area [214]. To evaluate the regenerative potential of ATRA in the context of disease, adult rats were intratracheally treated with elastase to induce emphysema and subsequently treated with ATRA. ATRA was found to restore the damaged alveoli in these rats and reversed pathological features of airspace enlargement observed [215]. Thus strengthening the potential role of ATRA as an exogenous agent inducing lung regeneration in animal models. Clinical studies performed using ATRA in patients with emphysema showed no changes in outcome measures with a delayed improvement in gas exchanged at a higher dose of ATRA [216, 217].

3-hydroxy 3-methyl glutaryl coenzyme A reductase inhibitor (simvastatin) was used to treat elastase-exposed mice and showed reversal of emphysema (reduced chord length) and an increase in proliferating alveolar epithelial cells [218]. Other studies have elucidated the role of simvastatin in blocking endothelial smooth muscle cell proliferation and in blocking vascular injury [219]. A number of growth factors have been assessed for their role in alveolar repair. Keratinocyte growth factor (KGF or fibroblast growth factor-7, FGF-7) has been implicated in alveologenesis, however when used to treat rats with elastase-induced emphysema it was unable to reverse the damage incurred. Pre-treatment with KGF nevertheless provided protection from subsequent elastase induced alveolar injury [220]. Hepatocyte growth factor (HGF), known to be a potent mitogen for alveolar type-II epithelial cells when transfected into rats with elastase induced emphysema displayed an increase in alveolar cell counts [221]. Mice treated with intranasal HGF showed reversal of elastase-induced emphysema [222]. The potential of HGF in treating human emphysema is yet to be assessed.

3.1.3 Pulmonary epithelial progenitor cell populations

Injury models have been widely helpful to identify and study various epithelial stem cell niches in the lung [223]. A population of cells (basal cells) found in the trachea and proximal airways has been shown to be resistant to injury caused by exposure to detergent polidocanol or sulfur dioxide exposure [224]. These basal cells have been shown to be a progenitor cell population for ciliated cells, clara cells and secretory cells lining the airways [225]. Bleomycin, a chemotherapeutic agent that damages several cell types in the alveolar compartment, led to the identification of some resistant AT-II cells capable of replicating and differentiating into AT-I

epithelial cells hence repopulating the alveolus [226]. The naphthalene injury model aided in the identification of two clara cell secretory protein (CCSP) expressing progenitor cell populations in the proximal and distal airways; one resistant population that is closely associated with neuroendocrine bodies (NEB) in the proximal airways [227-229] and the other resistant population located in the terminal bronchial duct junction [230]. Bronchoalveolar stem cells (BASCs) have been shown to repopulate Clara cells on naphthalene injury of distal airways and AT-II cells on bleomycin injury of the alveoli [231, 232]. Therefore by recognizing the molecular signals that activate these progenitor populations to proliferate and differentiate and other inhibitory signals that block this reparative function in the context of injury, we can hope to regenerate the damaged alveolus in emphysema.

3.1.4 Potential involvement of other cell lineages towards lung epithelial repair

Embryonic stem cells (ESCs) isolated from the inner cell mass of a blastocyst (from a fertilized egg) has the potential to give rise the cells types belonging to all three germ layers (pluripotency), namely ectoderm, mesoderm and endoderm. These ESCs may be cultured indefinitely, maintain their pluripotency and can be induced to differentiate into a specific cell type based on signaling molecules (cues) supplemented in their growth media. ESCs both from human and mouse have been successfully differentiated into alveolar type-II epithelial cells with lamellar bodies and surfactant protein production [233-236]. Mouse ESCs were shown to yield in greater endodermal differentiation in presence of activin and Wnt3a, than activin alone. On further treatment with fibroblast growth factor -2 (FGF-2) these cells began to express surfactant proteins and developed lamellar bodies characteristic of mature AT-II cells [237]. The challenge however in using ESCs for transplants/treatment remains the generation of pure differentiated

AT-II cells populations, without any undifferentiated ESCs, which can give rise to teratomas. The second challenge is an ethical one that involves generation and use of human ESCs.

The induced pluripotent stem cell (iPSC) technology has enabled us to overcome some of the limitations discussed earlier in using ESCs. iPSCs may be derived from an adult somatic cells, by transfecting them with 4 factors (Klf4, Sox2, Oct3/4 and c-Myc) previously described to re-program them into a pluripotent stem cell. Since iPSCs may be derived from an adult somatic cell, for example a skin cell from a patient with A1AT deficiency, it can then be reprogrammed into AT-II cells capable of expressing A1AT and transplanted back into the patient without the issue of immune rejection. Recent studies conducted using mouse fibroblast-derived iPSCs cultured in activin-A supplemented small airway growth media over 14 days, displayed differentiation into SP-C expressing AT-II epithelial cells and AQP-5 expressing AT-I cells [238]. Mouse models of endotoxin mediated acute lung injury demonstrated significant physiological improvement complimented by reduced levels of NF- κ B and neutrophils in their lungs on intravenous treatment with mouse iPSCs [239]. Although iPSCs have generated a lot of interest and present potential use in the field of lung regeneration, their clinical safety and efficacy as a therapeutic are yet to be ascertained.

Other cell types thought to have a reparative role in the lung include bone marrow derived cells injected intra-venously shown to migrate and engraft to the lung upon lung injury [240]. Although some of these studies have suggested that these cells are capable of differentiating to AT-I and AT-II cells within the lung [241], these results have been widely debated and hence very controversial [242, 243]. Further examination of lung histology from mice transplanted with eGFP tagged bone marrow cells indicated over-lapping fluorescence

intensities of AT-II SP-C+ cells with e-GFP positive bone marrow derived cells by deconvolution confocal microscopy [242].

Bone marrow derived stem cells are of two types hematopoietic stem cells (HSCs) capable of giving rise to the different blood cell types and bone marrow derived mesenchymal stem cells (BMDMSCs). The BMDMSCs have been described as a potential adult progenitor cell capable of homing to the lung under acute injury and giving rise to AT-I cells [244-246]. Other investigations have shown an increase in bone marrow derived cells in the lungs of elastase-injured mice post-treatment with granulocyte colony stimulating factor (G-CSF) [247]. Several studies have elucidated the contribution of these cells towards immunomodulation via suppression of pro-inflammatory factors and release of various growth factors in different injury models [244, 248-250]. The direct contribution of BMDMSCs towards repopulating the alveolar epithelium is still largely unclear, however they do appear to engraft in the lung in much smaller numbers (~1-2%) than initially described [251].

3.1.5 Bioengineering lung tissue *ex vivo*

While the intra-tracheal delivery of iPSCs holds considerable promise as cell-based therapy, one of the main challenges has remained the availability of bio-active lung scaffold that the epithelial cells can engraft on, form tight junctions between one another and functionally communicate with the underlying vasculature. Biologically engineered lung scaffolds that can support lung progenitor cells to replace lost/damaged regions of the lung are an alluring prospect and have generated a lot of interest in the past decade. Several groups have explored the use of synthetic and naturally derived scaffolds seeded with different adult lung epithelial and progenitor populations[252-254]. The progenitor cells populations seeded on these biological scaffolds

showed engraftment, differentiation into CC10 expressing Clara cells as well as SP-C expressing AT-II cells and development of distal airway like structures. The first successful clinical procedure involved treating a 30-year old woman with bronchomalacia (tracheal-defect) with a tracheal graft seeded with the patient's own cells. The scaffold used involved de-cellularizing cadaveric trachea, on one side of which the patients own bronchial epithelial cells were seeded and on the other MSC derived chondrocytes [255]. The bio-engineered tissue seems to have restored lost function in the patient, yet long-term follow-ups will determine if the procedure provided a life-long solution.

A more recent study conducted in rats, demonstrated this exciting potential of bio-engineered lung. The study involved decellularizing rat lungs in a bioreactor followed by transplanting microvascular lung endothelial cells into the pulmonary artery and pulmonary epithelial cells into the lung. Once the cells had seeded and repopulated the lungs, the distribution and phenotype of cells repopulating the vasculature and lung were confirmed by immunofluorescence staining. Further the bio-engineered rat lung was transplanted into the left lung of 4 rats to show functionality (gas-exchange), structural integrity and vascularization [256].

3.2 DBPC- MATERIALS AND METHODS

3.2.1 Lineage tracing of distal bronchial progenitor cells

3.2.1.1 Transgenic mouse model- CC10-Cre; ROSA-LacZ

A transgenic mouse line that stably expresses Cre recombinase (with SV40 promoter, intronic elements and polyA tail) under the rat CC10 promoter (generous gift of Dr. Jeffrey Whitsett) was

generated in our laboratory [257]. This mouse line was then bred with a Rosa 26 reporter mouse line that consisted of a constitutively active Rosa 26 promoter followed by a loxP-STOP-loxP codon that prevented active LacZ expression. The resultant progeny expressed Cre recombinase specifically in all CC10 positive cells, which cleaved the Lox-P sites flanking the STOP codon downstream of the constitutively active Rosa26 promoter and initiated transcription of LacZ. Consequently, the daughter cells of this parent (LacZ⁺ CC10⁺) cell then expressed LacZ irrespective of their CC10 expression status allowing one to trace their movement from their niche. LacZ transcription further led to the synthesis of β -galactosidase (β -gal) enzyme, which when exposed to 5-bromo-4-chloro-3-indolyl β -D-galactopyranoside (X-gal) substrate, produced an insoluble blue precipitate used to stain the lineage tagged daughter cells. These transgenic mice generated from crossing the ratCC10 Cre mouse with the Rosa26-LacZ reporter mice have been termed as CC10-Cre; ROSA-LacZ mice.

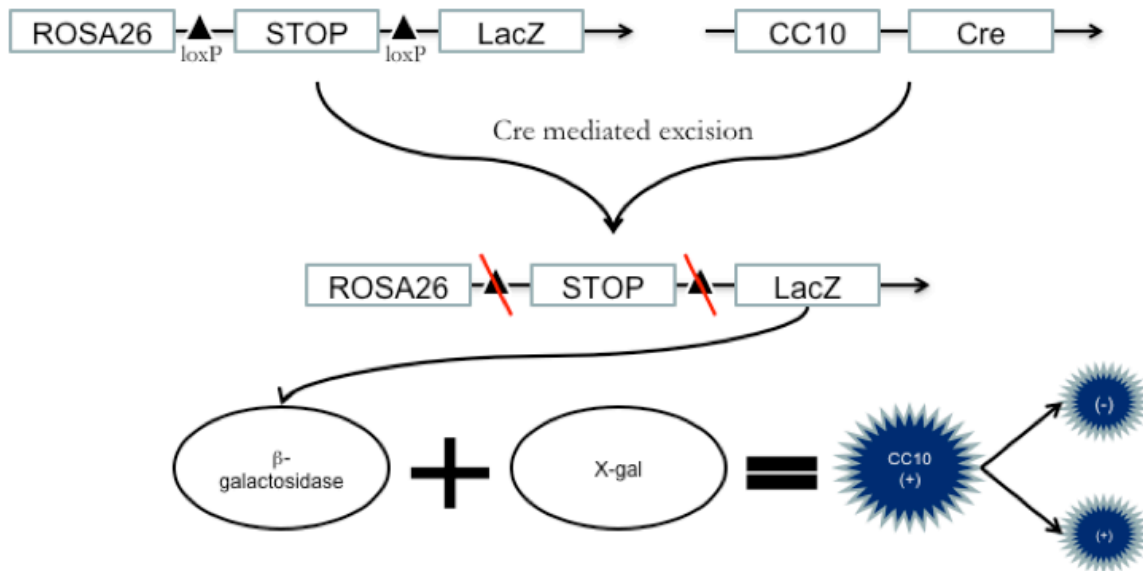


Figure 5: Lineage tracing distal bronchial epithelial cells

A schematic illustrating the breeding strategy used in the generation of CC10-Cre; Rosa26-LacZ progeny for lineage tracing DBPCs. A Rosa26-LacZ reporter mouse line was bred with a transgenic mouse line carrying Cre recombinase under the control of 2.4kb Rat CC10 promoter.

3.2.1.2 Cre specificity in the CC10-Cre; ROSA-LacZ transgenic mouse

We evaluated the specificity of ratCC10 promoter expression in the lungs of mice post-PPE induced injury/ PBS treated controls by immunofluorescence staining for ratCC10 on X-gal stained lung sections. Visualization of the stained sections indicated that ratCC10 expression was limited to β -Gal⁺ cells in the airways and not in the alveolar space both in the PPE treated mice and their controls that got treated with PBS (Appendix A, Figure 16). The protocol is detailed below under “3.2.7 Immunofluorescence staining” subsection.

Additionally to ascertain that Cre recombinase expression was selective to the airways, we immunofluorescence stained lung sections from PPE exposed transgenic mice for Cre. The stained sections on visualization by fluorescence microscopy confirmed Cre expression was specific to the airways in both the PPE as well as PBS treatment mice (Appendix A, Figure 15).

3.2.1.3 Constitutive knock-in mouse model- CC10-iCre; ROSA-LacZ

To completely rule out the possibility that there was any leakiness in Cre expression that was below our threshold of detection (as shown in Appendix A, Figure 15 & 16), we chose to use a constitutive knock-in mouse model to lineage trace the DBPCs. This knock-in mouse model with an improved version of Cre recombinase (iCre) was characterized by early embryonic expression and deeper penetration, which was knocked-in under the endogenous and constitutively active CC10 promoter (CC10-iCre) (obtained from Jackson laboratories). Dr. Francesco Demayo's group initially developed the CC10-iCre mouse (Li, Cho et al. 2008), which was later crossed

with a lipocalin2-loxP (LCN2-LoxP) mouse (Dr.Yvonne Chan at the University of Pittsburgh) and the progeny (CC10-iCre; LCN2-LoxP) banked at Jackson laboratories. These CC10-iCre; LCN2-LoxP mice were on a C57BL/6J background and then crossed with the Rosa26 reporter – LacZ mice (ROSA-LacZ) described earlier. The resultant progeny were genotyped to check for desired expression of Cre recombinase, Rosa26 reporter and the wild type lipocalin-2 gene. The mice with the appropriate genotype were termed as CC10-iCre; ROSA-LacZ mice.

3.2.2 Murine models of Emphysema

3.2.2.1 Porcine pancreatic elastase (PPE) model

The porcine pancreatic elastase (PPE) model is a well-documented model of emphysema. 8-12 week old female mice were anesthetized with ketamine/xylazine and their tracheas catheterized. The experimental group of mice received 1.5 units of PPE administered intra-tracheally and their lungs harvested over a course of 21 days. The control mice for the experiment were treated with PBS. Within the first 24 hours, the elastase caused direct alveolar damage and emphysema. This was followed by a macrophage predominant response over the remaining 20 days through an endogenous inflammatory feedback loop leading to extensive endogenous alveolar destruction.

3.2.2.2 Cigarette smoke model

The cigarette smoke exposure model has been considered the gold standard model of emphysema and involves regular exposure of mice to cigarette smoke over a span of 6 months. 8-12 week old female mice received smoke from 2 unfiltered 1R5F cigarettes, twice daily, 5 days a week, over 6 months. This model is characterized by an acute neutrophilic response, followed by the accumulation of T cells and macrophages over the next few days. These

inflammatory cells further release several elastolytic proteases that cleave the extracellular matrix, leading to slow yet progressive loss of the alveolar unit of the lung. The apparatus used to deliver the cigarette smoke to the animals has been described previously [8]. The mice tolerated 4 cigarettes per day with carboxyhaemoglobin levels under 15% and displayed no toxicity.

3.2.3 Lung tissue processing- X-Gal staining

Post-cigarette smoke exposure or PPE treatment, the animals were sacrificed at the appropriate time points by carbon dioxide narcosis. The chest cavity of the animal was exposed, their tracheas cannulated and lungs inflated with 10% normal buffered formalin (10%NBF) under 25cm H₂O pressure. Subsequently the inflated lungs were removed from the chest cavity of the mouse and fixed in 10% NBF for an hour at 4°C. The lungs were washed in 1X PBS and stained for β -galactosidase (β -gal) activity with X-Gal solution overnight at 37°C. 16-24 hours later, the lungs were washed in PBS and fixed for another 24 hours in 10% buffered formalin. These lungs were then washed once again in PBS, dehydrated in 70% ethanol, embedded in paraffin and sectioned for further analysis. Mid-sagittal sections obtained were stained and used for morphometric and histologic analysis.

3.2.4 β -gal⁺ lineage tagged cell quantification

Ten random fields per mouse lung section were selected to image at 20X magnification. The lung tissue previous stained with X-Gal for β -gal activity were used to quantify cells staining positive in the presence of X-Gal substrate, evident from the insoluble blue colored precipitate

produced. The numbers of β -gal+ cells are counted just adjacent to the BADJ junction. Additionally, β -gal+ cells that entered the alveolar compartment of the lung were counted and averaged to the number of fields counted. The β -gal+ cells in the airways were excluded for this purpose on the basis of gross histology. The average numbers of β -gal+ cells in the alveolar parenchyma determined were then normalized to the tissue density calculated from the mean chord length estimated by morphometry.

3.2.5 Morphometry

Ten random fields of modified gills stained sections per animal were captured under 200X magnification using NIS-elements program as described earlier (Nikon, Tokyo, Japan). The sections were then processed using Scion Image (Scion Corp., Fredrick, MD) avoiding all ambiguous areas, airways, smooth muscle and vasculature. The macros program computes the average chord length (alveolar diameter) of each alveolus and averages it to the total number of alveoli measured to produce a mean chord length value for each specimen.

3.2.6 Isolation of bronchoalveolar stem cells (BASCs) by fluorescence activated cell sorting (FACS)

Eight adult (> 6 weeks of age) female C57BL/6J mice were used to perform total lung digestion to isolate adequate numbers of BASCs. Mice were sacrificed by carbon dioxide narcosis. The outer layer of fur followed by the abdominal wall was incised to expose and sever the descending renal artery. Further the diaphragm was punctured to let the lungs collapse into the chest cavity and the chest wall exposed. The right ventricle (RV) of the heart was perfused using

5-10 mls of PBS. Following perfusion, the trachea was cannulated and 1.5ml of dispase (BD Pharmingen) was instilled. The lungs were then harvested and incubated with collagenase/dispase (Roche) and DNaseI (Sigma Aldrich) at 37°C for one hour to allow dissociation of the cells from the tissue. The resultant cell suspension was passed through a series of 70µm and 40µm filters to generate a single-cell suspension. The cells were resuspended in 10% fetal bovine serum (FBS) made in PBS, after red blood cell (RBC) lysis was performed.

Approximately 75-100 million cells in a single cell suspension were blocked with CD16/CD32 Fcγ III/II receptor antibody at 1µl/million cells (BD Pharmingen) on ice. The cells were subsequently stained with primary antibodies: Sca-1/FITC (BD Pharmingen), CD45-biotin (BD Pharmingen) & CD31-biotin-labelled antibodies (BD Pharmingen). After a brief wash to remove the primary antibody, the cells were incubated on ice with secondary antibodies (Streptavidin-phycoerythrin conjugated; SA-PE) (BD Pharmingen). All antibodies were used at a concentration of 1 µl/ million cells. To select for viable cells, DAPI (Molecular Probes) was used at a 200µg / ml concentration. The MoFlo-Cytomation machine was used for Fluorescent Activated Cell Sorting (FACS) at a low pressure (30Psi). The typical yield ranged approximately between 0.5~1.0% Sca-1-FITC positive/CD45-PE negative/PECAM-PE negative cells with 60-70% viability. The sorted cells were used for isolation of RNA or for cytopins to perform immunofluorescence staining. In order to assess purity, sorted cells were fixed with cytofix solution (BD Pharmingen), permeablized and stained in a single cell suspension for CC10 and SP-C using the same antibodies and concentrations mentioned in the dual immunofluorescence staining section (described below). The cells were re-suspended in the hardset mounting media with DAPI (Vector Labs), mounted on permafrost slides and cover slips were applied. The

BASCs were dual positive for SP-C and CC10 and recovered in a similar manner as described above, yielding an approximate purity of 80–90%.

3.2.7 Immunofluorescence staining

Lung sections were de-paraffinized and re-hydrated through a series of ethanols. 0.2% Triton-X-100 in 1X phosphate buffered saline (PBST) was used to permeabilize the sections and blocked with 10% normal donkey serum for an hour at room temperature. The sections were further incubated with rabbit polyclonal CC10 primary antibody (Millipore) at a 1:1000 dilution and goat polyclonal SP-C (Santa Cruz) at a 1:500 dilution overnight at 4°C. Subsequently after washing with PBST, the sections were incubated with secondary donkey anti-rabbit Alexa fluoro 594 antibody (Invitrogen) at a 1:200 dilution and donkey anti-goat Alexa fluoro 488 (Invitrogen) antibody at 1:200 dilution in PBS for 30 minutes at 37°C. The sections were washed, stained and cover-slipped using the 4', 6-diamidino-2-phenylindole (DAPI) vectastain (Vector labs) kit.

3.3 DBPC- RESULTS

3.3.1 Bronchoalveolar stem cells detected at the bronchoalveolar duct junction in normal lung tissue

Naïve C57BL/6J mice were sacrificed, their lungs processed for paraffin embedding and sections obtained were dual immunofluorescence stained for two specific cell markers: the Clara cell secretory protein -10 (CC10), which is a Clara cell specific marker and surfactant protein-C (SP-

C) that is an alveolar type-II (AT-II) cell specific marker. In addition, to decipher the nuclei of different cell types that populate the lung, the sections were stained with 4', 6-diamidino-2-phenylindole (DAPI). On imaging by fluorescence microscopy (FM), dual stained lung sections (Figure 6, panel A) indicated the presence of cells that stained positive for both CC10 (CC10+) and SP-C (SP-C+) at the bronchoalveolar duct junction (BADJ).

One of the major limitations of FM is the capture of non-specific background that arises from the illumination of the entire field by the light source. To overcome the possibility that the dual staining observed may be an artifact of this non-specific background, we pursued confocal microscopy (CM) imaging that utilizes point illumination in a single field to capture fluorescence emission from the tissue section. Imaging by CM confirmed true positive staining for CC10 and SP-C on a single cell (BASC) on dual stained lung sections as shown in Figure 6B. Thus, we were able to reproducibly detect the presence of BASCs at the BADJ as previously described by Tyler Jacks group.

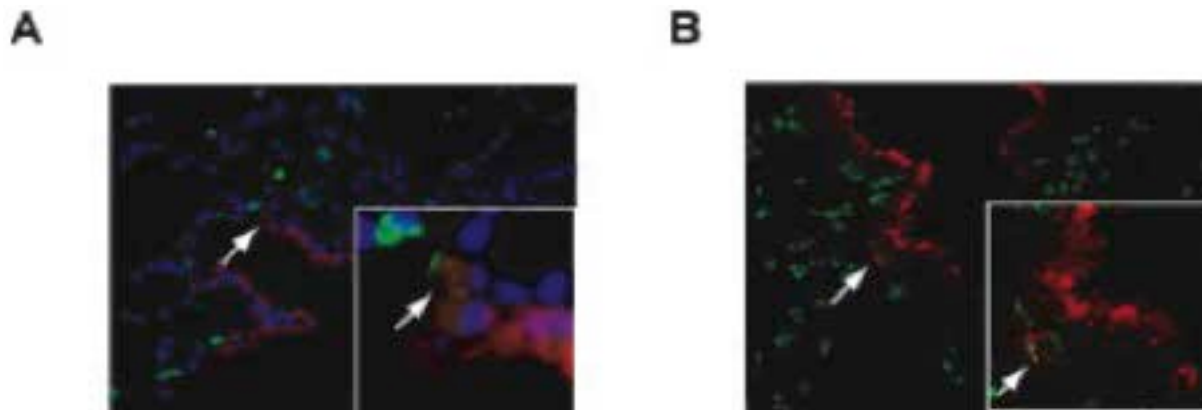


Figure 6: Detection of bronchoalveolar stem cells (BASCs) at the bronchoalveolar duct junction

Lung sections from naïve C57Bl/6J mice were stained for CC10 in red (Clara specific protein marker), SP-C in green (Alveolar type-II cell specific marker) and DAPI in blue (nuclear stain) (A) Fluorescence microscopy imaging of dual stained lung sections indicate the presence of dual positive BASCs at the BADJ (as indicated by the arrow)

(B) Confocal imaging confirms positive staining for CC10 (in red) and SP-C (in green) in the same cell (additionally seen in the magnified section of the image to the bottom right of the panel)

3.3.2 Expansion of BASC population with emphysema associated alveolar injury

To investigate if alveolar injury had any effect on the BASC population at the bronchoalveolar duct junction (BADJ), we exposed 8-12 week old female C57BL/6J mice to porcine pancreatic elastase (PPE) by intra-tracheal (IT) delivery while controls were exposed to an equivalent volume of phosphate buffered saline (PBS). The mice were sacrificed 1, 3, 5, 7, 10, 14 and 21 days post-exposure to PPE or PBS, their lungs processed for paraffin embedding and sectioning. The lung sections were dual stained for intracellular proteins, CC10 and SP-C and imaged by fluorescence microscopy (FM) as described in the methods section. The number of dual positive cells (CC10+ and SP-C+) was averaged to the number of BADJs considered per specimen and plotted as a function of day's post-PPE or PBS exposure. As seen in Figure 7A, PPE exposed mice exhibited a significant increase (1.5-fold) in the number of dual positive cells at their BADJ as early as 7 days post-exposure when compared to their PBS controls. At 21 days post-PPE exposure, a 2-fold increase ($p \leq 0.05$) was observed in the numbers of BASCs at the terminal BADJ when compared to their 21 day PBS controls (Figure 7A). Together, these findings show progressive expansion of the BASC population at the terminal bronchoalveolar duct junction (BADJ) with PPE-associated alveolar injury but not in their PBS-exposed counter-parts.

We examined the expansion of these distal BASCs in the cigarette smoke exposure model (gold-standard) of emphysema to confirm our observations in the PPE injury model, for this we exposed 8-12 week old female C57BL/6J mice to chronic cigarette smoke or room-air

over a period of 3 and 6 months before they were sacrificed. Whole lung isolations were performed and single-cell suspensions obtained were stained for cluster of differentiation 31 (CD31 or PECAM-platelet endothelial cell adhesion molecule), CD45 (hematopoietic cell marker) and stem cell antigen-1 (Sca-1). Since BASCs have been characterized to be CD31- CD45- Sca1+ (Tyler J et al., 2005); in the present study BASCs were isolated by employing fluorescent activated cell sorting (FACS) detailed in the methods section. The population of BASCs isolated was observed to be about 80% pure based on dual positive immunofluorescence staining for CC10 and SP-C (CC10+ SP-C+) on the sorted population. At 3 months post-cigarette smoke exposure, a 3.5-fold increase ($p \leq 0.05$) in CD31- CD45- Sca1+ BASCs was observed when compared to their room-air exposed counterparts (Figure 7B). Moreover, after 6 months exposure to chronic cigarette smoke the percentage of CD31- CD45- Sca1+ BASCs was observed to increase by 5-fold in contrast to their controls (Figure 7B). These results show a significant expansion of the BASC cell population in the cigarette smoke exposure model of emphysema (Figure 7B), similar to the results from the PPE injury model (Figure 7A).

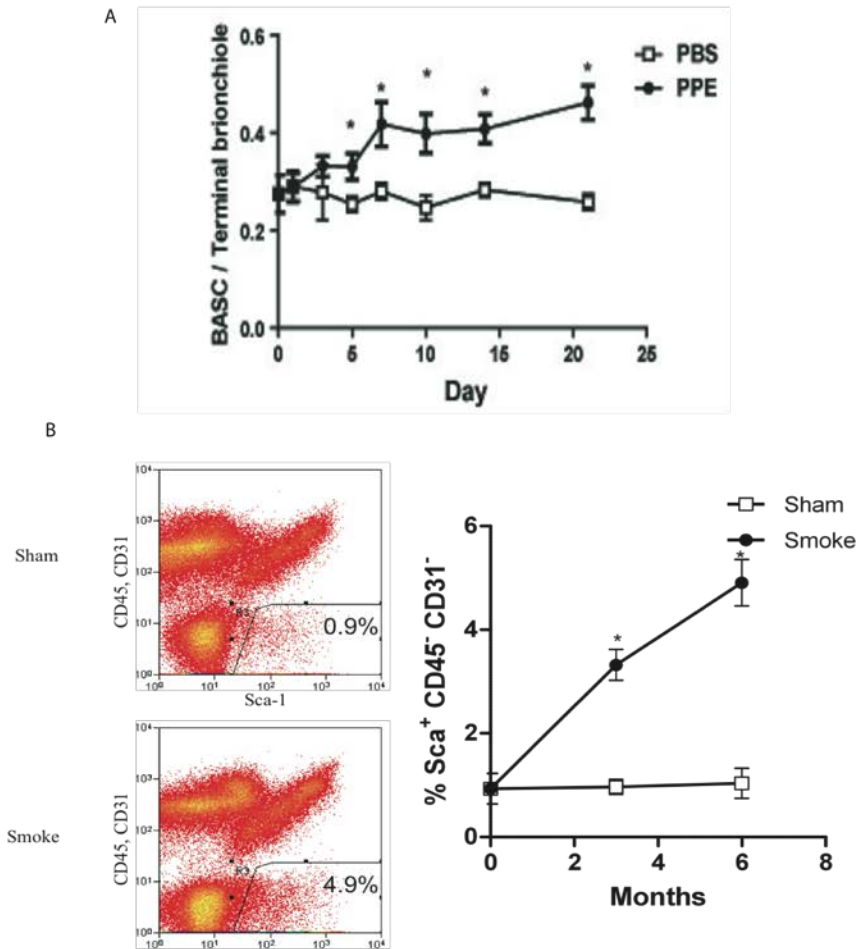


Figure 7: Expansion of BASC in the terminal BADC on emphysema-associated injury

Panel (A): Naïve C57BL/6J mice were treated IT with 1.5 units of PPE/PBS. Lung sections from the mice were dual stained for CC10 and SP-C. The number of dual positive (CC10+ SP-C+) cells were quantified over the course of 21 days and averaged to the number of BADCs counted per specimen. Panel (B): Whole lung cell isolates from 8-10 mice (C57BL/6J) exposed to chronic cigarette smoke for 3 months, 6 months and their room-air exposed controls were stained for CD31, CD45 and Sca-1. Fluorescence activated cell sorting (FACS) for the CD31⁻ CD45⁻ Sca-1⁺

population sorted the BASC population specifically. The percentage of CD31⁻ CD45⁻ Sca-1⁺ cells sorted was plotted as a function of month's post-cigarette smoke exposure.

3.3.3 Migration of distal bronchial progenitor cells from the terminal bronchiole in the context of alveolar injury

Alveolar injury has been shown to stimulate the proliferation, migration and differentiation of AT-II cells into AT-I cells on alveolar epithelial cell loss. Due to the lack of intracellular markers apart from CC10 that define Clara cells and SP-C that define AT-II cells, we were limited in our capacity to specifically follow the contribution of BASCs in the alveolar compartment and so chose to monitor the CC10 expressing distal bronchial progenitor cells (these include the BASCs as well) in the distal bronchi from this point on. To investigate the contribution of distal bronchial progenitor cells towards alveolar repair, transgenic CC10-Cre; ROSA-LacZ mice were exposed to PPE administered through the intra-tracheal route while their controls received an equivalent volume of PBS. The mice were sacrificed on 3, 5, 7, 10, 14 and 21 days post-exposure to PPE or PBS, their lungs processed for paraffin embedding and sectioning. Quantification of β -Gal⁺ cells just past the bronchoalveolar duct junction (BADJ), showed a significant and progressive increase in the number of cells that stained positive with X-Gal in the PPE exposed group in contrast to the PBS treated controls (Figure 8A). The number of β -Gal⁺ lineage tagged cells just past the bronchoalveolar duct junction (BADJ) increased from 2.4- to 3-fold between day 10 to day 21 post-PPE exposure compared to their respective PBS exposed controls (Figure 8A). Representative bright field images of lung sections shown in Figure 8B indicated a visual increase in the numbers of β -Gal⁺ cells emanating from the BADJ in the lung sections from mice that received PPE at 21 days post-exposure when compared to their PBS controls. These

observations when taken together, show a significant expansion in this progenitor cell population that proceed to migrate in significant numbers from their niche at the terminal bronchoalveolar duct junction into the adjacent injured alveolar parenchyma, as evidenced in the PPE injury model.

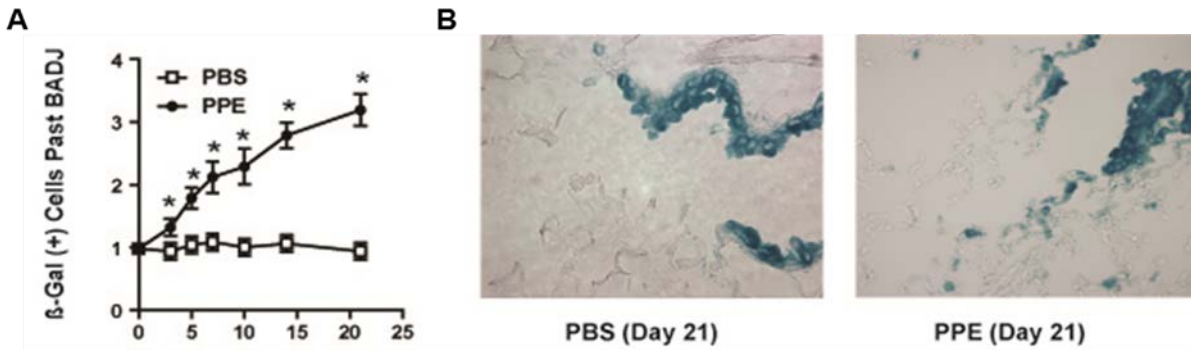


Figure 8: Migration of distal bronchial progenitor cells from the terminal bronchi in response to alveolar injury

CC10-Cre; ROSA-LacZ transgenic mice were exposed to 1.5 units of PPE (IT) and the control group received PBS. The mice were sacrificed at the various time points, their lungs inflated and stained in X-Gal solution. **(A)** Quantification of β -Gal⁺ cells just past the BADJ into the alveoli, indicating a progressive and significant increase in the numbers of β -Gal⁺ cells emanating from the BADJ in the PPE exposed mice over the course of 21 days as compared to their PBS controls. **(B)** Representative bright field images (at 60X magnification) of X-Gal stained lungs from mice 21 days post-PBS exposure (on left) and 21 days post-PPE exposure (on right) indicating blue (β -Gal⁺ lineage tagged) cells emanating from the distal bronchi of the lung.

3.3.4 Distal bronchial progenitor cells enter the alveolar space in response to emphysema associated alveolar injury

Following movement from the distal airway into the local alveolar junction, we also investigated migration throughout the alveolar space following PPE or cigarette smoke associated alveolar injury. We assessed this based on preliminary results, which indicated an increased migration of

these cells from their niche on PPE associated alveolar injury. Transgenic CC10-Cre; Rosa-LacZ mice were sacrificed at various time points post-PPE exposure and their lungs processed as elucidated earlier. The number of blue (β -Gal+ lineage tagged) cells were quantified from bright field images of X-Gal stained lung sections for each time point shown in Figure 9A. Morphometry was performed on the lung sections to determine their mean chord length, which was used to calculate their mean alveolar tissue density. The y-axis in Figure 9A shows the average numbers of β -Gal+ lineage tagged cells quantified per specimen that were normalized to their alveolar tissue density at each time-point post-exposure to PPE or PBS. The data indicated a significant increase in the numbers of blue-tagged cells in the alveolar space of mice that received PPE when compared to their PBS exposed controls. Additionally, a progressive increase in the migration of the β -Gal+ lineage tagged cells was observed into the injured alveolar compartment of the lung over the span of 21 days-post PPE exposure when compared to their PBS exposed counter-parts (Figure 9A). The bright field lung images shown in Figure 9B, reveal that more blue-tagged cells (β -Gal+) were present in the alveolar space at day 21 post-PPE exposure (right panel) when compared to their controls (left panel).

To elucidate if cigarette smoke induced injury had a similar effect on the migration of β -Gal+ lineage tagged cells into the alveolar space as seen with the PPE- injury model, 8-12 week old transgenic female mice were exposed to chronic cigarette smoke and sacrificed after 3 and 6 months smoke exposure while their controls were exposed to room-air. Quantification of the number of blue cells (β -Gal+ lineage tagged) in the alveolar space (Figure 9C) demonstrated a 2-fold increase in lineage tagged cells on 3 months exposure to cigarette smoke when compared to their room-air exposed controls. By 6 months of chronic smoke exposure, the number of blue cells (β -Gal+ lineage tagged) in the alveolar space was 3 times more in contrast to their room-air

exposed controls which were mostly unaltered over the course of 6 months (Figure 9C). This increase in numbers of blue cells (β -Gal+ lineage tagged) in the 6 month smoke exposed mice (right panel) in contrast to their room air-exposed controls (left panel) is reflected by representative bright field images of lung sections stained for X-Gal, as shown in Figure 9D. These results considered together indicate a critical contribution of the β -Gal+ lineage tagged terminal bronchial progenitor cells towards migrating into the injured alveolar compartment of the lung in response to PPE or cigarette smoke associated injury in a potential attempt to repair.

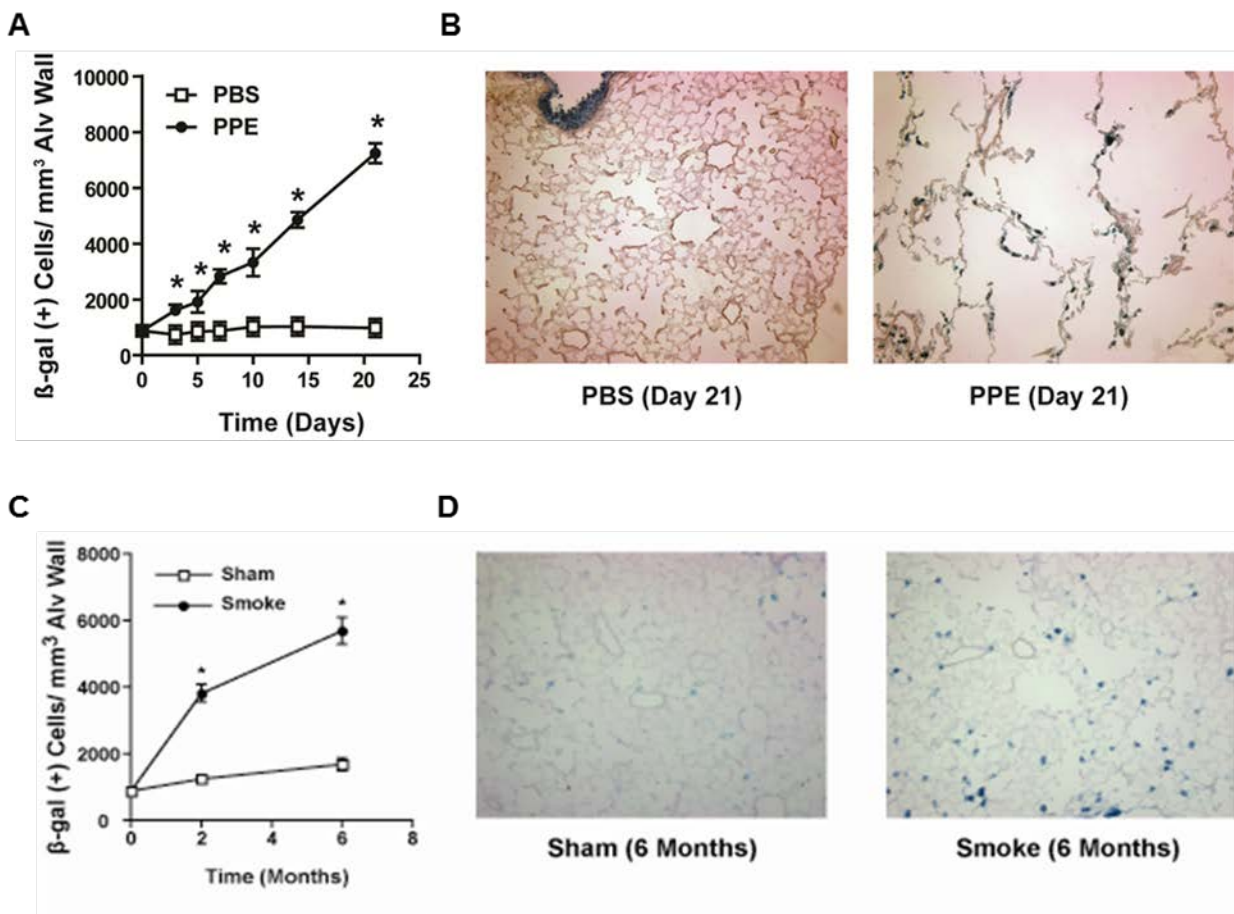


Figure 9: Migration of Distal bronchial progenitor cells from the BADJ into the injured alveolar compartment of the lung

Transgenic (CC10-Cre; ROSA-lacZ) mice were exposed to PPE/PBS over the course of 21 days (A&B) or exposed to chronic cigarette smoke/room-air for 3 and 6 months (C&D) before being sacrificed. The lungs from these mice

were inflated, stained with X-Gal and processed for sectioning as detailed in the methods. (A) β -Gal+ lineage tagged cells that enter the alveolar space were quantified and normalized to the alveolar tissue density. PPE exposed mice displayed a significant increase in the numbers of β -Gal+ cells in the alveolar space, which showed a linear progression as a function of days post-exposure in contrast to the PBS exposed controls. (B) Representative bright field (BF) images at 40x magnification of 21days post- PBS exposed (on left) and post-PPE exposed (on right) X-gal stained lung sections indicating the presence of blue (β -Gal+ lineage tagged) cells in the alveolar space. (C) Cigarette smoke exposure leads to ~ 2 fold increase in β -Gal+ cells at 3 months post-exposure and by 6 months this progresses to ~3 fold increase in lineage tagged cells entering the alveolar space when compared to their respective controls. (D) Visualization of representative BF image of a 6-month room-air exposed controls indicating relatively fewer blue (β -Gal+ lineage tagged) cells as compared to the 6 month cigarette smoke exposed (on right) lung section.

3.3.5 Lineage tagged distal bronchial progenitor cells give rise to alveolar type-II and alveolar type-I epithelial cells

The increased migration of lineage tagged terminal bronchial progenitor cells into the injured alveolar compartment of the lung leads to the question as to whether they differentiate into the local alveolar epithelial cell population or not. To investigate this, X-Gal stained lung sections obtained from transgenic CC10-Cre; Rosa-LacZ mice exposed to PPE or PBS through intratracheal (IT) instillation were examined. These lung sections demonstrated bright blue staining in their β -gal expressing parent (in the terminal bronchi) and daughter cells (in the alveolar space) irrespective of their CC10-expression status. As shown in Figure 10, bright blue staining was observed not only in the CC10-expressing airway epithelium (Figure 10, panels A and B) but also in the alveolar type-II (AT-II) epithelial cells that are present in the alveolar parenchyma in the PPE exposed group (Figure 10, panels B and D). Alveolar type-I (AT-I) epithelial cells however are thinner and have elongated cell bodies leading to poor visualization of the stain,

hence a blue speckling on staining with X-gal is observed. At 21 days post-PPE exposure the blue speckling in the AT-I epithelial cells was observed to be more predominant (indicated by arrows in Figure 10, panels B and D) when compared to their PBS exposed controls (Figure 10, panels A and C).

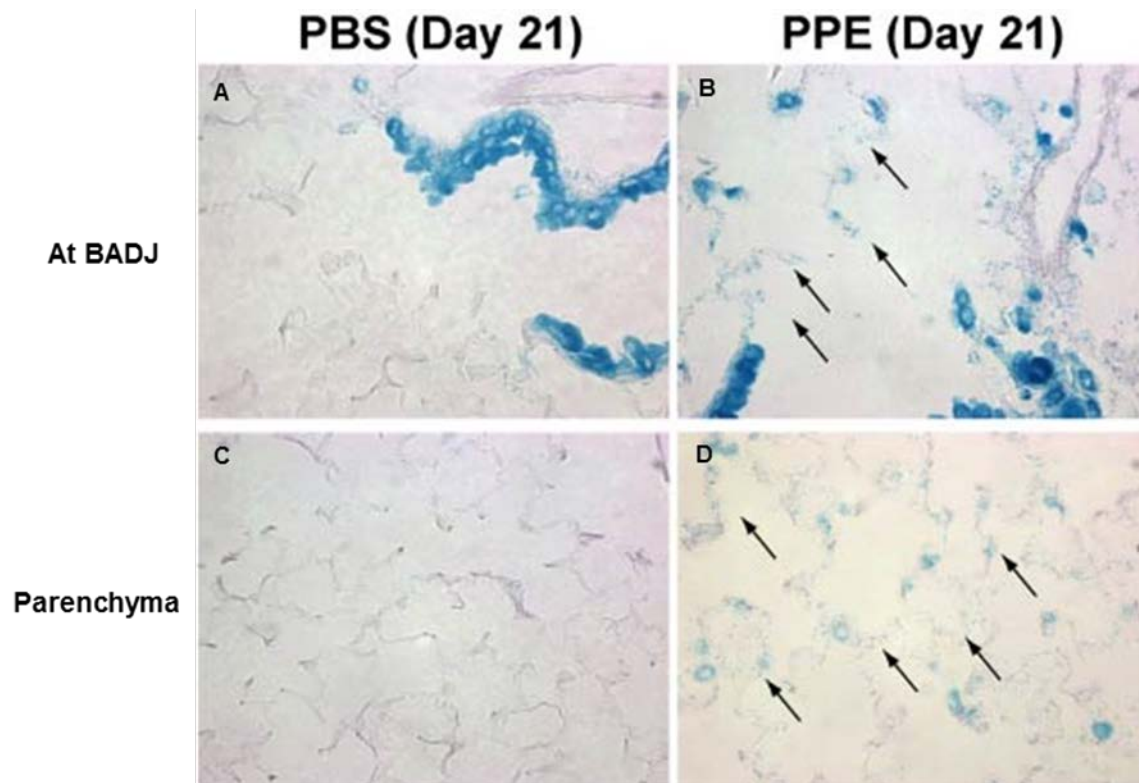


Figure 10: β -Gal⁺ lineage tagged cells arising from the terminal bronchi give rise to AT-I and AT-II epithelial cells post-PPE injury

Representative bright field images at 60X magnification from 21 day PBS treated mice stained with X-Gal show bright blue staining in their airways, some staining on the AT-II epithelial cells and no significant staining in their AT-I epithelial cells (A & C). The 21-day PPE exposed mouse lungs in contrary showed bright blue staining on their AT-II epithelial cells as well as blue speckling in their AT-I cells (indicated by the arrows) as shown in panels (B & D) on the right.

To validate if the lineage tagged β -Gal⁺ cells that enter the alveolar compartment from the BADJ truly differentiate into AT-II epithelial cells, lung sections were dual stained for SP-C

(AT-II cell specific marker) and CC10 (a Clara cell specific marker) to monitor the β -Gal+ tagged cells in the alveolar parenchyma. Comparing the representative bright field images (Figure 11B) to the dual IF stained fluorescence images (Figure 11D) of lung sections from PPE treated mice at 21 days post-exposure, a large number of blue (β -Gal+ lineage tagged) cells in the alveoli were found to stain positive for SP-C (indicated by arrows in Figures 11B and 11D). Additionally, similar expression of SP-C in the blue staining cells was observed in the alveoli of the PBS controls although fewer in number than in the PPE treated mice (Figures 11A and 11C). The loss of CC10 expression and the subsequent gain of SP-C expression by the lineage tagged (β -Gal+) cells originating from the BADJ confirms that the lineage tagged (β -Gal+) cells which originate from the BADJ truly differentiate into AT-II epithelial cell in the context of PPE associated alveolar injury.

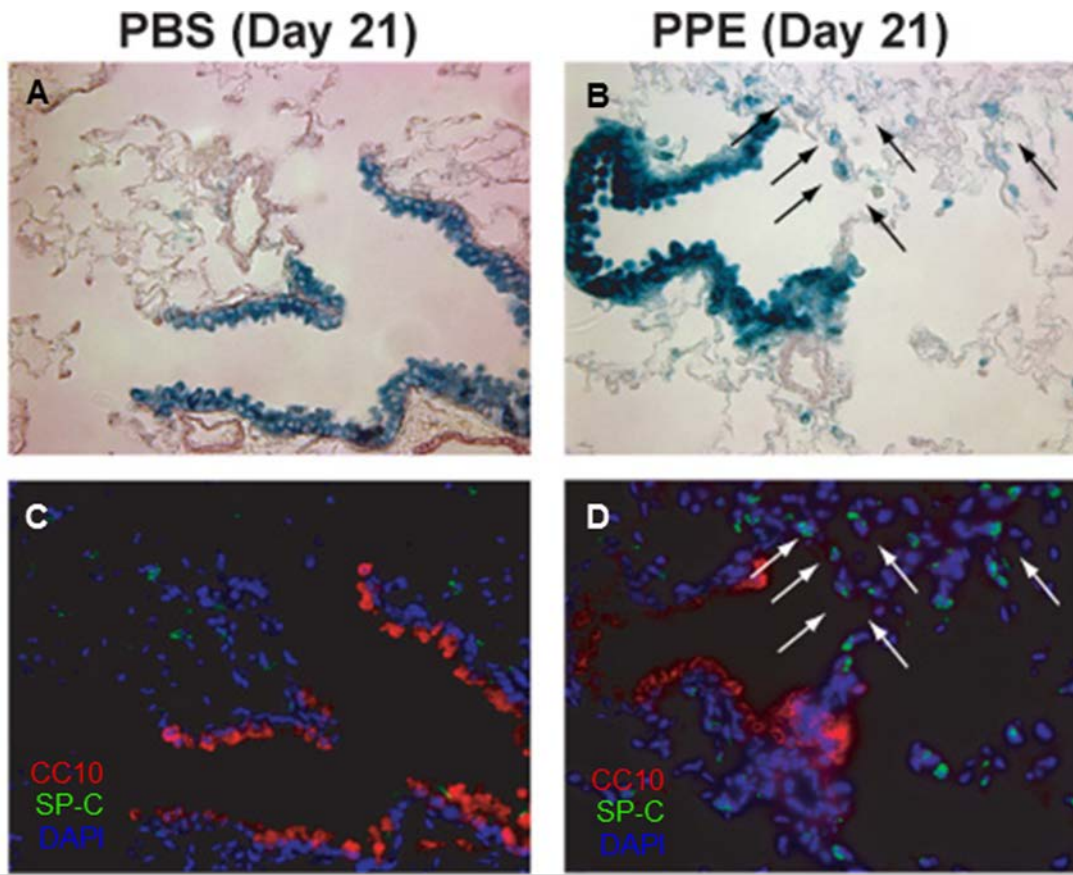


Figure 11: SP-C expressing β -Gal⁺ lineage tagged cells visualized around the BADJ on PPE exposure

X-Gal stained lungs from 21-day PPE exposed and PBS exposed mice were dual stained using immunofluorescence for CC10 (Clara specific) and SP-C (AT-II specific). Top panels indicate representative bright field images of a PBS exposed mouse lung (A) and a PPE exposed mouse lung (B), 21 days post-exposure. Bottom panels show corresponding fields imaged by fluorescence microscopy, indicating SP-C in green (AT-II specific marker) and CC10 in red (Clara cell specific). The β -Gal⁺ lineage tagged cells staining blue in the alveolar compartment additionally stain positive for SP-C (indicated by arrows) in both PPE exposed (D) mice and their PBS exposed controls (C) 21 days post-IT exposure.

Finally, we examined lung sections from transgenic (CC10-Cre; Rosa-LacZ) mice that had been exposed to chronic cigarette smoke/ room air for 6 months to trace the β -Gal⁺ lineage tagged cells from the distal airway into the alveolar space, to confirm our observations in the

PPE injury model. Representative bright field images from 6-month smoke exposed mice in Figure 12, panels B and D; indicated bright blue staining in the cuboidal AT-II epithelial cells as well as the wispy AT-I epithelial cells. The room-air exposed control mice did not show significant blue staining on the AT-I or AT-II epithelial cells around the BADJ (Figure 12A) or lining the alveolar space (Figure 12C). Together these observations, confirmed the true differentiation of β -Gal⁺ lineage tagged cells into AT-I and AT-II epithelial cells that repopulate the damaged alveoli.

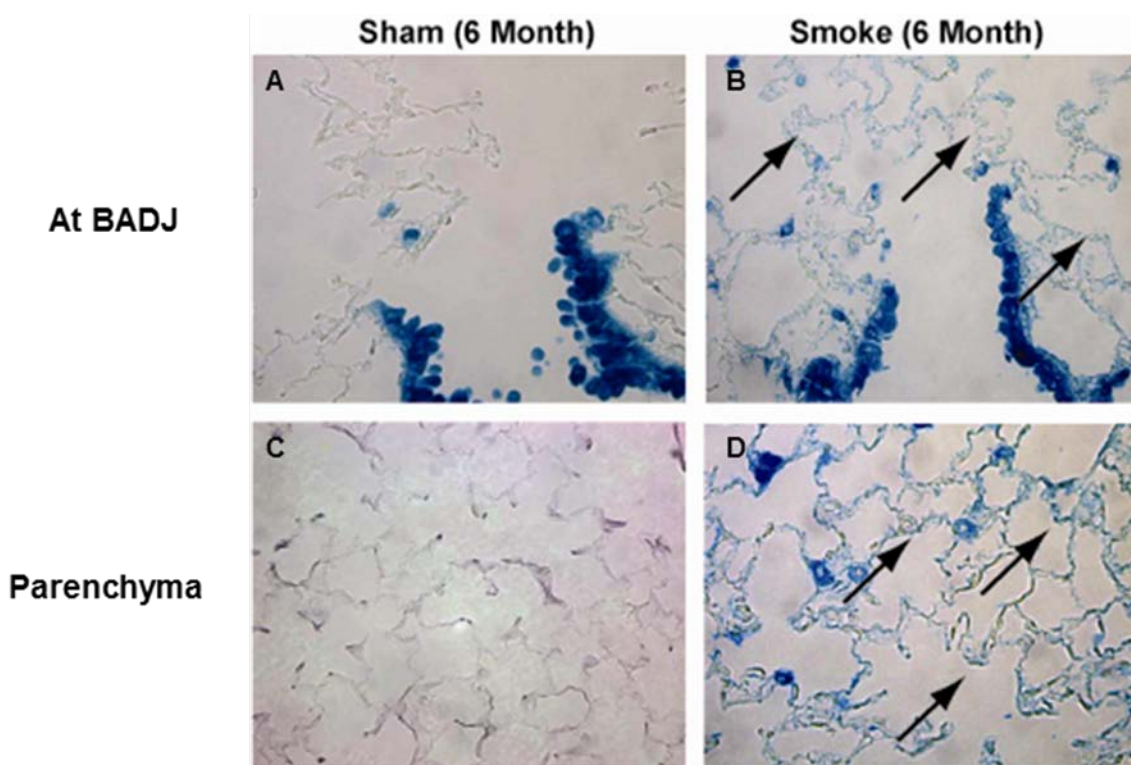


Figure 12: β -Gal⁺ lineage tagged cells arising from the terminal bronchi give rise to AT-I and AT-II epithelial cells post-cigarette smoke induced injury

Top panels (A & B) show representative bright field images at the BADJ of X-Gal stained lung tissue and the bottom panels (C & D) show images from the alveolar parenchyma at 60X magnification. The CC10-Cre; Rosa-LacZ transgenic mice were exposed to chronic cigarette smoke (B & D) over a period of 6 months and their controls to room-air (A & C). The black arrows (\rightarrow) point at blue speckling observed in the AT-I epithelial cells (β -Gal⁺ lineage tagged) predominantly in the 6 month cigarette smoke exposed mouse lung sections (B & D). Bright blue

staining was observed in the AT-II cells at the BADJ both in the chronic smoke exposed (B) as well as the shams (A).

3.3.6 Lineage tagged cells emanate from the BADJ and repopulate the alveoli in a constitutive CC10-iCre; Rosa-LacZ knock-in mouse line in the context of PPE associated injury

The transgenic (CC10-cre; Rosa-LacZ) mouse line developed in-house when tested for specificity and exclusivity of Cre expression in CC10 expressing cells showed no leakiness of Cre expression by immuno histochemistry. Nevertheless to rule out the possibility that the transgenic Rat CC10 promoter may have leaky expression below the threshold of detection of the tests performed; we used a knock-in CC10-iCre; Rosa –LacZ mouse line to validate our findings. To investigate if the distal bronchial progenitor cells present at the BADJ expressing lacZ emanated into the injured alveolar space, 8-12 week old female CC10-iCre; Rosa-LacZ knock-in mice were exposed to intra-tracheal (IT) instillation of PPE or PBS for 21 days. The mice were sacrificed at the end of 21 days, their lungs inflated and stained for X-Gal. Quantification of the numbers of β -Gal⁺ cells past the BADJ indicated a significant increase (3-fold) in the PPE-exposed mice when compared to their PBS exposed controls (Figure 13A). Visualization of representative bright field images (Figure 13B) of lung sections from the PPE-exposed mice (right panel) indicated more blue (β -Gal⁺ lineage tagged) cells adjacent to the terminal bronchi in contrast to their controls (left panel). These observations from the knock-in mouse line corroborated the initial findings described earlier in the transgenic mouse line and emphasized the critical contribution of the distal bronchial progenitor cells (initially CC10 expressing) in repopulating the injured alveolar compartment.

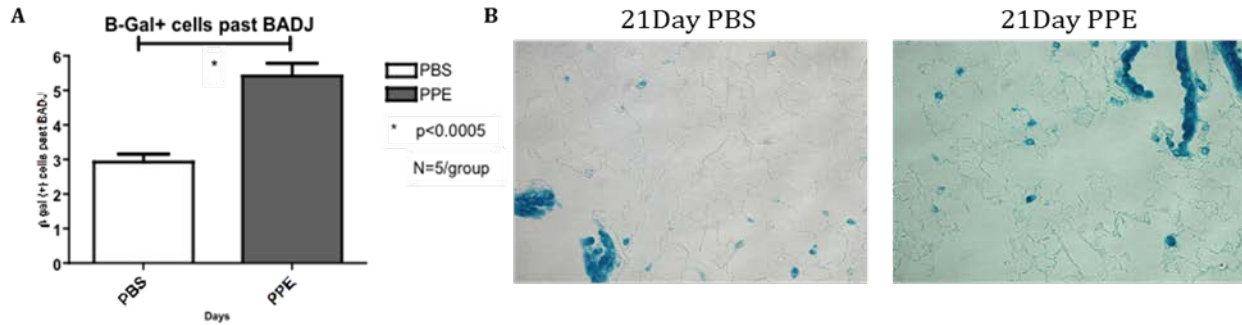


Figure 13: Migration of β -Gal⁺ lineage tagged cells from the BADJ into the damaged alveoli in the knock-in mouse model

Knock-in CC10-iCre; Rosa-LacZ mice were instilled IT with 1.5 units of PPE, the mice sacrificed at 21 days since exposure, their lungs inflated and stained with X-Gal. (A) Quantification of numbers of blue (β -Gal⁺ lineage tagged) cells near the BADJ indicated significantly increased lineage tagged cells emanating from the BADJ at 21 days post-PPE exposure as compared to their controls. (B) Representative bright field images of lung sections from mice exposed to PBS (on left) and PPE (on right) at 21 days post-exposure indicating lineage tagged cells near the BADJ at 40X magnification

In addition, dual immunofluorescence staining on lung sections from these knock-in mice were stained for CC10 and SP-C, this confirmed that the β -Gal⁺ lineage tagged cells emanating from the BADJ were truly giving rise to SP-C expressing AT-II cells in the alveolar epithelium. Comparative analysis of bright field images of X-Gal stained lung sections along with their dual immunofluorescence stained counterparts clearly showed that a number of blue (β -Gal⁺ lineage tagged) cells that had emanated into the alveolar space actively expressed SP-C (AT-II cell specific marker) as indicated by the arrows in Figure 14A and 14B. These findings in the knock-in mouse line when taken together with the increased recruitment of distal bronchial progenitor cells (DBPCs) into the damaged alveoli, confirm that the DBPCs emanating from the distal terminal bronchi lose their CC10- expression status and begin actively expressing SP-C as they

repopulate the alveolar parenchyma of the lung. Validation of our experimental observations in the transgenic mouse line using the knock-in mouse line highlighted the critical role of these DBPCs in mediating alveolar repopulation especially under alveolar-associated damage.

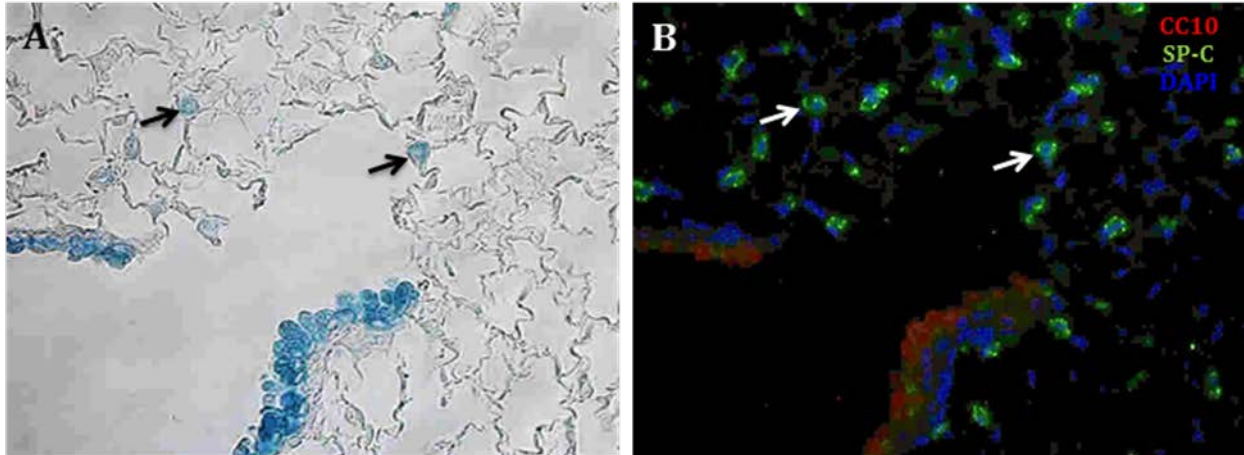


Figure 14: β -Gal⁺ lineage tagged cells emanating from the BADJ into the alveolar space express SP-C

Knock-in CC10-iCre; ROSA-LacZ mouse lungs stained for X-Gal and dual immunofluorescence stained. **Panel A:** representative bright field image at 40X magnification of the X-Gal stained lung. **Panel B** shows the same field imaged by fluorescence microscopy, indicating SP-C in green (AT-II specific marker), CC10 in red (Clara cell specific) and DAPI in blue. Arrows indicate β -Gal⁺ lineage tagged cells that have taken on active SP-C expression (AT-II epithelial cell specific) while no longer expressing CC10.

3.4 DBPC- DISCUSSION

Understanding the events that lead to lung tissue damage/destruction coupled with the activation of adult stem/progenitor cell populations facilitating lung repair and maintenance is critical to the study of regenerative medicine. Several adult lung progenitor cell populations have been implicated in repairing the airway or the alveolar compartment of the lung using a variety of chemical injury models, however the contribution of a single adult lung progenitor cell

population in both compartments of the lung has remained controversial. A number of lung pathologies have been characterized by the loss or modification of specific cell subsets in response to insult, including mutations in certain cell populations leading to cancers and oxidative/cellular stress leading to senescence, apoptosis or necrosis. Specifically in emphysema, a common manifestation of COPD, we observe a significant loss of the alveolar units within the lung parenchyma. In the present study, our data points towards compelling evidence highlighting the contribution of previously described (Giangreco, Reynolds et al. 2002, Kim, Jackson et al. 2005) distal bronchial progenitor cell populations (BASC and variant Clara cells) nestled in the terminal bronchoalveolar duct junction (BADJ) towards alveolar repair in the context of emphysema associated injury.

Bronchoalveolar stem cells (BASC), initially described to be resistant to airway (naphthalene) and alveolar (bleomycin) injury, were shown to proliferate in presence of oncogenic K-Ras. In vitro studies have indicated their capacity to differentiate into both CC10 expressing Clara cells as well as SP-C expressing alveolar type-II epithelial cells (Kim, Jackson et al. 2005). Although the BASCs were initially characterized to express cell surface markers: stem cell antigen- 1 (Sca-1) and cluster of differentiation 34 (CD34) and lack expression of CD31 (endothelial cell marker) and CD45 (a marker of hematopoietic cells); recent studies have questioned the exclusivity of these markers on these putative stem cells (McQualter, Brouard et al. 2009, Hittinger, Czyz et al. 2013). Aware of this limitation we decided to strictly monitor the contribution of CC10 expressing distal bronchial progenitor cells (DBPCs) using a transgenic CC10-Cre; Rosa-LacZ mouse strain as a tool for lineage tracing. Using this system, we studied the expansion and migration of these cells from the BADJ into the surrounding alveolar space under porcine pancreatic elastase (PPE) induced alveolar injury. The significantly elevated

numbers of β -gal+ lineage tagged progenitor cells at the BADJ and their subsequent migration into the (PPE mediated) injured alveolar parenchyma (Figure 8, Figure 9A and 9B) were corroborated in the GOLD standard 6-month cigarette smoke model (Figure 9C and 9D), which indicated a similar involvement of these progenitor cells in repopulating the damaged alveolar compartment of the lung.

Dual immunofluorescence staining for surfactant protein-C (SP-C), an alveolar type-II epithelial cell specific marker in addition to Clara cell specific secretory protein-10 (CC10) on X-Gal stained lung sections, enabled for the quantification of β -Gal+ cells that had migrated into the alveolar compartment and subsequently differentiated into alveolar type-II epithelial (AT-II) cells. Bright field imaging of X-gal stained transgenic mouse lung sections displayed bright blue staining on the AT-II cells; while the wispy and thin alveolar type-I epithelial (AT-I) cells displayed blue speckling in their stretched out cytoplasm (Figure 10, 11 and 12). Using a Rosa-eYFP reporter mouse crossed with the transgenic RatCC10-Cre mouse, we traced these bronchial progenitor cells that had given rise to both SP-C expressing AT-II cells and aquaporin-5 (AQP-5) expressing AT-I cells by dual immunofluorescence staining for enhanced yellow fluorescent protein (eYFP) (not shown). Our findings confirm the direct contribution of β -Gal positive lineage tagged cells (distal bronchial progenitor cell) that arose from the terminal bronchial duct junction and gave rise to both alveolar type-I and type-II epithelial cells in the injured alveolar parenchyma.

Contrary to findings from other studies that suggest that these CC10 positive lineage tagged bronchial progenitor cells do not play a role in alveolar repair (EL Rawlins et. al, 2009), results obtained from our transgenic mouse line used to lineage trace the CC10+ progenitor cells migrating from their niche in the terminal bronchiole showed a significant repopulation of the

injured alveolar compartment. The reasoning behind these differing observations could stem from the fact that different injury models (hyperoxia versus PPE) may have very different cellular and structural outcomes in vivo. Further, the tamoxifen inducible (dose-dependent) Cre expression system has its own limitations (dose dependency) when used to lineage trace cells from their niche. In a subsequent independent study, the CC10-CreERTM mouse line developed by Hogan's group was bred with an ACTB-mT-EGFP transgenic mouse line to develop a lineage tracing system that would enable the authors to look at the contribution of the CC10-expressing population stemming from the airways towards alveolar repair (Zheng, Limmon et al. 2012). Their results indicated similar regenerative potential of CC10 (also known as secretoglobulin1a1- scgb1a1) expressing distal airway-derived cells towards repopulating the damaged alveolar compartment under bleomycin and influenza associate injury (Zheng, Limmon et al. 2012). These observations support and further strengthen the results obtained in the present study utilizing the transgenic mouse model (RatCC10-Cre; Rosa26-LacZ).

The specificity of Cre expression on RatCC10 expressing cells lining the airways was investigated by immunofluorescence (IF) staining on lung sections from the transgenic mice (RatCC10-Cre; Rosa-LacZ) exposed to PPE over the course of 21 days. Visualization post-IF staining by fluorescence microscopy revealed that Cre recombinase expression was limited to RatCC10 expressing cells lining the airways of these transgenic mice (Appendix A, Figure 15 and 16). To overrule non-specific Cre expression or expression of Cre below our threshold for detection in the transgenic mouse line, we obtained a CC10-iCre knock-in mouse line that expressed an improved version of Cre recombinase under the endogenous mouse CC10 promoter (Li, Cho et al. 2008). This knock-in mouse line initially generated by DeMayo's group at Baylor college of medicine was bred with our Rosa26-LacZ reporter mouse line to generate a CC10-

iCre knock-in mouse strain (CC10-iCre; Rosa-LacZ) that expressed LacZ in all its endogenous CC10-expressing cells. Exposure of this knock-in mouse line to PPE over 21 days confirmed the migration of the CC10 expressing β -Gal⁺ lineage tagged cells into the damaged alveolar compartment (Figure 13). Additionally, we did observe β -Gal⁺ lineage tagged cells in the knock-in mouse line that enter the alveolar compartment actively expressing SP-C on losing their CC10 expression status, thereby differentiating into AT-II epithelial cells (Figure 14).

Alveolar type-II epithelial cells have long been implicated as a progenitor cell population for the more fragile alveolar type-I epithelial population (Evans, Cabral et al. 1975, Aso, Yoneda et al. 1976). However, whether all AT-II cells are uniformly able to regenerate and replenish AT-I cells is unclear. Under PPE and cigarette smoke related injury; loss of AT-I cells can lead to the proliferation and differentiation of AT-II cells into AT-I cells. Further as indicated in our transgenic and knock-in mouse models, we observe that the CC10 expressing terminal bronchial epithelial progenitor cells differentiated into AT-II cells and perhaps AT-I cells even (Figures 10,11,12 and 14). In staining for SP-C and Ki67 (a marker of proliferation) not only did we observe an increase in the SP-C expressing AT-II cell population post-injury but that these cells were actively proliferating (not shown). These findings suggest a multi-cellular approach towards repair of the damaged alveolus, although the specific sequence and extent of contributions are undetermined.

Our study defines a role for CC10⁺ distal bronchial progenitor cells towards repairing and repopulating the injured alveoli under emphysema-associated injury. By understanding the stimuli that potentiate the activation of these progenitor cells causing them to proliferate, migrate into the injured alveolar compartment and differentiate into local alveolar epithelium, we can aim at

recreating the same environment and triggers to elicit endogenous repair. Thus hope to treat this devastating disease.

3.5 DBPC- FUTURE DIRECTIONS

The results of this study demonstrate that distal bronchial progenitor cells in the terminal bronchiole are capable of re-populating damaged alveoli by giving rise to alveolar type-II and type-I epithelial cells. The nature of molecular cues that lead to the activation of these progenitor cells perhaps during early lung development may lead us to better understand how we may recapitulate the activation of these cells to repair in the context of injury. Fibroblast growth factor-10 (FGF10) and FGFR2b (fibroblast growth factor receptor 2 (III) b) null mice have been shown to have normal larynx and tracheal development, however they lacked distal bronchi. Several other studies as well have highlighted the importance of FGF10-FGFR2b signaling in amplifying peripheral progenitors in early lung development [106, 258, 259]. Inhibition of epidermal growth factor (EGF) expression during early mouse lung development showed a 75% decrease in branching lung morphogenesis [260]. Deficiency in Smad-3, a main intracellular mediator of transforming growth factor- β (TGF- β) receptor signaling caused early onset of emphysema due to disrupted organization of matrix and increased MMP activity [259]. Most of the studies outlined above point towards the involvement of growth factors and intracellular mediators in alveolar morphogenesis. In the future we would need to study the roles of these factors on the distal bronchial progenitor cell population and how they may potentiate a micro-environment suitable for repair in the context of cigarette smoke induced alveolar injury. One may argue that these distal bronchial progenitor cells being an adult progenitor cell population

with limited differentiation potential may find limited application while studying the role of developmental cues in the context of injury, however that said recent studies highlight epithelial adaptability and their capacity to reversibly express mesenchymal features to aid in tissue remodeling [261]. Hence the lung microenvironment and cross-talk between neighboring cells may largely dictate the activation of these progenitor cell populations in their niche to self-renew, migrate and differentiate into terminally differentiated epithelial cell populations especially in the context of injury.

In order to repair; progenitor cells need to be able to proliferate, migrate and differentiate into the local epithelial cell population. Matrix metalloproteinases (MMPs) have been implicated in regulating growth factor availability, remodeling cell-cell and cell-matrix contacts and promoting overall cell-survival [262]. Several MMPs have been shown to cause EGF release from the underlying basement membrane [263, 264]. MMP-7 or Matrilysin has been shown to contribute to airway epithelial cell repair [265]. MMP-9 null mutant mice were shown to have impaired alveolar bronchiolarization on bleomycin-induced injury when compared to their wild-type counter-parts [266]. Therefore our next steps would involve studying the expression of key MMPs and their involvement in DBPC migration in the context of cigarette smoke induced alveolar injury.

Identification of cell surface markers that specifically characterize progenitor cell populations in the lung coupled with the advancement of techniques that can enable us to specifically study progenitor population subsets will lead to a better understanding of relative contributions of these cells under homeostasis and in the context of injury. Recent approaches to characterizing cell surface markers involve isolating proteoglycans in the cell membrane using an enzyme-free cell dissociation solution and purified by affinity chromatography, known as cell

surface capture (CSC) technology. The isolated peptides (affinity purified) are further analyzed by mass spectrometry and the resultant spectra are analyzed using bioinformatic and hierarchical clustering databases to identify new cell surface proteins [267-269]. By systematically isolating and identifying the cell surface proteins on CC10 expressing DBPCs, CC10⁺ terminally differentiated Clara cells, CC10⁺ SP-C⁺ BASCs, SP-C⁺ alveolar type-II progenitor cells and terminally differentiated AT-II cells, we can hope to better dissect their independent roles in alveolar repopulation in the context of injury.

Aside from assessing the mechanistic roles of these progenitor cells, we do observe better repair responses in female mice in comparison to their male counterparts. Gender based differences in reparative responses and the extent of injury have been discussed in different injury models [270, 271]. Yet we do not completely understand how gender may impact an organ's ability to repair or sustain damage. Further, mouse models have their own limitations in that they do not entirely reflect the complexity seen in human disease. Environmental exposure, genetic susceptibility, variable response to treatment, variation in injury observed and general lifestyle habits have been shown to impact the extent of human disease. Hence finding an analogous human progenitor cell population sharing the same capacity to repair and regenerate the alveolus as investigated in a mouse model is a goal. Realization of which will enable us to translate these observations into potential treatments in the clinic.

APPENDIX A

SELECTIVITY AND SPECIFICITY OF RAT-CC10 PROMOTER EXPRESSION IN CC10-CRE; ROSA-LACZ TRANSGENIC MICE

In order to validate the specificity of Cre recombinase expression and exclude the possibility of a random insertion of the RatCC10 promoter - CRE construct in the mouse genome, we performed immunofluorescence staining for RatCC10 and Cre recombinase on transgenic mice that were exposed to PPE (intra-tracheal) and compared them to their controls that received PBS. The immunofluorescence staining for Cre and visualization by fluorescence microscopy confirms that Cre is expressed specifically in the airways and not in the alveolar parenchyma, both in the presence and absence of injury (Figure 15). Further staining for Rat CC10 confirms its expression to be limited to the airways in the lungs of the transgenic mice in the presence of PPE induced injury (Figure 16). These findings confirm that the Rat CC10 promoter is not leaky in its expression and that its subsequent expression of Cre recombinase is limited to epithelial cells lining the airways in the lungs of the transgenic mice.

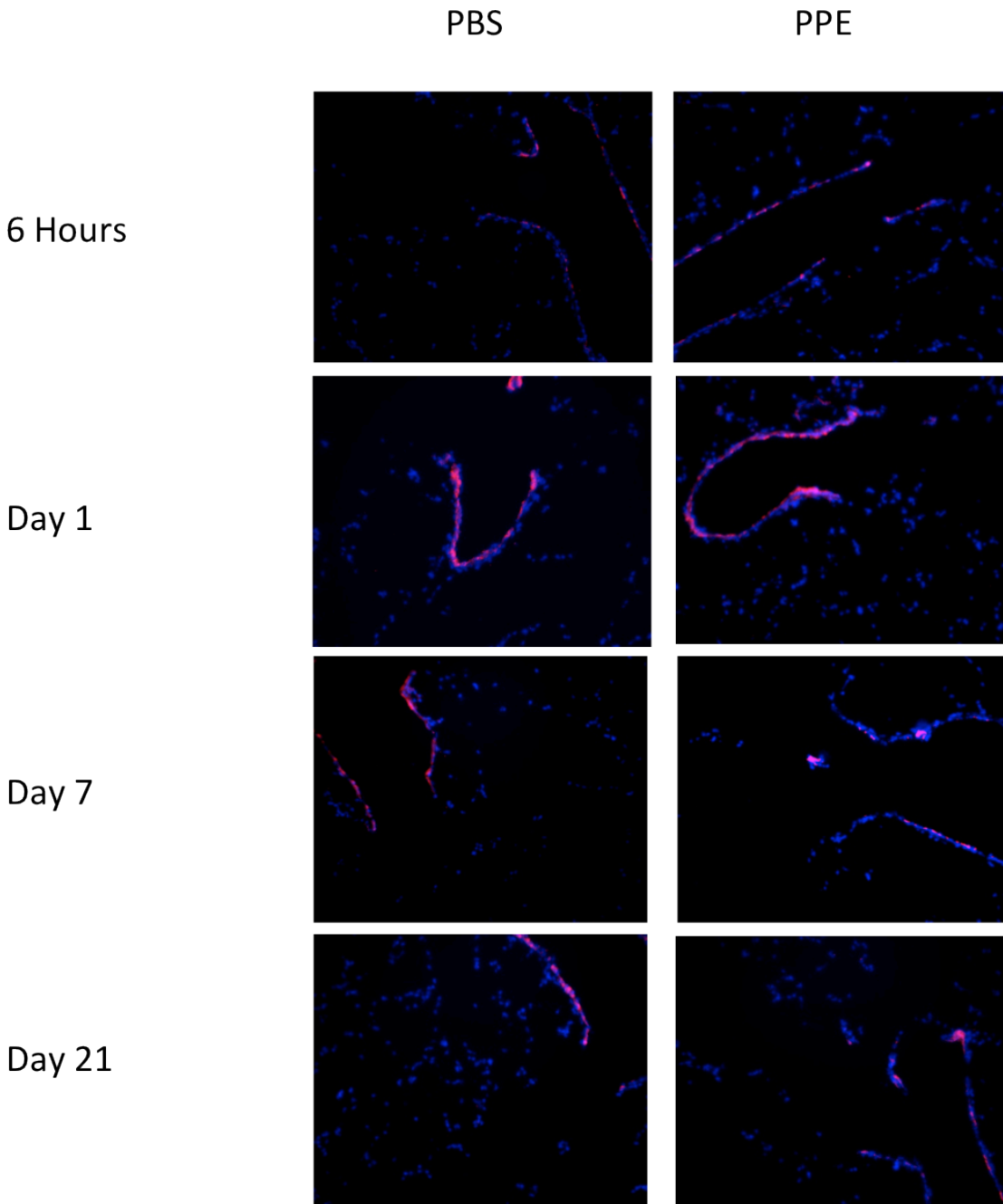


Figure 15: Cre expression limited to the airways and not found in the lung parenchyma.

Transgenic CC10-Cre; ROSA-LacZ mouse lungs exposed to PPE (panels on right) were stained for Cre expression over the course of 21 days and compared to their PBS controls (panels on left). The nuclear stain (DAPI) used stains blue and Cre stains in red.

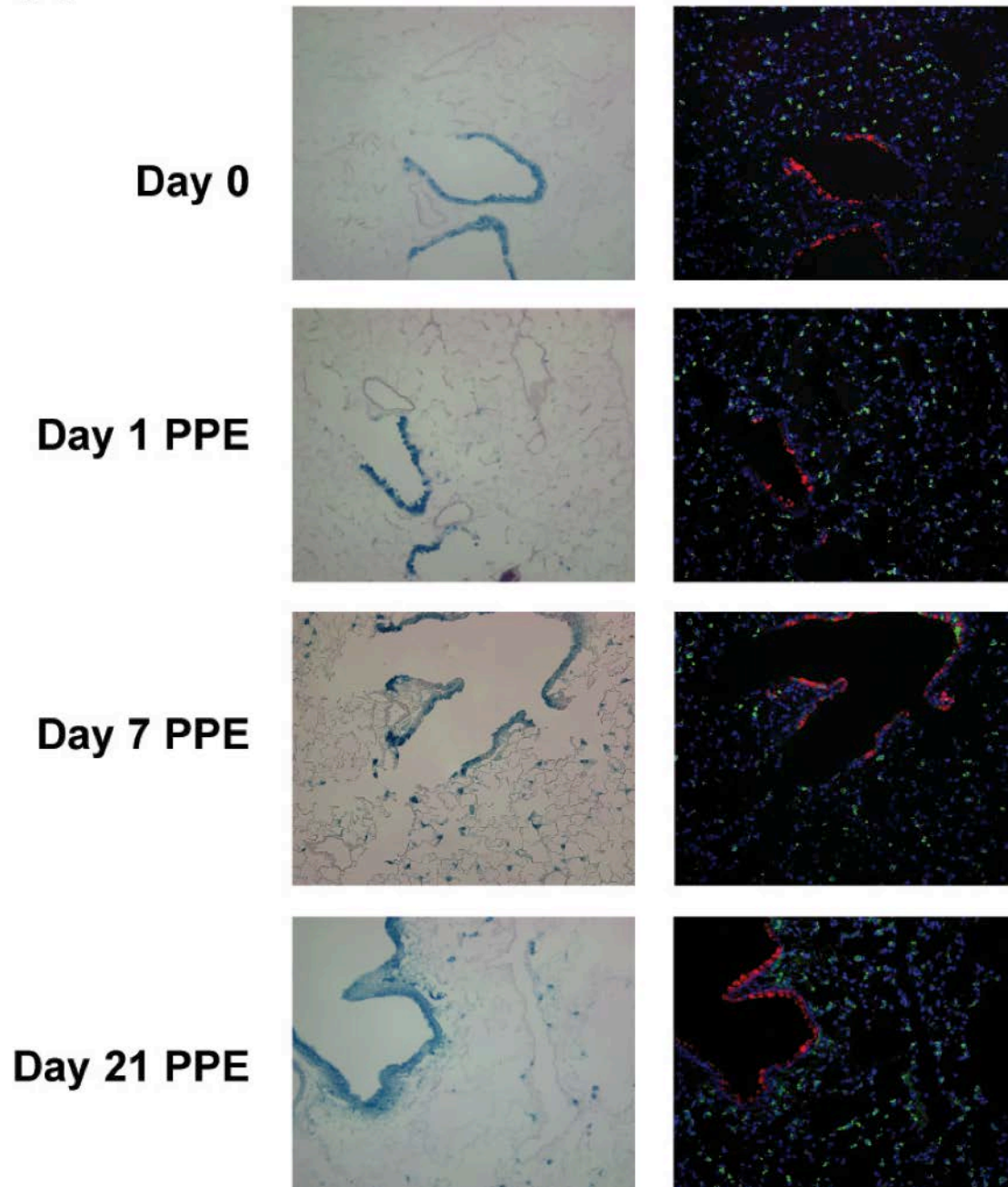


Figure 16: Rat CC10 promoter expression is airway specific even on injury.

Transgenic CC10-Cre; ROSA-LacZ mouse lungs exposed to PPE (panels on right) were stained for Rat CC10 expression over the course of 21 days and compared to their X-Gal stained bright field images (panels on left). In the immunofluorescence staining, blue indicates the nuclear staining (DAPI), red indicates the Rat CC10 staining and green indicates SP-C staining.

APPENDIX B

RAGE EXPRESSION ON CHRONIC CIGARETTE SMOKE EXPOSURE

B.1 BACKGROUND

The expression of RAGE on lung tissue from subjects with COPD was significantly elevated in the alveolar walls and not in their airways [158]. In vitro studies performed exposing a rat alveolar type-I epithelial cell line (R3/1), a macrophage cell line (RAW264.7) and a human lung adenocarcinoma cell line (A549) to cigarette smoke extract demonstrated an elevation in the expression of RAGE and its ligands [161]. These studies and others linking RAGE expression to the severity of disease led to the investigation of the expression of RAGE on wildtype mice (C57BL/6J background) that had been exposed to cigarette smoke over the course of 6 months.

B.2 MATERIALS AND METHODS

B.2.1 Mice

8-12 week old C57BL/6J female mice were used. N=8-10 mice per group per experimental condition.

B.2.2 Cigarette smoke exposure

C57BL/6J female mice were exposed to 4 unfiltered cigarettes (University of Kentucky) a day, 5 days a week for 6 months using a smoking apparatus [8]

B.2.3 RAGE immunofluorescence staining

Lung sections were de-waxed and rehydrated. Following antigen retrieval with 1mg/ml pepsin, slides were blocked in 2% BSA/PBST solution for 1hr room temperature. The sections were incubated with rabbit α -mouse RAGE antibody at 1:1000 dilution in 2% BSA/PBST [272]; at 4°C overnight. After washing the slides in PBS (3x), Donkey α Rabbit Alexa fluoro 594 antibody (Invitrogen) in 0.5% BSA/PBST was added and incubated for 1hr at room temperature. The slides were washed, nuclei stained with DAPI and coverslips were finally applied.

B.2.4 Tissue homogenization, protein quantification and immunoblotting

Whole lungs isolated from C57BL/6J mice exposed to 6 months of cigarette smoke and their respective controls were homogenized in isotonic buffer with CHAPS detergent (50 mM Tris-

HCl, pH 7.4, 150 mM NaCl, 10 mM CHAPS) with protease inhibitors (100 μ M 3,4-dichloroisocoumarin (DCI), 10 μ M trans-epoxysuccinyl-L-leucylamido- (4-guanidino) butane (E-64), 2 mM o-phenanthroline monohydrate- all from Sigma) and sonicated briefly [273]. The total lung homogenates were quantitated using the BCA standard protein assay kit (Thermo Fisher). 10 μ g of protein per sample was separated by SDS-PAGE and transferred to PVDF membranes as described previously [273]. The membranes were blocked overnight in 5% nonfat dry milk/PBST at 4°C. The membranes were then incubated with 1:5000 Rabbit anti-mouse RAGE primary and 1:10,000 anti-rabbit HRP secondary antibodies for 1 hr at room temperature. The membranes were washed with PBST (3x for 10 min) after each incubation. The reactive bands were visualized using the chemiluminescence method (SuperSignal West Pico, Pierce). The same membranes were probed with β -actin (1:1,000; Cell Signaling) as loading controls.

B.3 RESULTS

B.3.1 Immunofluorescence (IF) staining indicates no visible difference in RAGE expression

To test if there was any alteration in RAGE expression in mouse lung tissue on chronic cigarette smoke exposure, we stained lung sections from wildtype (C57BL/6J) mice that had been exposed to chronic cigarette smoke and compared them to their room air exposed controls. The antibody used in staining for RAGE expression showed specific binding to RAGE evident from the absence of staining in a RAGE deficient control (Figure 17, panel a). However, IF staining of

wildtype mouse lung sections indicated no visual difference in the intensity of staining irrespective of their exposure to cigarette smoke.

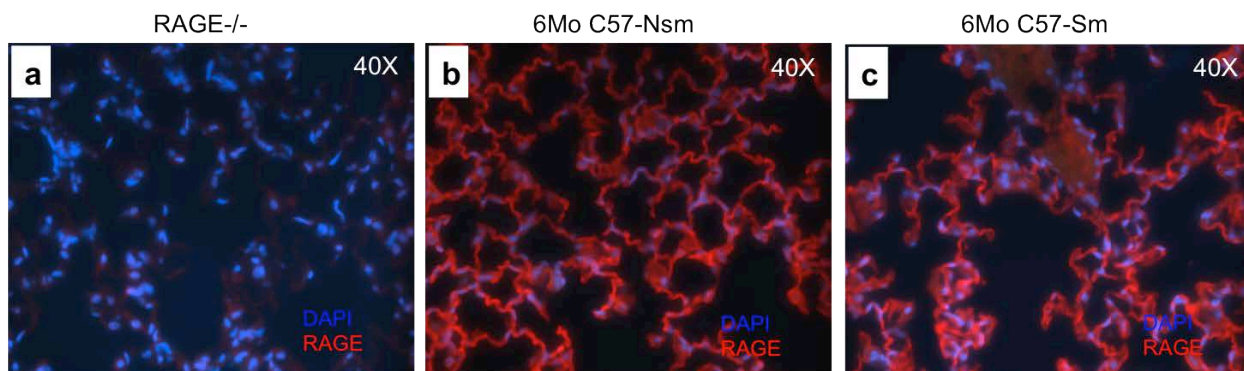


Figure 17: Immunofluorescence for RAGE shows no alteration of expression on cigarette smoke exposure

Representative images of IF staining performed on paraffin sections indicating RAGE expression (in RED) and DAPI (nuclear stain in BLUE). Representative images obtained at 40X magnification (a) naïve RAGE-/- (b) C57BL/6J (non-smoke) room air exposed mouse lung (c) C57BL/6J 6 month cigarette smoke-exposed mouse lung

B.3.2 Chronic cigarette smoke exposure led to the loss of X-RAGE

To quantitatively assay the expression of RAGE protein and its isoforms in mice, we analyzed total lung homogenates isolated from wildtype mice exposed to 6 months of cigarette smoke and compared them with their room air exposed controls. Western blotting for RAGE indicated to us the presence of three bands with molecular sizes 57.4 kDa, 52.6 kDa and 45.1 kDa corresponding to X-RAGE, membrane RAGE (mRAGE) and soluble RAGE (sRAGE) respectively as described previously [274]. Immunoblotting made apparent the loss of the X-RAGE isoform on chronic cigarette smoke exposure (Figure 18, top panel). Further quantification of band densities made clear that there was a significant loss in the X-RAGE isoform on chronic cigarette smoke exposure in the wildtype mice as compared to their room air exposed controls (Figure 18, bottom panel). However mRAGE and sRAGE levels remained

largely unaltered in the group that received chronic cigarette smoke exposure when compared to their controls (Figure 18).

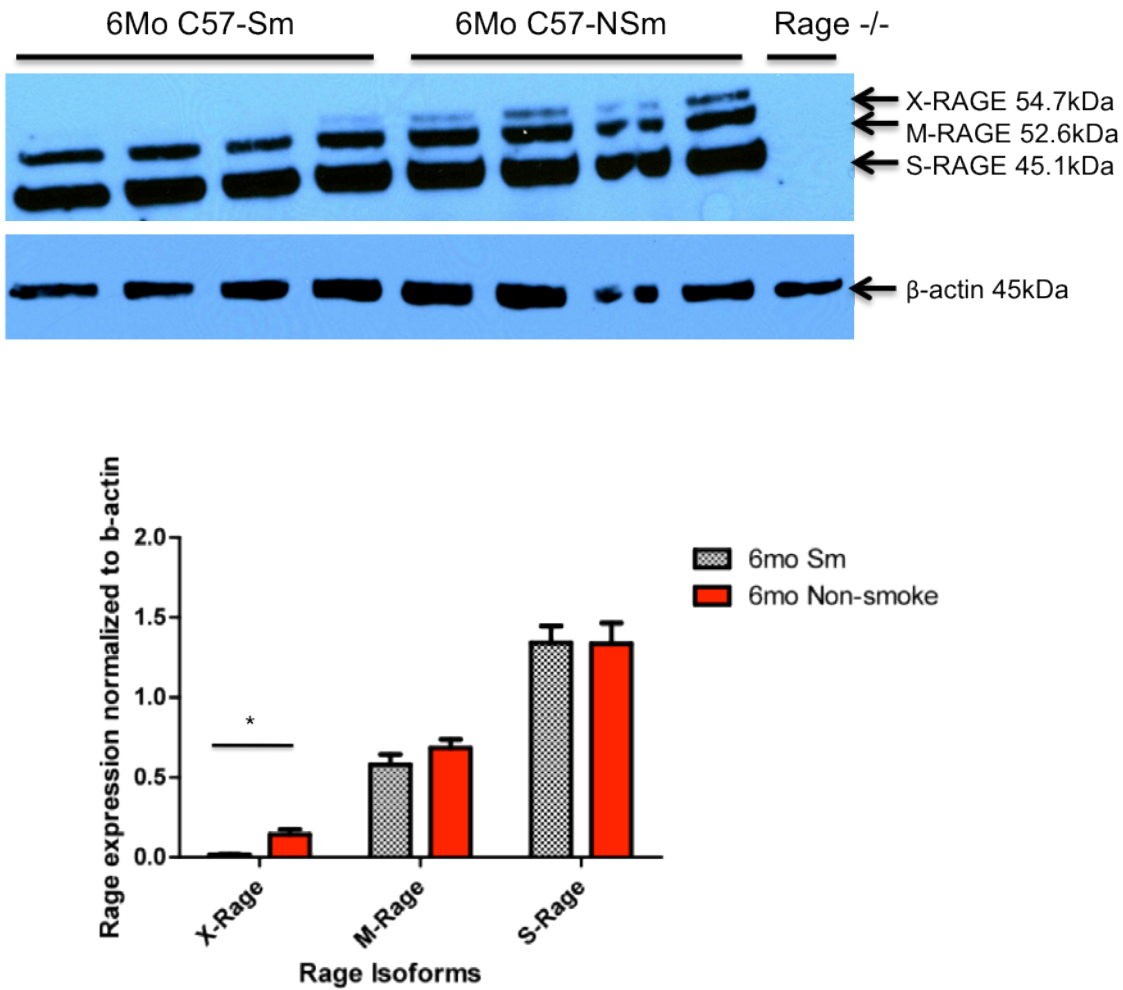


Figure 18: Quantification of RAGE isoforms indicates no alteration in membrane RAGE expression on chronic smoke exposure.

Immunoblotting for RAGE and β -actin (loading control) on whole lung homogenates from C57BL/6J mice exposed to 6months cigarette smoke and their non-smoke controls (**Top panel**). Quantification of RAGE signal intensity normalized to β -actin using ImageJ for each RAGE isoform (**Bottom panel**)

B.4 DISCUSSION

X-RAGE, a membrane bound isoform of RAGE is exclusively found in mouse lung tissue. Affinity column purified X-RAGE was analyzed by mass spectrometry and yielded identical peptide fragments as that obtained on analysis of mRAGE [274]. Hence there is no clear indication as to what could contribute to the difference in molecular sizes, however deglycosylation studies of RAGE point towards the possibility of an additional N-linked glycan of approximately 1.7kda in the case of X-RAGE [274]. X-RAGE was significantly reduced in the chronic smoke exposed group of mice when compared to their air-exposed controls. We are unsure of what the physiological indication of this could be in the context of cigarette smoke induced emphysema, given the nature of this isoform. However, we do not observe any significant alteration in mRAGE or sRAGE expression and this correlates with the lack of any visual alteration in immunofluorescence intensity of RAGE staining (Figure 17 and 18). These observations may not mirror observations reported in COPD subjects and may very well be attributed to the differences in model systems. Nevertheless, when we exposed RAGE null mutants to chronic cigarette smoke over a period of 6 months, we do observe that these mice display a significant protection in comparison to their wildtype counterparts (Figure 1E). These observations when considered together suggest a role for RAGE in mediating the progression of emphysema; at the same time they may also indicate the possible activation of alternate pathways that are capable of driving the disease phenotype in the absence of RAGE.

BIBLIOGRAPHY

1. *Chronic Obstructive Pulmonary Disease (COPD)*. CDC 2010 November 22, 2010 [cited 2010 November 22]; Available from: <http://www.cdc.gov/Features/COPD/>.
2. GOLD, *Global Initiative for Chronic Obstructive Lung Disease (GOLD): Global Strategy for the Diagnosis, Management, and Prevention of COPD*, 2014: <http://www.goldcopd.org/>.
3. Mathers, C.D. and D. Loncar, *Projections of Global Mortality and Burden of Disease from 2002 to 2030*. PLoS Med, 2006. **3**(11): p. e442.
4. Baty, F., et al., *Comorbidities and Burden of COPD: A Population Based Case-Control Study*. PLoS ONE, 2013. **8**(5): p. e63285.
5. Sullivan, S.D., S.D. Ramsey, and T.A. Lee, *The economic burden of COPD*. Chest, 2000. **117**(2 Suppl): p. 5S-9S.
6. Doll, R., et al., *Mortality in relation to smoking: 50 years' observations on male British doctors*. BMJ, 2004. **328**(7455): p. 1519.
7. Mannino, D.M. and A.S. Buist, *Global burden of COPD: risk factors, prevalence, and future trends*. The Lancet. **370**(9589): p. 765-773.
8. Hautamaki, R.D., et al., *Requirement for macrophage elastase for cigarette smoke-induced emphysema in mice*. Science, 1997. **277**(5334): p. 2002-4.
9. Niewoehner, D.E., J. Kleinerman, and D.B. Rice, *Pathologic changes in the peripheral airways of young cigarette smokers*. N Engl J Med, 1974. **291**(15): p. 755-8.
10. Hunninghake, G.M., et al., *MMP12, Lung Function, and COPD in High-Risk Populations*. New England Journal of Medicine, 2009. **361**(27): p. 2599-2608.
11. Mannino, D.M., et al., *Chronic obstructive pulmonary disease surveillance--United States, 1971-2000*. Respir Care, 2002. **47**(10): p. 1184-99.
12. Silverman, E.K., et al., *Gender-related differences in severe, early-onset chronic obstructive pulmonary disease*. Am J Respir Crit Care Med, 2000. **162**(6): p. 2152-8.
13. Sorheim, I.C., et al., *Gender differences in COPD: are women more susceptible to smoking effects than men?* Thorax, 2010. **65**(6): p. 480-5.
14. Hnizdo, E., et al., *Association between chronic obstructive pulmonary disease and employment by industry and occupation in the US population: a study of data from the Third National Health and Nutrition Examination Survey*. Am J Epidemiol, 2002. **156**(8): p. 738-46.
15. Bruce, N., R. Perez-Padilla, and R. Albalak, *Indoor air pollution in developing countries: a major environmental and public health challenge*. Bull World Health Organ, 2000. **78**(9): p. 1078-92.
16. H. W. de Koning, K.R.S., and J. M. Last, *Biomass fuel combustion and health*. Bull World Health Organ, 1985. **63**(1): p. 11-26.

17. Berndt, A., A.S. Leme, and S.D. Shapiro, *Emerging genetics of COPD*. EMBO Molecular Medicine, 2012. **4**(11): p. 1144-1155.
18. Tudor, R.M., S. McGrath, and E. Neptune, *The pathobiological mechanisms of emphysema models: What do they have in common?* Pulmonary Pharmacology & Therapeutics, 2003. **16**(2): p. 67-78.
19. Laurell, C.B. and S. Eriksson, *The electrophoretic alpha1-globulin pattern of serum in alpha1-antitrypsin deficiency*. . Scand. J. Clin. Invest., 1963. **15**: p. 132-140.
20. Kaplan, A. and L. Cosentino, *alpha1-Antitrypsin deficiency: Forgotten etiology*. Canadian Family Physician, 2010. **56**(1): p. 19-24.
21. Minakata, Y., et al., *High COPD prevalence in patients with liver disease*. Intern Med, 2010. **49**(24): p. 2687-91.
22. Saetta, M., et al., *Cellular and structural bases of chronic obstructive pulmonary disease*. Am J Respir Crit Care Med, 2001. **163**(6): p. 1304-9.
23. Hunninghake, G.W., et al., *Elastin fragments attract macrophage precursors to diseased sites in pulmonary emphysema*. Science, 1981. **212**(4497): p. 925-7.
24. Di Stefano, A., et al., *Cellular and molecular mechanisms in chronic obstructive pulmonary disease: an overview*. Clin Exp Allergy, 2004. **34**(8): p. 1156-67.
25. MacNee, W., *Pathogenesis of Chronic Obstructive Pulmonary Disease*. Proceedings of the American Thoracic Society, 2005. **2**(4): p. 258-266.
26. Retamales, I., et al., *Amplification of inflammation in emphysema and its association with latent adenoviral infection*. Am J Respir Crit Care Med, 2001. **164**(3): p. 469-73.
27. Punturieri, A., et al., *Regulation of elastolytic cysteine proteinase activity in normal and cathepsin K-deficient human macrophages*. J Exp Med, 2000. **192**(6): p. 789-99.
28. Russell, R.E.K., et al., *Alveolar macrophage-mediated elastolysis: roles of matrix metalloproteinases, cysteine, and serine proteases*. American Journal of Physiology - Lung Cellular and Molecular Physiology, 2002. **283**(4): p. L867-L873.
29. Tanino, M., et al., *Increased levels of interleukin-8 in BAL fluid from smokers susceptible to pulmonary emphysema*. Thorax, 2002. **57**(5): p. 405-411.
30. Traves, S.L., et al., *Increased levels of the chemokines GROalpha and MCP-1 in sputum samples from patients with COPD*. Thorax, 2002. **57**(7): p. 590-595.
31. MacNee, W., et al., *The effect of cigarette smoking on neutrophil kinetics in human lungs*. N Engl J Med, 1989. **321**(14): p. 924-8.
32. Witko-Sarsat, V., et al., *Proteinase 3, a potent secretagogue in airways, is present in cystic fibrosis sputum*. Am J Respir Cell Mol Biol, 1999. **20**(4): p. 729-36.
33. Sommerhoff, C.P., et al., *Neutrophil elastase and cathepsin G stimulate secretion from cultured bovine airway gland serous cells*. J Clin Invest, 1990. **85**(3): p. 682-9.
34. Finkelstein, R., et al., *Alveolar inflammation and its relation to emphysema in smokers*. American Journal of Respiratory and Critical Care Medicine, 1995. **152**(5): p. 1666-1672.
35. O'Shaughnessy, T.C., et al., *Inflammation in bronchial biopsies of subjects with chronic bronchitis: inverse relationship of CD8+ T lymphocytes with FEV1*. American Journal of Respiratory and Critical Care Medicine, 1997. **155**(3): p. 852-857.
36. Saetta, M., et al., *CD8+ve cells in the lungs of smokers with chronic obstructive pulmonary disease*. Am J Respir Crit Care Med, 1999. **160**(2): p. 711-7.

37. Takubo, Y., et al., *α 1-Antitrypsin Determines the Pattern of Emphysema and Function in Tobacco Smoke-exposed Mice*. American Journal of Respiratory and Critical Care Medicine, 2002. **166**(12): p. 1596-1603.
38. Hashimoto, S., et al., *Upregulation of two death pathways of perforin/granzyme and FasL/Fas in septic acute respiratory distress syndrome*. Am J Respir Crit Care Med, 2000. **161**(1): p. 237-43.
39. Ito, K., et al., *Cigarette smoking reduces histone deacetylase 2 expression, enhances cytokine expression, and inhibits glucocorticoid actions in alveolar macrophages*. FASEB J, 2001. **15**(6): p. 1110-2.
40. Marwick, J.A., et al., *Cigarette smoke alters chromatin remodeling and induces proinflammatory genes in rat lungs*. Am J Respir Cell Mol Biol, 2004. **31**(6): p. 633-42.
41. Schaberg, T., et al., *Superoxide anion release induced by platelet-activating factor is increased in human alveolar macrophages from smokers*. European Respiratory Journal, 1992. **5**(4): p. 387-393.
42. Rahman, I., et al., *Systemic oxidative stress in asthma, COPD, and smokers*. Am J Respir Crit Care Med, 1996. **154**(4 Pt 1): p. 1055-60.
43. Morrow, J.D., et al., *Increase in circulating products of lipid peroxidation (F2-isoprostanes) in smokers. Smoking as a cause of oxidative damage*. N Engl J Med, 1995. **332**(18): p. 1198-203.
44. Morrison, D., et al., *Epithelial permeability, inflammation, and oxidant stress in the air spaces of smokers*. Am J Respir Crit Care Med, 1999. **159**(2): p. 473-9.
45. Cantin, A. and R.G. Crystal, *Oxidants, antioxidants and the pathogenesis of emphysema*. Eur J Respir Dis Suppl, 1985. **139**: p. 7-17.
46. Laurent, P., A. Janoff, and H.M. Kagan, *Cigarette smoke blocks cross-linking of elastin in vitro*. Chest, 1983. **83**(5 Suppl): p. 63S-65S.
47. Cavalcante, A.G.d.M. and P.F.C.d. Bruin, *O papel do estresse oxidativo na DPOC: conceitos atuais e perspectivas*. Jornal Brasileiro de Pneumologia, 2009. **35**: p. 1227-1237.
48. MacNee, W., *Pulmonary and Systemic Oxidant/Antioxidant Imbalance in Chronic Obstructive Pulmonary Disease*. Proceedings of the American Thoracic Society, 2005. **2**(1): p. 50-60.
49. Owen, C.A., *Proteinases and oxidants as targets in the treatment of chronic obstructive pulmonary disease*. Proc Am Thorac Soc, 2005. **2**(4): p. 373-85; discussion 394-5.
50. Cantin, A.M., et al., *Antioxidant macromolecules in the epithelial lining fluid of the normal human lower respiratory tract*. J Clin Invest, 1990. **86**(3): p. 962-71.
51. Linden, M., et al., *Glutathione in bronchoalveolar lavage fluid from smokers is related to humoral markers of inflammatory cell activity*. Inflammation, 1989. **13**(6): p. 651-658.
52. Lian, X., et al., *Lysosomal acid lipase deficiency causes respiratory inflammation and destruction in the lung*. Am J Physiol Lung Cell Mol Physiol, 2004. **286**(4): p. L801-7.
53. Yan, C. and H. Du, *Alveolus formation: what have we learned from genetic studies?* J Appl Physiol (1985), 2004. **97**(4): p. 1543-8.
54. Ju, C.R., W. Liu, and R.C. Chen, *Serum surfactant protein D: biomarker of chronic obstructive pulmonary disease*. Dis Markers, 2012. **32**(5): p. 281-7.
55. Ozyurek, B.A., et al., *Value of serum and induced sputum surfactant protein-D in chronic obstructive pulmonary disease*. Multidiscip Respir Med, 2013. **8**(1): p. 36.

56. Yoshida, T. and R.M. Tuder, *Pathobiology of cigarette smoke-induced chronic obstructive pulmonary disease*. *Physiol Rev*, 2007. **87**(3): p. 1047-82.
57. Mouded, M., et al., *Epithelial cell apoptosis causes acute lung injury masquerading as emphysema*. *Am J Respir Cell Mol Biol*, 2009. **41**(4): p. 407-14.
58. Keatings, V.M., et al., *Differences in interleukin-8 and tumor necrosis factor-alpha in induced sputum from patients with chronic obstructive pulmonary disease or asthma*. *Am J Respir Crit Care Med*, 1996. **153**(2): p. 530-4.
59. Saetta, M., et al., *CD8+ T-lymphocytes in peripheral airways of smokers with chronic obstructive pulmonary disease*. *Am J Respir Crit Care Med*, 1998. **157**(3 Pt 1): p. 822-6.
60. Jeffery, P.K., et al., *Effects of Treatment on Airway Inflammation and Thickening of Basement Membrane Reticular Collagen in Asthma: A Quantitative Light and Electron Microscopic Study*. *American Review of Respiratory Disease*, 1992. **145**(4_pt_1): p. 890-899.
61. Keatings, V.M., et al., *Effects of inhaled and oral glucocorticoids on inflammatory indices in asthma and COPD*. *Am J Respir Crit Care Med*, 1997. **155**(2): p. 542-8.
62. Thomson, N.C., R. Chaudhuri, and E. Livingston, *Asthma and cigarette smoking*. *European Respiratory Journal*, 2004. **24**(5): p. 822-833.
63. Pellegrino, R., et al., *Interpretative strategies for lung function tests*. *European Respiratory Journal*, 2005. **26**(5): p. 948-968.
64. Wagner, P.D., *Possible mechanisms underlying the development of cachexia in COPD*. *Eur Respir J*, 2008. **31**(3): p. 492-501.
65. Lange, P., et al., *Ventilatory function and chronic mucus hypersecretion as predictors of death from lung cancer*. *Am Rev Respir Dis*, 1990. **141**(3): p. 613-7.
66. Skillrud, D.M., K.P. Offord, and R.D. Miller, *Higher risk of lung cancer in chronic obstructive pulmonary disease. A prospective, matched, controlled study*. *Ann Intern Med*, 1986. **105**(4): p. 503-7.
67. Tockman, M.S., et al., *Airways obstruction and the risk for lung cancer*. *Ann Intern Med*, 1987. **106**(4): p. 512-8.
68. Kishi, K., et al., *The correlation of emphysema or airway obstruction with the risk of lung cancer: a matched case-controlled study*. *Eur Respir J*, 2002. **19**(6): p. 1093-8.
69. Tonnesen, P., K. Mikkelsen, and L. Bremann, *Nurse-conducted smoking cessation in patients with COPD using nicotine sublingual tablets and behavioral support*. *Chest*, 2006. **130**(2): p. 334-42.
70. Lancaster, T., et al., *Effectiveness of interventions to help people stop smoking: findings from the Cochrane Library*. *BMJ*, 2000. **321**(7257): p. 355-358.
71. *A clinical practice guideline for treating tobacco use and dependence: A US Public Health Service report. The Tobacco Use and Dependence Clinical Practice Guideline Panel, Staff, and Consortium Representatives*. *JAMA*, 2000. **283**(24): p. 3244-54.
72. Fiore, M.C., Bailey, W.C., Cohen, S.J., Dorfman, S.F., Goldstein, and G. M.G., E.R. et al, *Treating tobacco use and dependence. Clinical practice guideline.*, 2000, U.S. Public health Service: Rockville, MD.
73. *In chronic obstructive pulmonary disease, a combination of ipratropium and albuterol is more effective than either agent alone. An 85-day multicenter trial. COMBIVENT Inhalation Aerosol Study Group*. *Chest*, 1994. **105**(5): p. 1411-9.
74. Barnes, P.J., *Current and future therapies for airway mucus hypersecretion*. *Novartis Found Symp*, 2002. **248**: p. 237-49; discussion 249-53, 277-82.

75. Calverley, P.M.A., et al., *Roflumilast in symptomatic chronic obstructive pulmonary disease: two randomised clinical trials*. The Lancet. **374**(9691): p. 685-694.
76. Francis, R.S., J.R. May, and C.C. Spicer, *Chemotherapy of bronchitis. Influence of penicillin and tetracycline administered daily, or intermittently for exacerbations. A report to the Research Committee of the British Tuberculosis Association by its Bronchitis Subcommittee*. Br Med J, 1961. **2**(5258): p. 979-85.
77. Members, A.T.F., et al., *Guidelines for the diagnosis and treatment of pulmonary hypertension: The Task Force for the Diagnosis and Treatment of Pulmonary Hypertension of the European Society of Cardiology (ESC) and the European Respiratory Society (ERS), endorsed by the International Society of Heart and Lung Transplantation (ISHLT)*. European Heart Journal, 2009. **30**(20): p. 2493-2537.
78. Celli, B.R. and W. MacNee, *Standards for the diagnosis and treatment of patients with COPD: a summary of the ATS/ERS position paper*. Eur Respir J, 2004. **23**(6): p. 932-46.
79. Wongsurakiat, P., et al., *Acute respiratory illness in patients with COPD and the effectiveness of influenza vaccination: a randomized controlled study*. Chest, 2004. **125**(6): p. 2011-20.
80. Li, J., et al., *Protective effect of a bacterial extract against acute exacerbation in patients with chronic bronchitis accompanied by chronic obstructive pulmonary disease*. Chinese medical journal, 2004. **117**(6): p. 828-834.
81. Stoller, J.K., et al., *Oxygen therapy for patients with COPD: current evidence and the long-term oxygen treatment trial*. Chest, 2010. **138**(1): p. 179-87.
82. McEvoy, R.D., et al., *Nocturnal non-invasive nasal ventilation in stable hypercapnic COPD: a randomised controlled trial*. Thorax, 2009. **64**(7): p. 561-6.
83. Cooper, J.D., et al., *Bilateral pneumectomy (volume reduction) for chronic obstructive pulmonary disease*. J Thorac Cardiovasc Surg, 1995. **109**(1): p. 106-16; discussion 116-9.
84. Fessler, H.E. and S. Permutt, *Lung volume reduction surgery and airflow limitation*. Am J Respir Crit Care Med, 1998. **157**(3 Pt 1): p. 715-22.
85. *Patients at high risk of death after lung-volume-reduction surgery*. N Engl J Med, 2001. **345**(15): p. 1075-83.
86. Theodore, J. and N. Lewiston, *Lung transplantation comes of age*. N Engl J Med, 1990. **322**(11): p. 772-4.
87. Mahadeva, R. and S.D. Shapiro, *Chronic obstructive pulmonary disease * 3: Experimental animal models of pulmonary emphysema*. Thorax, 2002. **57**(10): p. 908-14.
88. Gross, P., et al., *EXPERIMENTAL EMPHYSEMA: ITS PRODUCTION WITH PAPAINE IN NORMAL AND SILICOTIC RATS*. Arch Environ Health, 1965. **11**: p. 50-8.
89. Kuhn, C., et al., *The induction of emphysema with elastase. II. Changes in connective tissue*. Lab Invest, 1976. **34**(4): p. 372-80.
90. Kuhn, C., 3rd and B.C. Starcher, *The effect of lathyrogens on the evolution of elastase-induced emphysema*. Am Rev Respir Dis, 1980. **122**(3): p. 453-60.
91. Snider, G.L., E.C. Lucey, and P.J. Stone, *Animal models of emphysema*. Am Rev Respir Dis, 1986. **133**(1): p. 149-69.
92. Shapiro, S.D., *Animal Models for Chronic Obstructive Pulmonary Disease*. American Journal of Respiratory Cell and Molecular Biology, 2000. **22**(1): p. 4-7.
93. Wittels, E.H., et al., *Pulmonary intravascular leukocyte sequestration. A potential mechanism of lung injury*. Am Rev Respir Dis, 1974. **109**(5): p. 502-9.

94. Kasahara, Y., et al., *Endothelial cell death and decreased expression of vascular endothelial growth factor and vascular endothelial growth factor receptor 2 in emphysema*. Am J Respir Crit Care Med, 2001. **163**(3 Pt 1): p. 737-44.
95. Kasahara, Y., et al., *Inhibition of VEGF receptors causes lung cell apoptosis and emphysema*. J Clin Invest, 2000. **106**(11): p. 1311-9.
96. Wright, J.L. and A. Churg, *Cigarette smoke causes physiologic and morphologic changes of emphysema in the guinea pig*. Am Rev Respir Dis, 1990. **142**(6 Pt 1): p. 1422-8.
97. Wright, J.L., *The importance of ultramicroscopic emphysema in cigarette smoke-induced lung disease*. Lung, 2001. **179**(2): p. 71-81.
98. Hautamaki, R.D., et al., *Requirement for Macrophage Elastase for Cigarette Smoke-Induced Emphysema in Mice*. Science, 1997. **277**(5334): p. 2002-2004.
99. Dhimi, R., et al., *Acute cigarette smoke-induced connective tissue breakdown is mediated by neutrophils and prevented by alpha1-antitrypsin*. Am J Respir Cell Mol Biol, 2000. **22**(2): p. 244-52.
100. Shapiro, S.D., *Animal models for COPD*. Chest, 2000. **117**(5 Suppl 1): p. 223S-7S.
101. Kielty, C.M., et al., *The Tight skin mouse: demonstration of mutant fibrillin-1 production and assembly into abnormal microfibrils*. J Cell Biol, 1998. **140**(5): p. 1159-66.
102. Keil, M., et al., *A scanning electron microscopic investigation of genetic emphysema in tight-skin, pallid, and beige mice, three different C57 BL/6J mutants*. Lab Invest, 1996. **74**(2): p. 353-62.
103. Fisk, D.E. and C. Kuhn, *Emphysema-like changes in the lungs of the blotchy mouse*. Am Rev Respir Dis, 1976. **113**(6): p. 787-97.
104. Mercer, J.F., et al., *Mutations in the murine homologue of the Menkes gene in dappled and blotchy mice*. Nat Genet, 1994. **6**(4): p. 374-8.
105. Nagle, D.L., et al., *Identification and mutation analysis of the complete gene for Chediak-Higashi syndrome*. Nat Genet, 1996. **14**(3): p. 307-11.
106. Warburton, D., et al., *The molecular basis of lung morphogenesis*. Mech Dev, 2000. **92**(1): p. 55-81.
107. McGowan, S., et al., *Mice bearing deletions of retinoic acid receptors demonstrate reduced lung elastin and alveolar numbers*. Am J Respir Cell Mol Biol, 2000. **23**(2): p. 162-7.
108. Bostrom, H., et al., *PDGF-A signaling is a critical event in lung alveolar myofibroblast development and alveogenesis*. Cell, 1996. **85**(6): p. 863-73.
109. Nakamura, T., et al., *Fibulin-5/DANCE is essential for elastogenesis in vivo*. Nature, 2002. **415**(6868): p. 171-5.
110. Wendel, D.P., et al., *Impaired distal airway development in mice lacking elastin*. Am J Respir Cell Mol Biol, 2000. **23**(3): p. 320-6.
111. Weinstein, M., et al., *FGFR-3 and FGFR-4 function cooperatively to direct alveogenesis in the murine lung*. Development, 1998. **125**(18): p. 3615-23.
112. Yoshida, M., T.R. Korfhagen, and J.A. Whitsett, *Surfactant protein D regulates NF-kappa B and matrix metalloproteinase production in alveolar macrophages via oxidant-sensitive pathways*. J Immunol, 2001. **166**(12): p. 7514-9.
113. Leco, K.J., et al., *Spontaneous air space enlargement in the lungs of mice lacking tissue inhibitor of metalloproteinases-3 (TIMP-3)*. J Clin Invest, 2001. **108**(6): p. 817-29.

114. Hoyle, G.W., et al., *Emphysematous lesions, inflammation, and fibrosis in the lungs of transgenic mice overexpressing platelet-derived growth factor*. Am J Pathol, 1999. **154**(6): p. 1763-75.
115. Kuhn, C., 3rd, et al., *Airway hyperresponsiveness and airway obstruction in transgenic mice. Morphologic correlates in mice overexpressing interleukin (IL)-11 and IL-6 in the lung*. Am J Respir Cell Mol Biol, 2000. **22**(3): p. 289-95.
116. Hardie, W.D., et al., *Dose-dependent lung remodeling in transgenic mice expressing transforming growth factor-alpha*. Am J Physiol Lung Cell Mol Physiol, 2001. **281**(5): p. L1088-94.
117. Wang, Z., et al., *Interferon gamma induction of pulmonary emphysema in the adult murine lung*. J Exp Med, 2000. **192**(11): p. 1587-600.
118. Zheng, T., et al., *Inducible targeting of IL-13 to the adult lung causes matrix metalloproteinase- and cathepsin-dependent emphysema*. J Clin Invest, 2000. **106**(9): p. 1081-93.
119. D'Armiento, J., et al., *Collagenase expression in the lungs of transgenic mice causes pulmonary emphysema*. Cell, 1992. **71**(6): p. 955-61.
120. Shipley, J.M., et al., *Metalloelastase is required for macrophage-mediated proteolysis and matrix invasion in mice*. Proc Natl Acad Sci U S A, 1996. **93**(9): p. 3942-6.
121. Shapiro, S.D., et al., *Neutrophil elastase contributes to cigarette smoke-induced emphysema in mice*. Am J Pathol, 2003. **163**(6): p. 2329-35.
122. Lucey, E.C., et al., *Severity of elastase-induced emphysema is decreased in tumor necrosis factor-alpha and interleukin-1beta receptor-deficient mice*. Lab Invest, 2002. **82**(1): p. 79-85.
123. Atkinson, J.J., et al., *The role of matrix metalloproteinase-9 in cigarette smoke-induced emphysema*. Am J Respir Crit Care Med, 2011. **183**(7): p. 876-84.
124. Schmidt, A.M., et al., *Isolation and characterization of two binding proteins for advanced glycosylation end products from bovine lung which are present on the endothelial cell surface*. J Biol Chem, 1992. **267**(21): p. 14987-97.
125. Neeper, M., et al., *Cloning and expression of a cell surface receptor for advanced glycosylation end products of proteins*. J Biol Chem, 1992. **267**(21): p. 14998-5004.
126. Thomas, V., et al., *Mrp8 and Mrp14 are endogenous activators of Toll-like receptor 4, promoting lethal, endotoxin-induced shock*. Nature Medicine, 2007. **13**(9): p. 1042-1049.
127. Yang, H., et al., *A critical cysteine is required for HMGB1 binding to Toll-like receptor 4 and activation of macrophage cytokine release*. Proc Natl Acad Sci U S A, 2010. **107**(26): p. 11942-7.
128. Yu, M., et al., *HMGB1 signals through toll-like receptor (TLR) 4 and TLR2*. Shock, 2006. **26**(2): p. 174-9.
129. Kalea, A.Z., et al., *Alternative splicing of the murine receptor for advanced glycation end-products (RAGE) gene*. FASEB J, 2009. **23**(6): p. 1766-74.
130. Raucci, A., et al., *A soluble form of the receptor for advanced glycation endproducts (RAGE) is produced by proteolytic cleavage of the membrane-bound form by the sheddase a disintegrin and metalloprotease 10 (ADAM10)*. FASEB J, 2008. **22**(10): p. 3716-27.
131. Zhang, H., et al., *Role of soluble receptor for advanced glycation end products on endotoxin-induced lung injury*. Am J Respir Crit Care Med, 2008. **178**(4): p. 356-62.

132. Galichet, A., M. Weibel, and C.W. Heizmann, *Calcium-regulated intramembrane proteolysis of the RAGE receptor*. *Biochem Biophys Res Commun*, 2008. **370**(1): p. 1-5.
133. Hori, O., et al., *The receptor for advanced glycation end products (RAGE) is a cellular binding site for amphotericin. Mediation of neurite outgrowth and co-expression of RAGE and amphotericin in the developing nervous system*. *J Biol Chem*, 1995. **270**(43): p. 25752-61.
134. Leclerc, E., et al., *Binding of S100 proteins to RAGE: an update*. *Biochim Biophys Acta*, 2009. **1793**(6): p. 993-1007.
135. Ramasamy, R., S.F. Yan, and A.M. Schmidt, *Arguing for the motion: yes, RAGE is a receptor for advanced glycation endproducts*. *Mol Nutr Food Res*, 2007. **51**(9): p. 1111-5.
136. Mizumoto, S. and K. Sugahara, *Glycosaminoglycans are functional ligands for receptor for advanced glycation end-products in tumors*. *FEBS J*, 2013. **280**(10): p. 2462-70.
137. Yan, S.D., et al., *RAGE and amyloid-beta peptide neurotoxicity in Alzheimer's disease*. *Nature*, 1996. **382**(6593): p. 685-91.
138. Milutinovic, P.S., et al., *Clearance kinetics and matrix binding partners of the receptor for advanced glycation end products*. *PLoS One*, 2014. **9**(3): p. e88259.
139. Demling, N., et al., *Promotion of cell adherence and spreading: a novel function of RAGE, the highly selective differentiation marker of human alveolar epithelial type I cells*. *Cell Tissue Res*, 2006. **323**(3): p. 475-88.
140. Orlova, V.V., et al., *A novel pathway of HMGB1-mediated inflammatory cell recruitment that requires Mac-1-integrin*. *EMBO J*, 2007. **26**(4): p. 1129-39.
141. Park, J.S., et al., *High mobility group box 1 protein interacts with multiple Toll-like receptors*. *Am J Physiol Cell Physiol*, 2006. **290**(3): p. C917-24.
142. Park, J.S., et al., *Involvement of toll-like receptors 2 and 4 in cellular activation by high mobility group box 1 protein*. *J Biol Chem*, 2004. **279**(9): p. 7370-7.
143. Hudson, B.I., et al., *Interaction of the RAGE cytoplasmic domain with diaphanous-1 is required for ligand-stimulated cellular migration through activation of Rac1 and Cdc42*. *J Biol Chem*, 2008. **283**(49): p. 34457-68.
144. Lander, H.M., et al., *Activation of the receptor for advanced glycation end products triggers a p21(ras)-dependent mitogen-activated protein kinase pathway regulated by oxidant stress*. *J Biol Chem*, 1997. **272**(28): p. 17810-4.
145. Perkins, N.D., *Integrating cell-signalling pathways with NF-kappaB and IKK function*. *Nat Rev Mol Cell Biol*, 2007. **8**(1): p. 49-62.
146. Hofmann, M.A., et al., *RAGE mediates a novel proinflammatory axis: a central cell surface receptor for S100/calgranulin polypeptides*. *Cell*, 1999. **97**(7): p. 889-901.
147. Ishihara, K., et al., *The receptor for advanced glycation end-products (RAGE) directly binds to ERK by a D-domain-like docking site*. *FEBS Lett*, 2003. **550**(1-3): p. 107-13.
148. Huttunen, H.J., C. Fages, and H. Rauvala, *Receptor for advanced glycation end products (RAGE)-mediated neurite outgrowth and activation of NF-kappaB require the cytoplasmic domain of the receptor but different downstream signaling pathways*. *J Biol Chem*, 1999. **274**(28): p. 19919-24.
149. Schmidt, A.M., et al., *The multiligand receptor RAGE as a progression factor amplifying immune and inflammatory responses*. *J Clin Invest*, 2001. **108**(7): p. 949-55.
150. Schraml, P., et al., *Identification of genes differentially expressed in normal lung and non-small cell lung carcinoma tissue*. *Cancer Res*, 1994. **54**(19): p. 5236-40.

151. Schraml, P., I. Bendik, and C.U. Ludwig, *Differential messenger RNA and protein expression of the receptor for advanced glycosylated end products in normal lung and non-small cell lung carcinoma*. *Cancer Res*, 1997. **57**(17): p. 3669-71.
152. Schenk, S., et al., *A novel polymorphism in the promoter of the RAGE gene is associated with non-small cell lung cancer*. *Lung Cancer*, 2001. **32**(1): p. 7-12.
153. Hofmann, H.S., et al., *Discrimination of human lung neoplasm from normal lung by two target genes*. *Am J Respir Crit Care Med*, 2004. **170**(5): p. 516-9.
154. Stav, D., I. Bar, and J. Sandbank, *Usefulness of CDK5RAP3, CCNB2, and RAGE genes for the diagnosis of lung adenocarcinoma*. *Int J Biol Markers*, 2007. **22**(2): p. 108-13.
155. Rho, J.H., M.H. Roehrl, and J.Y. Wang, *Glycoproteomic analysis of human lung adenocarcinomas using glycoarrays and tandem mass spectrometry: differential expression and glycosylation patterns of vimentin and fetuin A isoforms*. *Protein J*, 2009. **28**(3-4): p. 148-60.
156. Uchida, T., et al., *Receptor for advanced glycation end-products is a marker of type I cell injury in acute lung injury*. *Am J Respir Crit Care Med*, 2006. **173**(9): p. 1008-15.
157. Su, X., et al., *Receptor for advanced glycation end-products (RAGE) is an indicator of direct lung injury in models of experimental lung injury*. *Am J Physiol Lung Cell Mol Physiol*, 2009. **297**(1): p. L1-5.
158. Wu, L., et al., *Advanced glycation end products and its receptor (RAGE) are increased in patients with COPD*. *Respiratory Medicine*, 2011. **105**(3): p. 329-336.
159. Sukkar, M.B., et al., *RAGE: a new frontier in chronic airways disease*. *British Journal of Pharmacology*, 2012. **167**(6): p. 1161-1176.
160. Miniati, M., et al., *Soluble receptor for advanced glycation end products in COPD: relationship with emphysema and chronic cor pulmonale: a case-control study*. *Respir Res*, 2011. **12**: p. 37.
161. Reynolds, P.R., et al., *RAGE: developmental expression and positive feedback regulation by Egr-1 during cigarette smoke exposure in pulmonary epithelial cells*. *Am J Physiol Lung Cell Mol Physiol*, 2008. **294**(6): p. L1094-101.
162. Stogsdill, J.A., et al., *Embryonic overexpression of receptors for advanced glycation end-products by alveolar epithelium induces an imbalance between proliferation and apoptosis*. *Am J Respir Cell Mol Biol*, 2012. **47**(1): p. 60-6.
163. Constien, R., et al., *Characterization of a novel EGFP reporter mouse to monitor Cre recombination as demonstrated by a Tie2 Cre mouse line*. *Genesis*, 2001. **30**(1): p. 36-44.
164. Houghton, A.M., et al., *Elastin fragments drive disease progression in a murine model of emphysema*. *J Clin Invest*, 2006. **116**(3): p. 753-9.
165. Dunnill, M.S., *Quantitative Methods in the Study of Pulmonary Pathology*. *Thorax*, 1962. **17**(4): p. 320-328.
166. Shirasawa, M., et al., *Receptor for advanced glycation end-products is a marker of type I lung alveolar cells*. *Genes Cells*, 2004. **9**(2): p. 165-74.
167. Fehrenbach, H., et al., *Receptor for advanced glycation endproducts (RAGE) exhibits highly differential cellular and subcellular localisation in rat and human lung*. *Cell Mol Biol (Noisy-le-grand)*, 1998. **44**(7): p. 1147-57.
168. Fineschi, S., et al., *Receptor for advanced glycation end products contributes to postnatal pulmonary development and adult lung maintenance program in mice*. *Am J Respir Cell Mol Biol*, 2013. **48**(2): p. 164-71.

169. Smith, D.J., et al., *Reduced soluble receptor for advanced glycation end-products in COPD*. Eur Respir J, 2011. **37**(3): p. 516-22.
170. Shifren, A. and R.P. Mecham, *The Stumbling Block in Lung Repair of Emphysema: Elastic Fiber Assembly*. Proceedings of the American Thoracic Society, 2006. **3**(5): p. 428-433.
171. Senior, R.M., G.L. Griffin, and R.P. Mecham, *Chemotactic activity of elastin-derived peptides*. J Clin Invest, 1980. **66**(4): p. 859-62.
172. Janoff, A., et al., *Experimental emphysema induced with purified human neutrophil elastase: tissue localization of the instilled protease*. Am Rev Respir Dis, 1977. **115**(3): p. 461-78.
173. Shapiro, S.D., *The pathogenesis of emphysema: the elastase:antielastase hypothesis 30 years later*. Proc Assoc Am Physicians, 1995. **107**(3): p. 346-52.
174. Clynes, R., et al., *Receptor for AGE (RAGE): weaving tangled webs within the inflammatory response*. Curr Mol Med, 2007. **7**(8): p. 743-51.
175. Bierhaus, A., D.M. Stern, and P.P. Nawroth, *RAGE in inflammation: a new therapeutic target?* Curr Opin Investig Drugs, 2006. **7**(11): p. 985-91.
176. Herold, K., et al., *Receptor for advanced glycation end products (RAGE) in a dash to the rescue: inflammatory signals gone awry in the primal response to stress*. J Leukoc Biol, 2007. **82**(2): p. 204-12.
177. Bierhaus, A., et al., *Understanding RAGE, the receptor for advanced glycation end products*. J Mol Med (Berl), 2005. **83**(11): p. 876-86.
178. Basta, G., et al., *Advanced glycation end products activate endothelium through signal-transduction receptor RAGE: a mechanism for amplification of inflammatory responses*. Circulation, 2002. **105**(7): p. 816-22.
179. Schmidt, A.M., et al., *Advanced glycation endproducts interacting with their endothelial receptor induce expression of vascular cell adhesion molecule-1 (VCAM-1) in cultured human endothelial cells and in mice. A potential mechanism for the accelerated vasculopathy of diabetes*. J Clin Invest, 1995. **96**(3): p. 1395-403.
180. Chavakis, T., et al., *The pattern recognition receptor (RAGE) is a counterreceptor for leukocyte integrins: a novel pathway for inflammatory cell recruitment*. J Exp Med, 2003. **198**(10): p. 1507-15.
181. Osawa, M., et al., *De-N-glycosylation or G82S mutation of RAGE sensitizes its interaction with advanced glycation endproducts*. Biochim Biophys Acta, 2007. **1770**(10): p. 1468-74.
182. Park, S.J., T. Kleffmann, and P.A. Hessian, *The G82S polymorphism promotes glycosylation of the receptor for advanced glycation end products (RAGE) at asparagine 81: comparison of wild-type rage with the G82S polymorphic variant*. J Biol Chem, 2011. **286**(24): p. 21384-92.
183. Li, Y., et al., *Association of Polymorphisms of the Receptor for Advanced Glycation End Products Gene with COPD in the Chinese Population*. DNA Cell Biol, 2014. **33**(4): p. 251-8.
184. Bohlender, J.M., et al., *Advanced glycation end products and the kidney*. American Journal of Physiology - Renal Physiology, 2005. **289**(4): p. F645-F659.
185. RONG, L.L., et al., *RAGE modulates peripheral nerve regeneration via recruitment of both inflammatory and axonal outgrowth pathways*. The FASEB Journal, 2004. **18**(15): p. 1818-1825.

186. Stogsdill, M.P., et al., *Conditional overexpression of receptors for advanced glycation end-products in the adult murine lung causes airspace enlargement and induces inflammation*. Am J Respir Cell Mol Biol, 2013. **49**(1): p. 128-34.
187. Clark, J.G., et al., *Lung connective tissue*. Int Rev Connect Tissue Res, 1983. **10**: p. 249-331.
188. Pasquali-Ronchetti, I. and M. Baccarani-Contri, *Elastic fiber during development and aging*. Microsc Res Tech, 1997. **38**(4): p. 428-35.
189. Al-Robaiy, S., et al., *The receptor for advanced glycation end-products supports lung tissue biomechanics*. Am J Physiol Lung Cell Mol Physiol, 2013. **305**(7): p. L491-500.
190. Starcher, B.C., *Determination of the elastin content of tissues by measuring desmosine and isodesmosine*. Analytical Biochemistry, 1977. **79**(1-2): p. 11-15.
191. Veloso, C.A., et al., *TLR4 and RAGE: similar routes leading to inflammation in type 2 diabetic patients*. Diabetes Metab, 2011. **37**(4): p. 336-42.
192. Zhang, X., et al., *Toll-like receptor 4 deficiency causes pulmonary emphysema*. The Journal of Clinical Investigation, 2006. **116**(11): p. 3050-3059.
193. Turovskaya, O., et al., *RAGE, carboxylated glycans and S100A8/A9 play essential roles in colitis-associated carcinogenesis*. Carcinogenesis, 2008. **29**(10): p. 2035-2043.
194. Vogl, T., A.L. Gharibyan, and L.A. Morozova-Roche, *Pro-Inflammatory S100A8 and S100A9 Proteins: Self-Assembly into Multifunctional Native and Amyloid Complexes*. Int J Mol Sci, 2012. **13**(3): p. 2893-917.
195. Yamamoto, Y., et al., *Septic Shock Is Associated with Receptor for Advanced Glycation End Products Ligation of LPS*. The Journal of Immunology, 2011. **186**(5): p. 3248-3257.
196. Visintin, A., et al., *Lysines 128 and 132 Enable Lipopolysaccharide Binding to MD-2, Leading to Toll-like Receptor-4 Aggregation and Signal Transduction*. Journal of Biological Chemistry, 2003. **278**(48): p. 48313-48320.
197. Watanabe, T., et al., *Increased levels of HMGB-1 and endogenous secretory RAGE in induced sputum from asthmatic patients*. Respir Med, 2011. **105**(4): p. 519-25.
198. Bezerra, F.S., et al., *Long-term exposure to cigarette smoke impairs lung function and increases HMGB-1 expression in mice*. Respir Physiol Neurobiol, 2011. **177**(2): p. 120-6.
199. Rouhiainen, A., et al., *Regulation of monocyte migration by amphotericin (HMGB1)*. Blood, 2004. **104**(4): p. 1174-82.
200. Wang, Y., et al., *sRAGE Induces Human Monocyte Survival and Differentiation*. The Journal of Immunology, 2010. **185**(3): p. 1822-1835.
201. Pullerits, R., et al., *Soluble receptor for advanced glycation end products triggers a proinflammatory cytokine cascade via β 2 integrin Mac-1*. Arthritis & Rheumatism, 2006. **54**(12): p. 3898-3907.
202. Bannister, L.H., *Respiratory system*. In Gray's Anatomy, ed. R.W. P.L. Williams, M. Dyson, and L.H. Bannister. 1999, New York: Churchill Livingstone.
203. Weibel, E.R., *The Pathway for Oxygen : Structure and Function in the Mammalian Respiratory System*. 1984, Cambridge, MA, USA: Harvard University Press.
204. Dobbs, L.G., et al., *Highly water-permeable type I alveolar epithelial cells confer high water permeability between the airspace and vasculature in rat lung*. Proc Natl Acad Sci U S A, 1998. **95**(6): p. 2991-6.
205. Johnson, M.D., et al., *Alveolar epithelial type I cells contain transport proteins and transport sodium, supporting an active role for type I cells in regulation of lung liquid homeostasis*. Proc Natl Acad Sci U S A, 2002. **99**(4): p. 1966-71.

206. Sloniewsky, D.E., et al., *Leukotriene D4 activates alveolar epithelial Na,K-ATPase and increases alveolar fluid clearance*. Am J Respir Crit Care Med, 2004. **169**(3): p. 407-12.
207. Ashino, Y., et al., *[Ca(2+)](i) oscillations regulate type II cell exocytosis in the pulmonary alveolus*. Am J Physiol Lung Cell Mol Physiol, 2000. **279**(1): p. L5-13.
208. Fehrenbach, H., *Alveolar epithelial type II cell: defender of the alveolus revisited*. Respir Res, 2001. **2**(1): p. 33-46.
209. Massaro, D. and G.D. Massaro, *Estrogen regulates pulmonary alveolar formation, loss, and regeneration in mice*. Am J Physiol Lung Cell Mol Physiol, 2004. **287**(6): p. L1154-9.
210. Massaro, D., et al., *Calorie-related rapid onset of alveolar loss, regeneration, and changes in mouse lung gene expression*. Am J Physiol Lung Cell Mol Physiol, 2004. **286**(5): p. L896-906.
211. Shifren, A. and R.P. Mecham, *The stumbling block in lung repair of emphysema: elastic fiber assembly*. Proc Am Thorac Soc, 2006. **3**(5): p. 428-33.
212. Okabe, T., et al., *Isolation and characterization of vitamin-A-storing lung cells*. Exp Cell Res, 1984. **154**(1): p. 125-35.
213. McGowan, S.E., C.S. Harvey, and S.K. Jackson, *Retinoids, retinoic acid receptors, and cytoplasmic retinoid binding proteins in perinatal rat lung fibroblasts*. Am J Physiol, 1995. **269**(4 Pt 1): p. L463-72.
214. Massaro, G.D. and D. Massaro, *Postnatal treatment with retinoic acid increases the number of pulmonary alveoli in rats*. Am J Physiol, 1996. **270**(2 Pt 1): p. L305-10.
215. Massaro, G.D. and D. Massaro, *Retinoic acid treatment abrogates elastase-induced pulmonary emphysema in rats*. Nat Med, 1997. **3**(6): p. 675-7.
216. Mao, J.T., et al., *All-trans retinoic acid modulates the balance of matrix metalloproteinase-9 and tissue inhibitor of metalloproteinase-1 in patients with emphysema*. Chest, 2003. **124**(5): p. 1724-32.
217. Mao, J.T., et al., *A pilot study of all-trans-retinoic acid for the treatment of human emphysema*. Am J Respir Crit Care Med, 2002. **165**(5): p. 718-23.
218. Takahashi, S., et al., *Reversal of elastase-induced pulmonary emphysema and promotion of alveolar epithelial cell proliferation by simvastatin in mice*. Am J Physiol Lung Cell Mol Physiol, 2008. **294**(5): p. L882-90.
219. Indolfi, C., et al., *Effects of hydroxymethylglutaryl coenzyme A reductase inhibitor simvastatin on smooth muscle cell proliferation in vitro and neointimal formation in vivo after vascular injury*. J Am Coll Cardiol, 2000. **35**(1): p. 214-21.
220. Plantier, L., et al., *Keratinocyte growth factor protects against elastase-induced pulmonary emphysema in mice*. Am J Physiol Lung Cell Mol Physiol, 2007. **293**(5): p. L1230-9.
221. Shigemura, N., et al., *Amelioration of pulmonary emphysema by in vivo gene transfection with hepatocyte growth factor in rats*. Circulation, 2005. **111**(11): p. 1407-14.
222. Hegab, A.E., et al., *Intranasal HGF administration ameliorates the physiologic and morphologic changes in lung emphysema*. Mol Ther, 2008. **16**(8): p. 1417-26.
223. Otto, W.R., *Lung epithelial stem cells*. J Pathol, 2002. **197**(4): p. 527-35.
224. Borthwick, D.W., et al., *Evidence for stem-cell niches in the tracheal epithelium*. Am J Respir Cell Mol Biol, 2001. **24**(6): p. 662-70.

225. Rock, J.R., S.H. Randell, and B.L. Hogan, *Airway basal stem cells: a perspective on their roles in epithelial homeostasis and remodeling*. *Dis Model Mech*, 2010. **3**(9-10): p. 545-56.
226. Aso, Y., K. Yoneda, and Y. Kikkawa, *Morphologic and biochemical study of pulmonary changes induced by bleomycin in mice*. *Lab Invest*, 1976. **35**(6): p. 558-68.
227. Reynolds, S.D., et al., *Conditional clara cell ablation reveals a self-renewing progenitor function of pulmonary neuroendocrine cells*. *Am J Physiol Lung Cell Mol Physiol*, 2000. **278**(6): p. L1256-63.
228. Hong, K.U., et al., *Clara cell secretory protein-expressing cells of the airway neuroepithelial body microenvironment include a label-retaining subset and are critical for epithelial renewal after progenitor cell depletion*. *Am J Respir Cell Mol Biol*, 2001. **24**(6): p. 671-81.
229. Reynolds, S.D., et al., *Neuroepithelial bodies of pulmonary airways serve as a reservoir of progenitor cells capable of epithelial regeneration*. *Am J Pathol*, 2000. **156**(1): p. 269-78.
230. Giangreco, A., S.D. Reynolds, and B.R. Stripp, *Terminal bronchioles harbor a unique airway stem cell population that localizes to the bronchoalveolar duct junction*. *Am J Pathol*, 2002. **161**(1): p. 173-82.
231. Kim, C.F., et al., *Identification of bronchioalveolar stem cells in normal lung and lung cancer*. *Cell*, 2005. **121**(6): p. 823-35.
232. Nolen-Walston, R.D., et al., *Cellular kinetics and modeling of bronchioalveolar stem cell response during lung regeneration*. *Am J Physiol Lung Cell Mol Physiol*, 2008. **294**(6): p. L1158-65.
233. Denham, M., T.J. Cole, and R. Mollard, *Embryonic stem cells form glandular structures and express surfactant protein C following culture with dissociated fetal respiratory tissue*. *Am J Physiol Lung Cell Mol Physiol*, 2006. **290**(6): p. L1210-5.
234. Samadikuchaksaraei, A., et al., *Derivation of Distal Airway Epithelium from Human Embryonic Stem Cells*. *Tissue Eng*, 2006. **12**(4): p. 867 - 75.
235. Van Vranken, B.E., et al., *The differentiation of distal lung epithelium from embryonic stem cells*. *Curr Protoc Stem Cell Biol*, 2007. **Chapter 1**: p. Unit 1G 1.
236. Van Haute, L., et al., *Generation of lung epithelial-like tissue from human embryonic stem cells*. *Respiratory Research*, 2009. **10**(1): p. 105.
237. Roszell, B., et al., *Efficient derivation of alveolar type II cells from embryonic stem cells for in vivo application*. *Tissue Eng Part A*, 2009. **15**(11): p. 3351-65.
238. Lavinia Iuliana, I., et al., *Induced Pluripotent Stem Cells (iPSC) Differentiate Into Alveolar Epithelial Cells In Vitro And Improve Lung Function Following Hyperoxia-Induced Lung Injury*, in *D99. REPAIR BY STEM CELLS: PARACRINE MECHANISMS AND INDUCED PLURIPOTENT STEM CELLS (IPSCS)*. American Thoracic Society. p. A6535-A6535.
239. Yang, K.Y., et al., *IV delivery of induced pluripotent stem cells attenuates endotoxin-induced acute lung injury in mice*. *Chest*, 2011. **140**(5): p. 1243-53.
240. Krause, D.S., et al., *Multi-organ, multi-lineage engraftment by a single bone marrow-derived stem cell*. *Cell*, 2001. **105**(3): p. 369-77.
241. Kotton, D.N., et al., *Bone marrow-derived cells as progenitors of lung alveolar epithelium*. *Development*, 2001. **128**(24): p. 5181-8.

242. Kotton, D.N., A.J. Fabian, and R.C. Mulligan, *Failure of bone marrow to reconstitute lung epithelium*. Am J Respir Cell Mol Biol, 2005. **33**(4): p. 328-34.
243. Chang, J.C., et al., *Evidence that bone marrow cells do not contribute to the alveolar epithelium*. Am J Respir Cell Mol Biol, 2005. **33**(4): p. 335-42.
244. Ortiz, L.A., et al., *Mesenchymal stem cell engraftment in lung is enhanced in response to bleomycin exposure and ameliorates its fibrotic effects*. Proc Natl Acad Sci U S A, 2003. **100**(14): p. 8407-11.
245. Rojas, M., et al., *Bone marrow-derived mesenchymal stem cells in repair of the injured lung*. Am J Respir Cell Mol Biol, 2005. **33**(2): p. 145-52.
246. Aliotta, J.M., et al., *Bone marrow production of lung cells: the impact of G-CSF, cardiotoxin, graded doses of irradiation, and subpopulation phenotype*. Exp Hematol, 2006. **34**(2): p. 230-41.
247. Ishizawa, K., et al., *Bone marrow-derived cells contribute to lung regeneration after elastase-induced pulmonary emphysema*. FEBS Lett, 2004. **556**(1-3): p. 249-52.
248. Ortiz, L.A., et al., *Interleukin 1 receptor antagonist mediates the antiinflammatory and antifibrotic effect of mesenchymal stem cells during lung injury*. Proc Natl Acad Sci U S A, 2007. **104**(26): p. 11002-7.
249. Gupta, N., et al., *Intrapulmonary delivery of bone marrow-derived mesenchymal stem cells improves survival and attenuates endotoxin-induced acute lung injury in mice*. J Immunol, 2007. **179**(3): p. 1855-63.
250. Haynesworth, S.E., M.A. Baber, and A.I. Caplan, *Cytokine expression by human marrow-derived mesenchymal progenitor cells in vitro: effects of dexamethasone and IL-1 alpha*. J Cell Physiol, 1996. **166**(3): p. 585-92.
251. Van Arnem, J.S., et al., *Engraftment of bone marrow-derived epithelial cells*. Stem Cell Rev, 2005. **1**(1): p. 21-7.
252. Cortiella, J., et al., *Tissue-engineered lung: an in vivo and in vitro comparison of polyglycolic acid and pluronic F-127 hydrogel/somatic lung progenitor cell constructs to support tissue growth*. Tissue Eng, 2006. **12**(5): p. 1213-25.
253. Mondrinos, M.J., et al., *Engineering three-dimensional pulmonary tissue constructs*. Tissue Eng, 2006. **12**(4): p. 717-28.
254. Andrade, C.F., et al., *Cell-based tissue engineering for lung regeneration*. Am J Physiol Lung Cell Mol Physiol, 2007. **292**(2): p. L510-8.
255. Macchiarini, P., et al., *Clinical transplantation of a tissue-engineered airway*. Lancet, 2008. **372**(9655): p. 2023-30.
256. Petersen, T.H., et al., *Tissue-Engineered Lungs for in Vivo Implantation*. Science, 2010. **329**(5991): p. 538-541.
257. Stripp, B.R., et al., *cis-acting elements that confer lung epithelial cell expression of the CC10 gene*. J Biol Chem, 1992. **267**(21): p. 14703-12.
258. Warburton, D., *Developmental biology: order in the lung*. Nature, 2008. **453**(7196): p. 733-5.
259. Warburton, D., et al., *Lung development and susceptibility to chronic obstructive pulmonary disease*. Proc Am Thorac Soc, 2006. **3**(8): p. 668-72.
260. Seth, R., et al., *Role of Epidermal Growth Factor Expression in Early Mouse Embryo Lung Branching Morphogenesis in Culture: Antisense Oligodeoxynucleotide Inhibitory Strategy*. Developmental Biology, 1993. **158**(2): p. 555-559.

261. Vaughan, A.E. and H.A. Chapman, *Regenerative activity of the lung after epithelial injury*. *Biochimica et Biophysica Acta (BBA) - Molecular Basis of Disease*, 2013. **1832**(7): p. 922-930.
262. Newby, A.C., *Matrix metalloproteinases regulate migration, proliferation, and death of vascular smooth muscle cells by degrading matrix and non-matrix substrates*. *Cardiovascular Research*, 2006. **69**(3): p. 614-624.
263. Suzuki, M., et al., *Matrix metalloproteinase-3 releases active heparin-binding EGF-like growth factor by cleavage at a specific juxtamembrane site*. *J Biol Chem*, 1997. **272**(50): p. 31730-7.
264. Lucchesi, P.A., et al., *Involvement of metalloproteinases 2/9 in epidermal growth factor receptor transactivation in pressure-induced myogenic tone in mouse mesenteric resistance arteries*. *Circulation*, 2004. **110**(23): p. 3587-93.
265. Dunsmore, S.E., et al., *Matrilysin expression and function in airway epithelium*. *J Clin Invest*, 1998. **102**(7): p. 1321-31.
266. Betsuyaku, T., et al., *Gelatinase B is required for alveolar bronchiolization after intratracheal bleomycin*. *Am J Pathol*, 2000. **157**(2): p. 525-35.
267. Schiess, R., et al., *Analysis of cell surface proteome changes via label-free, quantitative mass spectrometry*. *Mol Cell Proteomics*, 2009. **8**(4): p. 624-38.
268. Gundry, R.L., et al., *A cell surfaceome map for immunophenotyping and sorting pluripotent stem cells*. *Mol Cell Proteomics*, 2012. **11**(8): p. 303-16.
269. Hofmann, A., et al., *Proteomic cell surface phenotyping of differentiating acute myeloid leukemia cells*. *Blood*, 2010. **116**(13): p. e26-34.
270. Laura Van, W., et al., *Sex Differences In Lung Repair Following Sidestream Smoke Exposure*, in A68. *AN ENDOCRINE STUDY OF THE LUNG: GLUCOCORTICOIDS, SEX, AND OTHER HORMONES*. American Thoracic Society. p. A2136-A2136.
271. Oliver, J.R., et al., *Gender differences in pulmonary regenerative response to naphthalene-induced bronchiolar epithelial cell injury*. *Cell Prolif*, 2009. **42**(5): p. 672-87.
272. Milutinovic, P.S., et al., *The receptor for advanced glycation end products is a central mediator of asthma pathogenesis*. *Am J Pathol*, 2012. **181**(4): p. 1215-25.
273. Hanford, L.E., et al., *Regulation of receptor for advanced glycation end products during bleomycin-induced lung injury*. *Am J Respir Cell Mol Biol*, 2003. **29**(3 Suppl): p. S77-81.
274. Gefter, J.V., et al., *Comparison of distinct protein isoforms of the receptor for advanced glycation end-products expressed in murine tissues and cell lines*. *Cell Tissue Res*, 2009. **337**(1): p. 79-89.